The Effect of Maximum MLC Speed and Dose Rate Constraints on VMAT Plan Quality, Accuracy and Efficiency

A thesis
submitted in partial fulfilment
of the requirements for the Degree
of
Master of Science in Medical Physics

by

Neil A Campbell

Department of Physics and Astronomy
University of Canterbury
Christchurch, New Zealand
2013

Abstract

Volumetric modulated arc therapy (VMAT) is an efficient and conformal radiation therapy technique. It accomplishes this by dynamically varying multi-leaf collimator (MLC) positions, dose rates and gantry velocity. This work investigated the effect of varying the maximum MLC speed and maximum dose rate on the quality, efficiency and accuracy of treatment plans.

The Pinnacle^3 SmartArc treatment planning software was used to generate plans on prostate and head and neck (H&N) sites. A range of maximum MLC leaf speeds (0.55 cm/s to 2.20 cm/s) and maximum dose rates (200 MU/min to 600 MU/min) restrictions were applied to each plan to investigate their effect on the treatment quality, efficiency and accuracy. Each plan had their monitor units (MU) per fraction, delivery time, mean dose rate and leaf speed analysed. The dose volume histogram (DVH) data was used in the assessment of the conformity, homogeneity and plan quality. The treatments were delivered on Varian iX accelerator equipped with 120-leaf millennium MLC. Quality assurance measurements were performed using the ArcCHECK™ 3D diode array and results were assessed based on gamma analysis of dose fluence maps, beam delivery statistics and Dynalog data.

The number of VMAT fields was found to be a key factor in how significant the maximum MLC leaf speed affected the plan parameters investigated. Single arc treatments were shown to have lower MU, dose rate and plan quality, while also exhibiting a slight increase in estimated delivery time. For dual arc treatments, MU, delivery time, dose rate and plan quality were largely independent of the maximum MLC speed allowed. The QA showed that higher MLC leaf speeds were prone to an increase in the discrepancy between planned and delivered control point (CP) fluence and higher MLC positioning errors. None of these were at a clinically significant level, and the overall fluence distribution and point dose comparisons were independent of maximum MLC leaf speed.

The only clinically significant effect that modulation of the maximum dose rate had was on the delivery time. Lower maximum dose rates resulted in longer treatment delivery, which is an important consideration in minimising the intra-fractional motion during treatment.

The results of the MLC leaf speed evaluation showed that the lower the maximum leaf speed the more accurate the delivered treatment, -however the quality of the plan is reduced. This indicates that there could be an optimum maximum MLC leaf speed which produces high quality plans that can be accurately delivered. Based on this work a maximum MLC leaf speed of 1.38 cm/s was shown to have no reduction in plan quality however it showed improvement in delivery accuracy. There was no justification found for reducing the maximum dose rate below the recommended 600 MU/min.

Acknowledgments

First and foremost I must thank my supervisor Dr Gerard Bengua. Without his constant support, advice and deadlines throughout this project (especially during these final few months) there would likely still be many months more to go.

I would like to thank all the members of staff at Auckland Oncology physics department for being accessible and willing to answer the many questions that I had. As well as providing a work environment that gave me the time and ability to conduct this research.

I would like to express my gratitude to Dr Juergen Meyer for his supervision in the initial stages of the project, as well as his willingness to support his student even after leaving UC.

For the support that my family has offered me through encouragement, advice, food and ambitions bets (cheers Viv), I thank you all.

To my friends, thanks for being there to take my mind off the project whenever I needed it and many times I didn't. I would especially like to thank Kaidi, Leanne and Alison for enabling me to multi task and discuss the project at the pub even if you didn't always know what I was talking about.

Contents

List of Figures

List of Tables

Glossary

3D	Three-dimensional
3DCRT	Three-Dimensional Conformal Radiation Therapy
ADHB	Auckland District Health Board
BOT	Beam on time
CHHiP	Conventional or Hypofractionated High dose Intensity-modulated radiotherapy for Prostate cancer
CI	Conformity Index
CP (s)	Control points (s)
CT	Computed tomography
CTV	Clinical tumour volume
*d*DVH	Differential dose volume histogram
DICOM	Digital Imaging and Communications in Medicine
DNA	Deoxyribose nucleic acid
DTA	Distance to agreement
DVH	Dose volume histogram
EBRT	External beam radiation therapy
EUD	Equivalent uniform dose
GTV	Gross tumour volume
Gy	Gray (J/kg)
H&N	Head and Neck
HI	Homogeneity Index
ICRU	International Commission on Radiation Units and measurements
IMAT	Intensity-modulated arc therapy
IMRT	Intensity-modulated radiation therapy
LET	Linear energy transfer
Linac (s)	Linear Accelerator (s)
MLC	Multi-leaf collimator
MU(s)	Monitor unit (s)
MV	Mega-voltage
NTCP	Normal tissue complication probability
OAR (s)	Organ(s) at risk
OBI	On-board imaging
PMMA	Poly-methyl methacrylate

PRV	Planning risk volume
PTV	Planning target volume
QA	Quality assurance
QUANTEC	Quantitative Analysis of Normal Tissue Effects in the Clinic
ROI (s)	Region(s) of interest
RT	Radiation therapy
SIB	Simultaneous integrated boost
STDV	Standard deviation value
TCP	Tumour control probability
TPS	Treatment planning system
VMAT	Volumetric modulated arc therapy

1. Introduction

Cancer is the leading cause of death worldwide with over 7.5 million deaths attributed to cancer in 2008 and more than 12 million new cases diagnosed[1]. Over the next 10 years, as the world population ages and the developing world adopts cancer associated lifestyle choices and a " westernised" diet [1], it is predicted to reach nearly 17 million new cancer cases per year and causing in excess of 10 million deaths. This increasing trend is reflected in the Australian and New Zealand statistics where the increase in new cancers is predicted to rise by over 31% between 2008 and 2020[2]. To address this increase in cancer incidences, all areas of oncology will need to improve the efficiency, effectiveness and economics of the methods for treating this disease. Currently, surgery, chemotherapy and radiation therapy (RT) are used to treat cancer sometimes independently but more often in conjunction with at least one of the other treatment modality. More than half the patients that are treated for cancer will, at some point, be treated using radiation therapy.

1.1 Radiobiology

Radiation can be classified into two categories - ionising and non-ionising radiation; the former is used in cancer therapy. As a radioactive particle travels through matter it deposits energy based on its linear energy transfer (LET). The higher the LET of the radiation, the higher the frequency of energy deposition. The energy deposited can cause ionisation events. If these events occur in a cell it can lead to the damage of the DNA in the cell via a double strand break or the production of free radicals which have a high chemical reactivity and are also capable of causing DNA breaks. A healthy cell is normally capable of repairing a single strand break without any significant detriment. However, if there is a double stand break (where both strands of the helix are broken), it is more difficult for the cell to repair the damaged DNA. Provided that the number of breaks is small, this process is usually repaired successfully. If the cell is unable to repair itself correctly then it will either become inactive (permanently or temporarily) or signal apoptosis (programmed cell death). How a cell reacts to DNA damage is complex and beyond the scope of this paper however if the cell cannot repair itself then it usually either dies or becomes incapable of replicating. The more damage that occurs means a cell is less likely to be able to repair itself and thus cell death has a greater chance of occurring. Radiation therapy aims to maximise the dose delivered to a tumour volume while minimising the dose that is delivered to the healthy tissues.

1.2 Radiation Therapy

Wilhelm Röntgen discovered x-rays in 1895 and within a year Leoplod Freund, an Austrian surgeon, demonstrated the disappearance of a hairy mole following treatment with x-rays[3]. In the early days very little was understood about radiobiology and due to the limitation in dosimetry and the accuracy of delivery it often resulted in quite severe side effects including induction of secondary tumours in healthy tissues. Over the past century, dramatic improvements have been made in the methods that are used in radiation therapy and the biological effects of radiation such that nowadays radiotherapy plays a major role in most cancer treatments.

In the early days the energies available were only useful for treating superficial diseases and it was soon realised that higher energies were required to treat deeper tumours. The development of cobalt-60 and other isotope-based teletherapy machines addressed the need for a more penetrating radiation beam. Although cobalt-60 machines are still used in a few radiotherapy applications, mega-voltage (MV) linear accelerators (linacs) are the equipment of choice for generating high-energy photon and electron beams for treatment. Some of the notable advantages of linacs are its configurability to have multiple electron and photon energies, its ability to deliver in higher dose rates and the sharper dose fall-off at the beam edge[4]. Shown in Figure 1.1 a and b are the early model of a linac and one of the modern linacs, respectively.

Initially, treatments were planned based on 2D orthogonal images and using bony anatomy to localise targets, dose calculations were all done manually and radiation fields used were mostly simple squares or rectangles. The introduction of computed tomography (CT) as a tool to visualise tumours in 3D provided better tumour delineation and led to the development of more conformal treatment methods, the simplest of which is 3D conformal radiation therapy (3DCRT). In its early implementation, 3DCRT was delivered using multiple beams from different angles and the fields were shaped to closely resemble the shape of the tumour. The beams were weighted to give the optimal dose distribution at the tumour site. The practicality of this technique was initially limited by the requirement to alter the field shape for each angle which would require the changing of shield trays manually as well as the cost and time of manufacturing one for each field. This limitation was the driving force behind the development of the multi leaf collimator (MLC).

a.

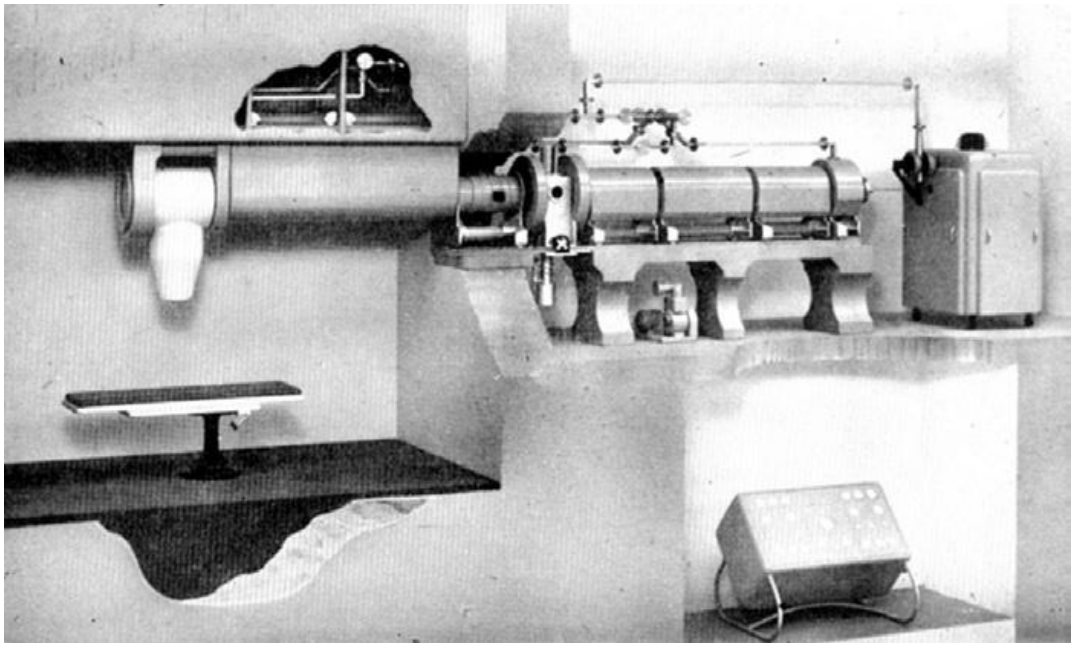

b.

Figure 1.1 a) Model of the 8 MeV accelerator installed in Hammersmith Hospital in 1953. b) Varian iX linear accelerator installed in Auckland Hospital.

MLC's (Figure 1.2) are two banks of interlocking tungsten leaves opposed over the central plane, these leaves initially had a projected thickness of 1.0 cm at isocentre but have since been reduced to 0.5 cm in most non-stereotactic systems. The leaves are able to move independently of their neighbour to form more complex shapes allowing a more conformal field to be delivered. Currently the two major linac manufacturers implement MLC leaves in slightly different ways. Eleckta replaces one of the secondary collimators with a set of MLC

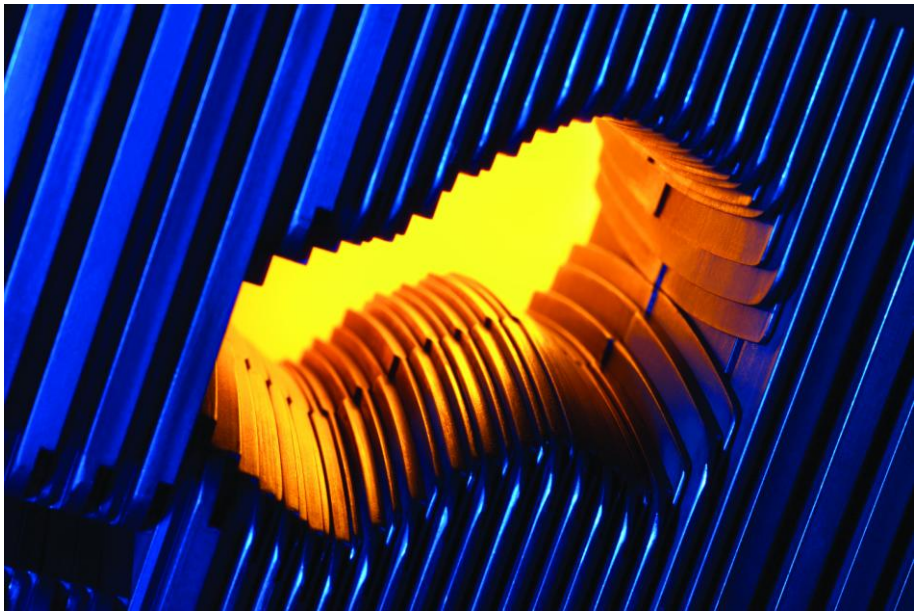

Figure 1.2 Multi Leaf Collimator, reproduced from Varian.

leaves which allows additional space in the head of the linac. They move in and out of the field along a curved track so that the flat leaf end always exposes a constant attenuating thickness to the primary beam regardless of the field size. On the other hand, Varian machines use an MLC bank in combination with the secondary jaws, they used leaves that travel linearly in and out of the beam. To ensure that they have constant leaf attenuation at the leaf tips, they are rounded and this gives the same effect as the curved track of Eleckta MLCs. In both machines, MLC leaves can be electronically driven to any specified shape within their maximum field size (40 cm × 30 cm) and generate the same beam conformity to the tumour that physical blocks once provided. The flat beam profiles used in 3DCRT usually cannot effectively limit the dose to organs at risk, within or close to the treatment target volumes, without compromising the intended dose to be delivered the tumour. A solution to this is to use modulated beam fluences which is discussed in the next section.

1.3 Intensity Modulated Radiation Therapy

Intensity modulated radiation therapy (IMRT) is a treatment modality where at least one beam is intentionally delivered with a non-uniform intensity profile. Anders Brahme[5] was the first to publish the concept in 1988 when he showed that a higher degree of conformity can be achieved by delivering a beam with a modulated intensity profile. The intensity profile was modulated so that paths that travel through a larger volume of tumour will have a higher intensity, while paths which travel through less tumour volume will have a lower intensity as seen in Figure 1.3. The inverse planning required for this treatment did not have a single exact solution and Bortfeld[6] demonstrated that by using a quadratic objective function, local minimum will not be generated allowing the use of fast gradient descent methods, thus reducing the optimisation times.

The early concepts of IMRT offered a significant improvement on dose conformity, however they had the significant limitation in the range of modifiers that would be required to alter the intensity of each beam for each patient. The required intensity modulation, however, was easily achieved with the use of MLCs.

Two methods of delivering IMRT treatments have been developed - step and shoot and sliding window. The step and shoot involves the use of fixed fields formed by the MLCs of varying sizes being delivered from the same angle. Each field, known as segments, delivers a fraction of the dose required from that angle to achieve the required dose fluence. Once all the fields have been delivered the process is repeated for the remaining fields at different angles. The superposition of successive segments from each field results in an intensity modulated dose fluence, despite each delivered field having a flat profile. With this method, no dose is delivered while the MLC leaves are moving from one position to the next.

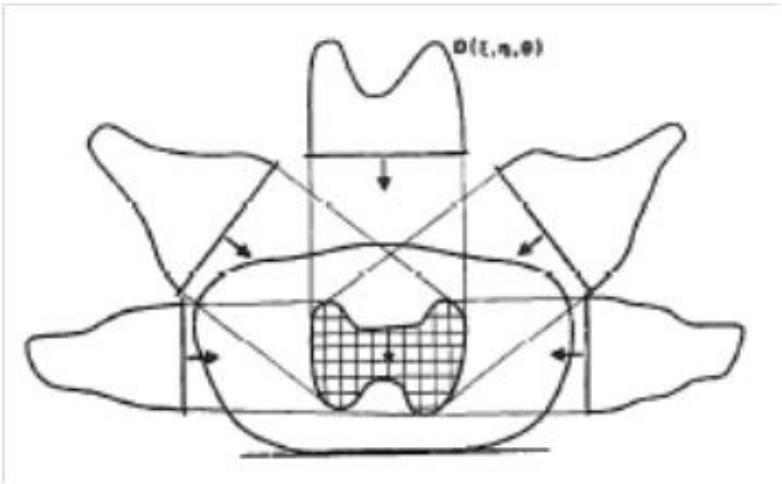

Figure 1.3 The original IMRT schematic diagram by Brahme [5], it shows five intensity modulated beams incident on the target volume (hatched area). The intensity profile is dependent on the volume of the target that the beam would see when traversing the tumour volume.

However, this means that the step and shoot method requires longer total treatment time due to time needed for the MLC leaves to travel between segments. The sliding window (or dynamic IMRT) method involves the leaves moving in a unilateral direction across the field from each of the delivery angles. The variation in the duration of exposure to the open field results in the overall intensity modulation of the beam from that angle. Restrictions on the leaf motion are imposed, as there is a physical limitation on how fast MLC leaves can travel, meaning that the successive fields that are used to plan sliding window cannot change more than the leaf can move.

IMRT offers a significant improvement on the conformity compared to 3DCRT and earlier methods. This improved conformity not only allows for greater organ at risk (OAR) sparing and reduction of the normal tissue complication probability (NTCP) but it also provides a chance for dose escalation, which means that a higher dose can be delivered to the tumour volume increasing the tumour control probability (TCP). However, the complexity of IMRT resulted in an increased demand on planning computational power, quality assurance (QA) requirements, patient positioning restrictions, delivery time and monitor units (MU) per fraction.

Traditional forward planning methods would have been impractical to generate IMRT treatment plans, thus, inverse planning techniques were developed. In this technique, the desired dose objectives are initially defined and optimisation algorithms in treatment planning computers (TPS) attempt to get as close as possible to these specified objectives. A robust QA regimen is likewise required prior to the clinical delivery of an IMRT plan to ensure that the optimised plan is deliverable and the doses predicted by the TPS are accurate within acceptable tolerances. The plan QA may include point dose or dose fluence measurements or both. A disadvantage of IMRT treatments is that it takes longer to deliver compared to 3DCRT which reduces the daily patient throughput. However, of bigger concern is the increased chance of intra-fractional motion for longer treatment times which could affect the outcome of the treatment. The longer a patient is required to hold the treatment position the more likely they are to move if the position becomes uncomfortable. Other causes of intra-fractional motion are respiration, changes in rectal and bladder filling or bowel gas movement.

One of the main characteristics of IMRT plans is the high conformity of dose distributions to target volumes which means that there is less tolerance to target localisation errors that could result in the target volume being underdosed or the surrounding healthy tissues being overdosed. This is why IMRT requires better immobilisation and on-board imaging (OBI) systems to ensure that the tumour volume localised as accurately as possible. In order to achieve the higher conformity in IMRT, more small fields (or segments) are required. This increases the number of MU per fraction which in turn increases the amount of scatter from the head of the linac that can induce secondary cancers[7-10]. Overall, the limitations of

IMRT are outweighed by the improved cure rates and improved OAR sparing that comes from its superior conformity when compared to 3DCRT and other simple RT treatments.

1.4 Volumetric-Modulated Arc Therapy

Intensity-modulated arc therapy (IMAT) is an alternative way of generating and delivering intensity modulated beams, first proposed by Yu in 1995 [11]. Instead of using fields at discrete angles with a set number of segments, an arc, or combinations of multiple arcs with different constant dose rates, are used. In IMAT, the MLC leaves move dynamically, like in sliding window IMRT, as the gantry rotates. The initial implementation of IMAT was computationally demanding and required a large number of MU to be delivered per fraction and long delivery times, just like IMRT. The technique was further improved and developed by Otto who coined the term 'volumetric modulated arc therapy' (VMAT) and described it as *IMRT in a single arc*[12]. In VMAT, both the dose rate and gantry speed are allowed to vary in addition to MLC leaf positions to generate a highly conformal isodose distribution at reduced delivery time and MU.

To make the optimisation time practical the VMAT model assumes that a full arc can be represented by a set number of control points (CPs). It also assumes that all of the MU are given at the angle of the CPs and to the field shape defined at that CP. However, the field is changing shape during the entire beam delivery and the set MU at the CP is delivered over the length of the segment between CPs. With a small enough CP spacing the model becomes valid. If the total number of CPs were optimised from the start then planning would be prohibitively long. Otto's solution was to use coarse sampling initially with wide gaps between CPs and during the optimisation these gaps are filled until the desired CP space is achieved. The accuracy of the model is dependent on the CP spacing but the closer the CPs are the longer the optimisation time becomes. As such, at ADHB our current practice is to use 4° spacing in our VMAT plans allowing a compromise between the accuracy of the model and the planning time.

Since the original paper by Otto [12]there has been extensive work done in comparing the dose distributions between 3DCRT, IMRT and VMAT[13,14]. The general consensus of these papers is that both IMRT and VMAT provide significant improvements in dose distributions for both tumour coverage and OAR sparing. When compared to each other, VMAT is shown to provide equal or better dose distribution and a reduction in both MU and delivery times. VMAT has been shown to deliver a more efficient treatment and although long term survival statistics are still limited, it is predicted that the OAR sparing will prove it to be more effective than IMRT. Figure 1.4 provides a good example of the typical dose distributions in 3DCRT, IMRT and VMAT.

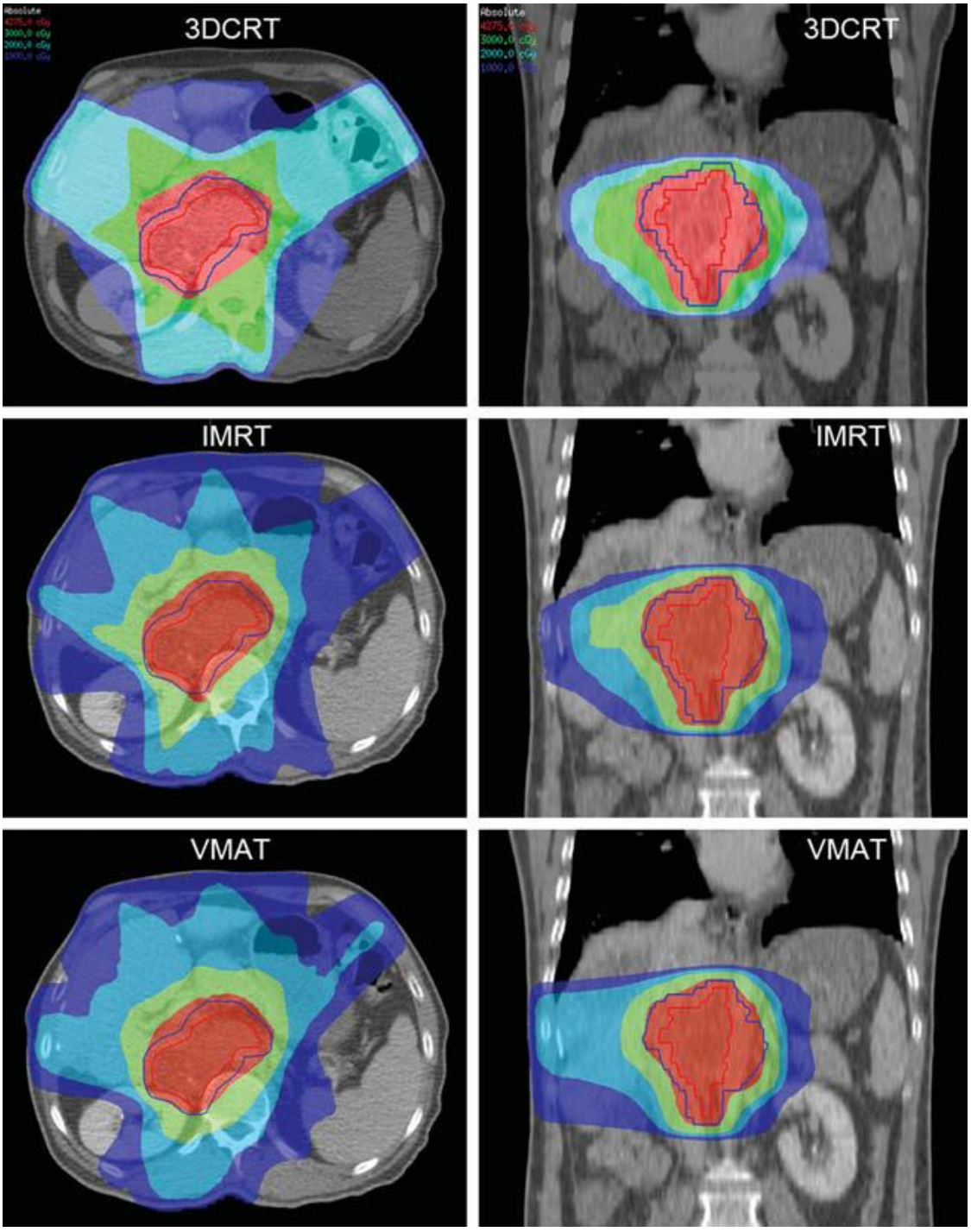

Figure 1.4 Shows the typical dose distributions for the treatment of an abdominal Lymph node metastasis, using 3DCRT (top), IMRT (middle) and VMAT (bottom)[13].

1.5 Literature Review

A significant number of research papers published about VMAT in the past five years have focused on the practical applications of the technique with reference to a particular site, tumour type and how it compares with other available modalities such as static IMRT, tomotherapy or 3DCRT [13,14] . There have also been a number of papers related to methods of undertaking machine and patient QA specific to VMAT[15,16], however the interplay between machine input and output parameters on plan quality, efficiency and accuracy is largely unexplored and there is a lack of a general theory governing VMAT[17]. There are, however, limited publications on the dependence of the quality of plans and QA results on the limitations applied on MLC leaf motion, the MLC positional errors and the constraints applied to usable dose rates during beam delivery.

Chen et al.[18] investigated how leaf motion constraints affect the quality, accuracy and efficiency of IMAT plans. Using fluences imported into an in-house sequencer designed to generate IMAT plans, they investigated the effect of applying a restriction on the MLC leaf motion in terms of the distance that the MLC leaves can travel per degree over a range of 1 to 30 mm/deg. They found that there was a significant impact on the quality, efficiency and accuracy of the plans delivered especially in complex treatments. They recommended a leaf motion constraint of 2 to 3 mm/deg and noted that as the motion constraint was relaxed the delivery times increased.

Tatsumi et al.[19] has published a paper on the effects of MLC positional error on dose distribution. They applied a systematic error to the MLC leaf positions and compared the QA results from the delivery of the original plans to the plans with the error applied and found that there was a range of tolerances in the MLC leaf positioning error depending on the TPS used. To maintain pass rates with under a 2% dose difference, any systematic error would have to be less than 0.5 mm for SmartArc. SmartArc is part of the Pinnacle treatment planning system intended for generating VMAT plans in this study.

The dose rate modulation is important in order for VMAT to deliver efficient intensity modulated therapy. Nicolini et al.[20] looked into how restricting the maximum dose rate effects the gantry rotation. They applied the same objective weights to a single arc for each dose rate and showed that the RapidArc algorithm, a Varian Medical System's implementation of VMAT, was able to modulate the gantry speed to compensate for the restriction in dose rates available. The study also showed a slight improvement in the plan quality and an increase in the treatment time for a more restricted plan.

1.6 Objectives

Chen et al.[18] covered a broad range of MLC motions, a large portion of which would require a significant decrease in the speed of the gantry rotation. Their recommendations based on the data obtained from their in-house sequencer are not easily implementable in the TPS at our hospital. It was also not clear whether the reported effects on plan quality was brought about by the limitations applied on the MLC or the TPS/sequencer itself.

It is clear from the work of Tatsumi et al.[19] that a small systematic error can cause significant change in agreement between planned and delivered VMAT. However, they did not look into the effects of random errors which would be more representative of those expected to occur in a normal treatment delivery.

When the objectives and weights are optimised to produce an optimal plan they are dependent on the initial physical constraints applied to the machine. The dose rate study, mentioned in section 1.4, applied the same objectives and weights to all the restricted dose rate tests, meaning they were not optimised for the initial constrains in the restricted dose rate cases. It is therefore possible for the TPS to minimise the effects if the objectives and weights were set taking into account these restrictions. Additionally only single arc treatments were trialled for head and neck (H&N) cases while earlier publications recommended at least two arcs [21-23] to compensate for the increased complexity.

In terms of plan verifications, previous studies were conducted using a 2D detector device and analysed as an overall fluence pattern. However, with this method the effects of gantry rotation could be hidden by the overall dose fluence.

The main objective of this thesis was to determine the effect of the maximum allowed MLC speed and dose rate on VMAT plans generated in the Pinnacle® treatment planning system. Specifically, prostate and H&N VMAT plans were evaluated to establish the dependence on the maximum allowed MLC speed and dose rate of the following parameters:

(1) the optimum plan parameters, including the number of required MU, delivery time and mean dose rate;
(2) the dose conformity and homogeneity of the generated plans;
(3) the plan quality score, which was computed based on the weighted importance of the dose objectives set by radiation oncologists;
(4) the pass-fail rate of plan QA using a 3D diode array;
(5) the accuracy of MLC leaf positions during beam delivery which was obtained from linac Dynalog data.

2. Methods and Materials

The data gathering, analysis methods applied and the materials used in this research are discussed in this chapter. The tumour sites selected for this study are described in section 2.1. The succeeding section discusses the various aspects of treatment planning, including the treatment planning system used, the planning objectives in addition to constraints for the different tumour sites considered, and the parameters survey in this research. Section 2.4 explains the metrics used for the assessment of the quality of the plans generated. In order to verify the deliverability and the dosimetry of the plans, the QA regimen for clinical patients used in our institution was performed on all the plans. The details of the QA regimen and the equipment used in the plan verification are described in section 2.5.

2.1 Tumour Sites

We are currently treating a broad range of sites with a variety of external beam radiation therapy (EBRT) techniques. IMRT is used primarily in the radical treatment of prostate and H&N cases. Prostates are treated with VMAT while H&N treatments are delivered using step and shoot IMRT. The latter is likewise planned to move towards the use of VMAT as future resources become available.

Prostate (Figure 2.1a) was the first choice for the tumour site to be evaluated in this study due to a number of reasons. Firstly, they represent a simple treatment planning case study because of the size and shape of the target volumes and the number of organs at risk. Secondly, we already have extensive experience in terms of VMAT delivery for this site given our current practice to treat all prostates with VMAT. Therefore, we were able to use our established planning and QA protocols to create and assess the VMAT plans used in this study. Additionally, the results of this study may also become useful in further improvement of our present protocols. Finally, there are also a significant amount of literature available about prostate cancer treatment using VMAT that would allow us to compare and validate the results of this research.

The second site evaluated in this study was H&N. This site was selected as an example of treatment cases with higher levels of complexity compared to prostate cases. Specifically, a nasopharynx and an oropharynx case were chosen. The nasopharynx case was a paediatric patient that involved a single volume located in close proximity to critical organs in the head (Figure 2.1b), which included the optic structures and the brainstem. The plans generated in this research were further complicated by the constraints requested by the radiation oncologist

in the original clinical plan because of the age of the patient; paediatric patients have higher susceptibility to adverse effects due to a longer life expectancy and the developing tissue being more sensitive to radiation damage. The oropharynx case had two tumours with vastly different prescriptions; this is in addition to similar critical organs as the nasopharynx treatment site. This increases the complexity of the treatments and provided a good test for any effects that may occur when treating tumours in more complex sites.

a)

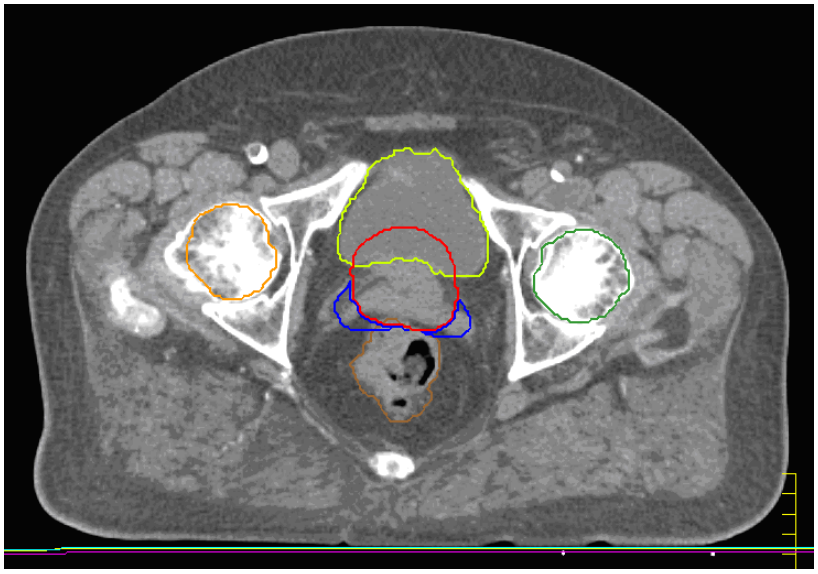

b)

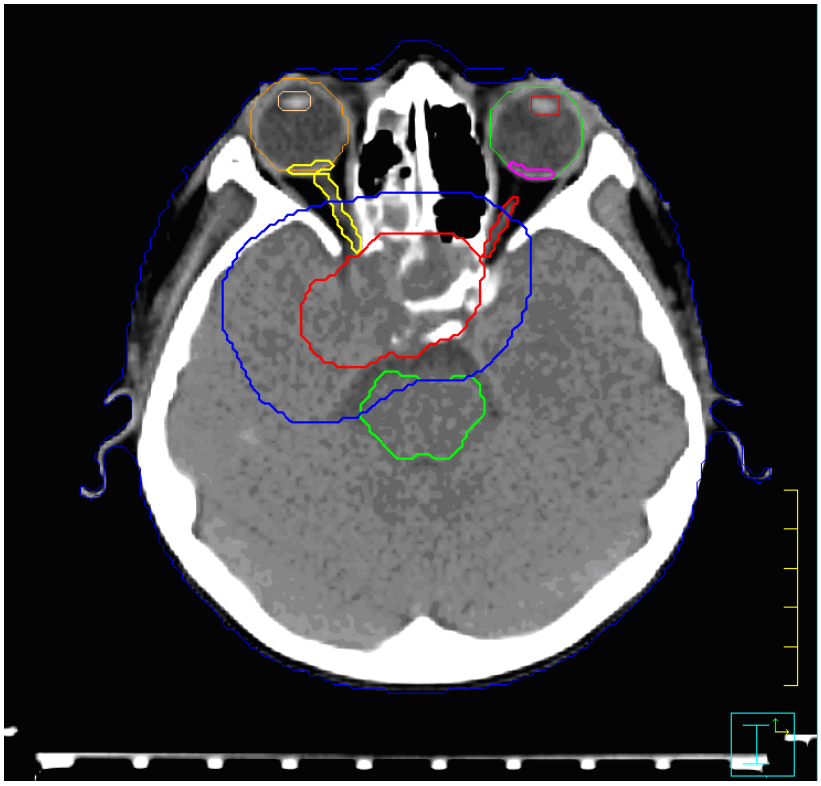

Figure 2.1 Screen captures from Pinnacle showing two of the patient data sets. The top image is a prostate site with the prostate, the seminal vesicles, femoral heads, bladder and rectum contoured. The bottom image is the paediatric nasopharaynx cases showing the gross tumour volume, prescribed tumour volume, brainstem, and the left and right optic nerve, lens, eye and retina.

2.2 Treatment Planning

2.2.1 Pinnacle Treatment Planning with SmartArc

The Treatment Planning System that was used in this research was Pinnacle[3] version 9.2 (Phillips Radiation Oncology Systems, Fitchburg, WI) with the SmartArc planning module. The SmartArc module in Pinnacle requires certain parameters to be specified such as machine characteristics, regions of interest (ROIs), plan parameters and planning objectives. The machine characteristics set the physical limitations of the linac components; these are typically set to the maximum safe level that it can operate within. These include the physical range of each parameter (e.g., maximum and minimum jaw position), the maximum speed that something can move (e.g. leaf, gantry and collimator speeds) and the rates at which the movements of these components can vary (e.g. gantry acceleration). These parameter settings and limitations apply to all plans; they must be adhered to by the TPS to generate a deliverable plan.

ROIs need to be contoured for a plan to be generated and evaluated. This is generally done on CT images although other imaging modalities can be used provided they are co-registered to the CT images. ROIs are used in two ways, firstly is to create a volume that planning objectives can be applied to, which are used by the TPSs optimisation algorithm when producing a plan. Secondly they are used to evaluate the dose that a particular volume of tissue would receive based on the current treatment plan. ROIs can be used as both planning objectives and evaluation volumes.

The plan parameters must be selected by the user for each plan. These include the number of arcs, the isocentre, the direction of rotation, the length of the arc, the plane of the arc rotation, the energy of the beam, the control point spacing and collimator rotation.

Finally optimisation objectives are specified to reflect the target dose requirements and the dose constraints to OAR. The dose objectives can be specified using any one of the objective types listed in Table 2.1. The dose optimisation algorithm then attempts to achieve an optimum plan by prioritising the objectives based on their defined weights.

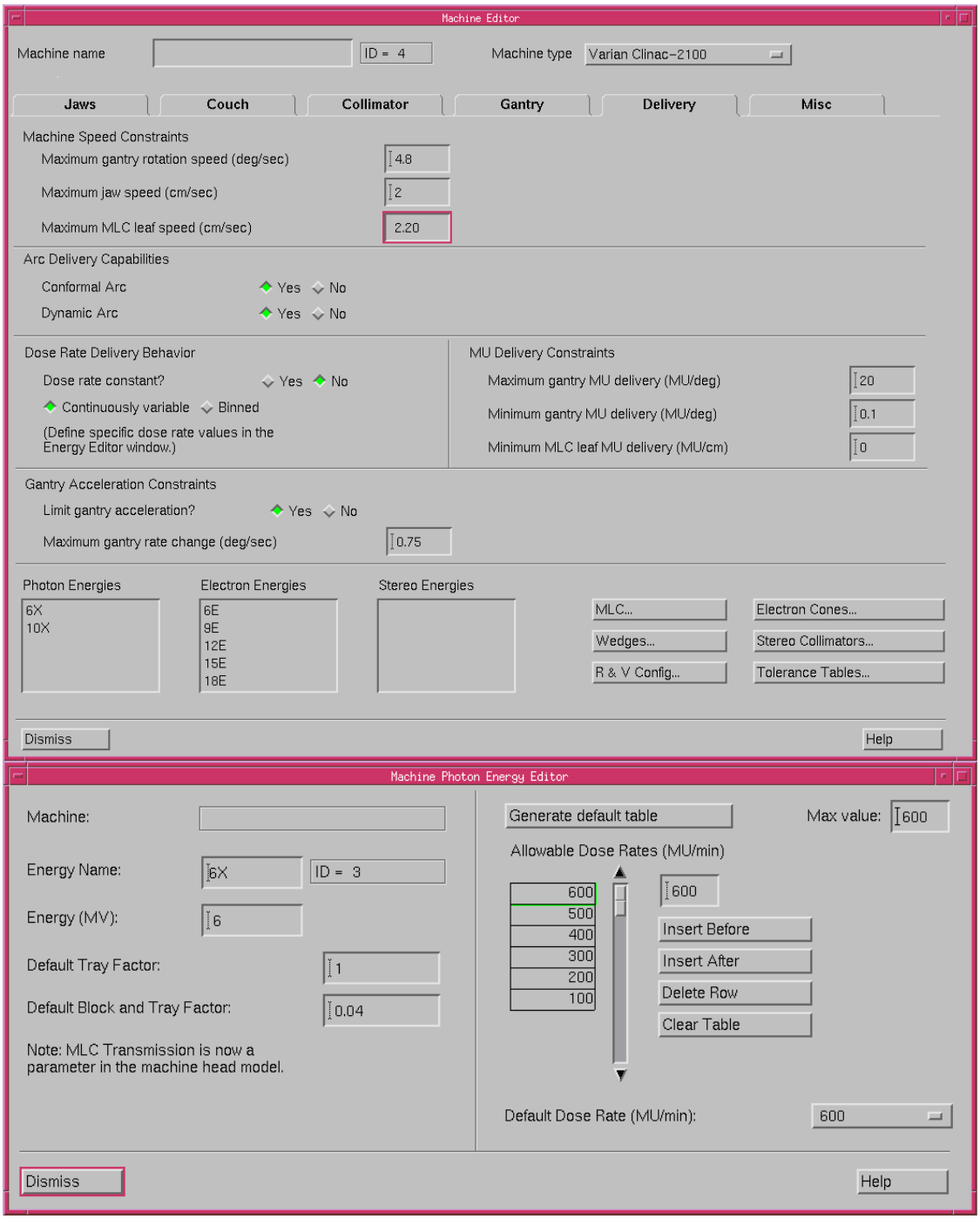

Figure 2.2 Screen shots of some or the machine characteristics that are required when setting up a machine in Pinnacle. The top image shows delivery parameters such as leaf gantry and jaw speed. The bottom image shows where the dose rates available can be modified.

Table 2.1 Definitions of optimisation objective types in Pinnacle

Objective type	Description
Max Dose	sets the desired maximum dose in a ROI; usually set with a low weight in PTVs (when combined with the Min Dose and Uniform Dose objective) and a higher weight for serial organs (e.g. spine, brainstem, optic structures)
Min Dose	sets the desired minimum dose in a ROI; used only in PTVs and usually set at 95% of the PTV's dose prescription (e.g. 57 Gy for PTV60); provides an additional control of the PTV coverage when used together with the Uniform Dose objective;
Uniform Dose	sets the desired uniform dose in a ROI; must only be used in PTVs and given the same (or comparable) weight as that of the Min Dose;
Max EUD and Min EUD	used to control hotspots, cold spots or the mean dose in an ROI; requires a parameter "a" where: i. a < 1 is appropriate for ROIs representing targets. A smaller (or more negative) "a-value" can remove cold spots; used with Min EUD ii. a = 1 corresponds to the mean dose; used with Max EUD iii. a > 1 is appropriate for ROIs representing critical structures. A larger "a-value" can remove hot spots; used with Max EUD
Max DVH	used for ROIs with maximum dose-volume constraints (e.g. $V_{50\ Gy} < 30\%$);
Min DVH	used for ROIs with minimum dose-volume constraints (e.g. $V_{95\%\ of\ Dose} > 95\%$); not often used unless the Min Dose objective is not working

In this study, the effect of the maximum dose rates and the maximum MLC leaf speed on plan quality were investigated by varying these machine settings while maintaining all the other machine characteristics mentioned earlier. The same plan parameters were applied in all the VMAT plans generated such that the length of the arc was 358°, collimator angle was set at 10°, control point spacing was 4°, and beam energy was 6 MV. Depending on the site, a single or dual arc was used with the initial arc always being counter clockwise. All arcs were attached to the same isocentre.

All regions of interest were contoured by radiation therapists and doctors. An example of the set of optimisation objectives used in the prostate and H&N plans are given in Figure 2.3.

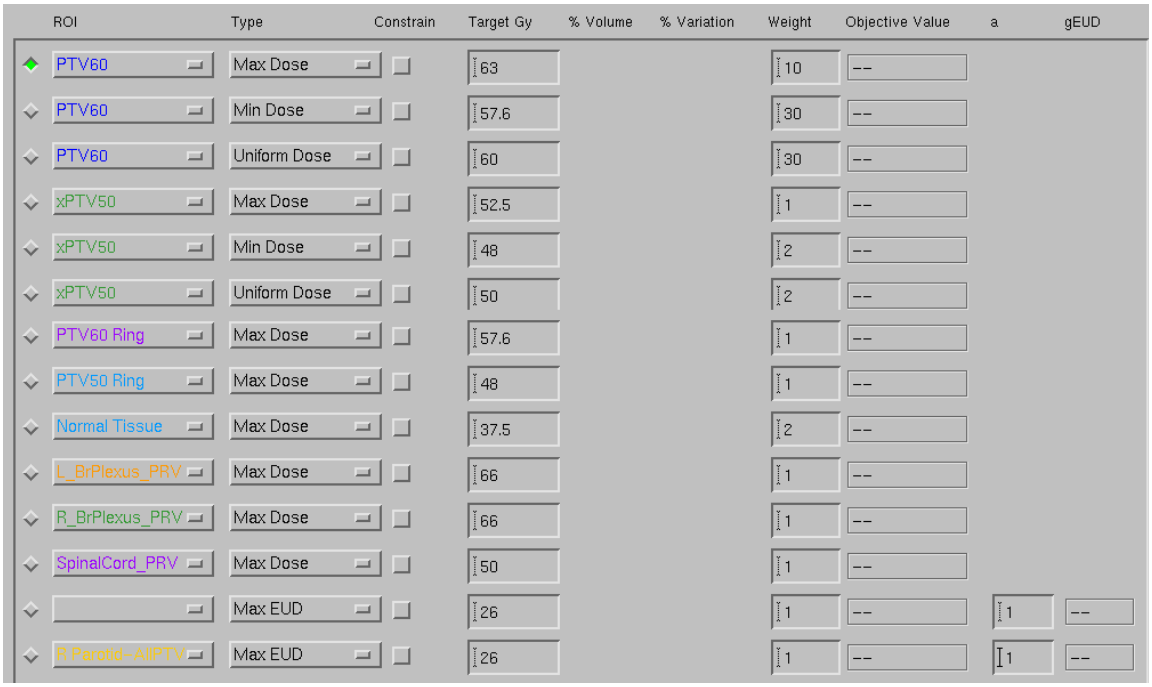

ROI	Type	Constrain	Target Gy	% Volume	% Variation	Weight	Objective Value	a	gEUD
PTV60	Max Dose		63			10	--		
PTV60	Min Dose		57.6			30	--		
PTV60	Uniform Dose		60			30	--		
xPTV50	Max Dose		52.5			1	--		
xPTV50	Min Dose		48			2	--		
xPTV50	Uniform Dose		50			2	--		
PTV60 Ring	Max Dose		57.6			1	--		
PTV50 Ring	Max Dose		48			1	--		
Normal Tissue	Max Dose		37.5			2	--		
L_BrPlexus_PRV	Max Dose		66			1	--		
R_BrPlexus_PRV	Max Dose		66			1	--		
SpinalCord_PRV	Max Dose		50			1	--		
	Max EUD		26			1	--	1	--
R Parotid - AllPTV	Max EUD		26			1	--	1	--

Figure 2.3 An example of the optimisation objectives that were used in the planning the two volume H&N site.

2.2.2 Clinical Plan Requirements

2.2.2.1 Prescriptions

The prescriptions used in the treatment plans generated for this study are summarised in Table 2.2. In our institution, the standard prescription for prostate cases is 74 Gy to the prostate planning target volume (PTV) and 65 Gy to the seminal vesicle PTV delivered in 37 fractions in a simultaneous integrated boost (SIB) plan. The same prescription doses were used in the two prostate cases that were evaluated in this study.

A prescription of 50.4 Gy in 28 fractions was applied to the single-volume nasopharynx case. On the other hand, a SIB prescription of 60 Gy and 50 Gy delivered in 30 fractions were given to the two target volumes of the oropharynx case.

Table 2.2 Prescriptions and target volumes for the cases evaluated in this study

Patient	Tumour Site	Prescription		
		Target Volume	Dose	Fractions
A and B	Prostate + Seminal Vesicle	PTV74 *(prostate)*	74 Gy	37 (SIB)
		PTV65 *(seminal vesicle)*	65 Gy	
C	Oropharynx	PTV60 *(primary)*	60 Gy	30 (SIB)
		PTV50 *(nodes)*	50 Gy	
D	Nasopharynx	PTV50.8 *(primary)*	50.8 Gy	28

2.2.2.2 Target Dose Objectives and OAR Constraints

Listed in Table 2.3 are the dose objectives for the target volumes in our prostate plan. These dose objectives are based on the ICRU83 recommended way of prescribing and evaluating IMRT (or VMAT) plans [24]. Instead of maximum or minimum point doses, the dose objectives are expressed in terms of the near maximum dose and near minimum doses, which are represented by the $D_{2\%}$ and $D_{98\%}$ dose objectives, respectively. Additionally, the minimum dose received by 50% of the target volume was also used as an evaluation metric via the reported $D_{50\%}$ dose objective. The required target doses and organ at risk doses were adapted from the CHHiP [25]. The OAR constraints for prostate treatments are given in Table 2.4. Some constraints differ from those specified in the clinical trial, they were instead set to reflect the expectations developed from what was achieved in previous patients within our centre.

Table 2.3 Dose objectives for target volumes in prostate plans

Target volume	Dose Objective
CTV *(prostate)*	$D_{98\%} \geq 98\%$ of prostate prescription
	$D_{2\%} \leq 101\%$ of prostate prescription
PTV *(prostate or seminal vesicle)*	$D_{98\%} \geq 96\%$ of prescription
	$D_{2\%} \leq 101\%$ of prescription
	$D_{50\%}$ for reporting *(Ideally equal to the PTV prescription dose)*

Table 2.4 Dose constraints for organs at risk in prostate plans

Organs at risk	Dose Constraint
Rectum	$V_{40Gy} \leq 60\%$ $V_{60Gy} \leq 30\%$ $V_{70Gy} \leq 15\%$ $V_{74Gy} \leq 3\%$ D_{mean} for reporting $D_{2\%}$ for reporting
Bladder	$V_{50Gy} \leq 50\%$ D_{mean} for reporting $D_{2\%}$ for reporting
Femoral head	$V_{50Gy} \leq 50\%$ D_{mean} for reporting $D_{2\%}$ for reporting
Urethral bulb	$V_{70Gy} \leq 20\%$ $D_{2\%} \leq 71$ Gy D_{mean} for reporting
Intra-prostatic urethra	$V_{75\ Gy} \leq 10\%$
Extra-prostatic urethra	$V_{72\ Gy} \leq 10\%$
Global maximum dose	$D_{max} < 103\%$ of highest PTV prescription

Listed in Table 2.5 are the target volumes dose objectives for the H&N using the near-minimum and near-maximum dose in conjunction with $V_{100\%}$, $V_{95\%}$, D_{max} and $D_{50\%}$. The dose constraints applied to the OARs (Table 2.6) are based on the recommendations from the Quantitative Analyses of Normal Tissue Effects in the Clinic (QUANTEC) [26] and have been scaled to reflect the dose fractionation schemes that were delivered.

Table 2.5 Dose objectives for target volumes in head and neck plans.

Target volume	**Dose Objective**
GTV	$V_{100\%\ of\ Presc.} \geq 100\%$
PTV	$V_{95\%\ of\ Presc.} \geq 95\%$ $D_{max} \leq 110\%$ of prescription $D_{98\%} \geq 92\%$ of prescription $D_{2\%} \leq 101\%$ of prescription $D_{50\%}$, D_{mean} for reporting *(Ideally equal to the PTV prescription dose)*

Table 2.6 Dose constraints for organs at risk in head and neck plans

Organs At Risk	Dose Constraint	
	Oropharynx (2Gy/fr)	Nasopharynx (1.8Gy/fr)
Spinal cord	D_{max} < 39 Gy	D_{max} < 32 Gy
Spinal cord PRV	D_{max} < 43 Gy	D_{max} < 36 Gy
Brainstem	D_{max} < 46 Gy	D_{max} < 39 Gy
Brainstem PRV	D_{max} < 51 Gy	D_{max} < 43 Gy
Eyes	D_{max} < 43 Gy	D_{max} < 36 Gy
Lens	D_{max} < 7 Gy	D_{max} < 6 Gy
Optic nerve	D_{max} < 43 Gy	D_{max} < 36 Gy
Optic nerve PRV	D_{max} < 46 Gy	D_{max} < 39 Gy
Chiasm	D_{max} < 43 Gy	D_{max} < 36 Gy
Chiasm PRV	D_{max} < 46 Gy	D_{max} < 39 Gy
Cochlea	D_{max} for reporting	D_{max} for reporting
Temporal lobe	D_{max} < 60 Gy $V_{56Gy} \leq 1\%$	D_{max} < 50 Gy $V_{46Gy} \leq 1\%$
Parotid	D_{mean} < 22 Gy $V_{26Gy} \leq 50\%$	D_{mean} < 19 Gy $V_{21Gy} \leq 50\%$
Sub-mandibular gland	D_{mean} for reporting	D_{mean} for reporting
Lips	D_{mean} < 17 Gy	D_{mean} < 14 Gy
Oral cavity *(vol. outside PTV)*	D_{mean} < 26 Gy	D_{mean} < 21 Gy
Pharynx *(vol. outside PTV)*	D_{mean} < 39 Gy $V_{43Gy} \leq 33\%$ $V_{51Gy} \leq 15\%$	D_{mean} < 32 Gy $V_{36Gy} \leq 33\%$ $V_{43Gy} \leq 15\%$
Glottic and supra-glottic larynx	D_{mean} < 17 Gy	D_{mean} < 14 Gy
Oesophagus	D_{mean} < 26 Gy	D_{mean} < 21 Gy
Brachial plexus	D_{max} < 57 Gy	D_{max} < 47 Gy
Brachial plexus PRV	D_{max} for reporting	D_{max} for reporting
Mandible *(whole)*	D_{max} < 60 Gy $V_{57Gy} \leq 1\%$	D_{max} < 50 Gy $V_{47Gy} \leq 1\%$
Mandible *(left or right)*	D_{max} < 60 Gy $V_{57Gy} \leq 1\%$ V_{43Gy} for reporting	D_{max} < 50 Gy $V_{47Gy} \leq 1\%$ V_{36Gy} for reporting

2.2.3 VMAT Plan Parametric Survey

This research investigated the effect of maximum MLC leaf speed and the effect of the maximum dose rate settings in Pinnacle on the quality and deliverability of treatment plans created with these settings. Our planning system was according to the manufacturers recommendations; part of which was to limit the gantry acceleration when a Varian linac is used in combination with Aria record and verify system. This means that the option to constrain leaf motion cannot simply be turned on and off while planning. As a result, an entirely new machine with a specified constraint for leaf motion had to be setup in the TPS. This was done by duplicating one of our current treatment machines that are capable of VMAT treatment (they are all beam matched and have the same physical components as well as beam model within Pinnacle). Using this template, all machine settings were left unchanged, except for those which were related to the leaf speed or dose rate.

The range of MLC maximum leaf speeds chosen for this work was 2.20 cm/s (full speed), 1.93, 1.65, 1.10, 0.70, 0.60 and 0.55 cm/s (25% of full speed). This range of values provided a good spread of leaf speeds, with the lower limit being a condition where there was significant detriment to the plans efficiency in terms of delivery time and/or plan quality.

The range of dose rates that were available for study was limited by the input into the Varian linacs. The system required the maximum dose rate to be a multiple of 100 MU such that it could be match to a preset value; without this match delivery would not be possible. Since our linacs are used clinically, this requirement on the dose rate setting cannot be modified for the purpose of this research.

One of the reasons for using VMAT was to accelerate delivery times compared to other techniques. Therefore, the lower limit for the dose rate for each site was set to ensure that the estimated delivery times for treatment plans were not significantly increased. This resulted in two different lower limits between the two sites evaluated, the single arc treatments were modulated down to a maximum of 300 MU/min, the H&N plans were allowed to have a dose rate setting of 200 MU/min.

For each site a plan was generated using the standard machine characteristics so that the objectives and weights produced the optimal plan. These same parameters were applied to produce new plans using the restricted machine characteristics. From heron, these plans are referred to as plans with ‘original objectives’. An additional plan was made using the restricted characteristics where the objectives and weights were re-optimised to achieve an optimum plan. From heron, these plans are referred to as plans with ‘re-optimised objectives’.

2.3 Planning Analysis

In this section the tools and methods used in the analysis of the plans will be described. The analysis is done using the dose volume histogram (DVH) data from Pinnacle which is used to assess the quality of the plans as well as the dose conformity and homogeneity in the target volumes. In addition to what is described here, the physical characteristics of the plans were also extracted from Pinnacle for analysis and are presented in sections 3.1.1 and 3.2.1.

2.3.1 DVH Analysis

In our clinic, IMRT plans are evaluated based on in-house assessment sheets that are designed as an aid to the analysis of DVH data. The DVH data of the regions of interest (both targets and OAR) are exported from Pinnacle and read into an in-house spreadsheet which calculates the dose requirement for that region (i.e. $D_{x\%}$ or $V_{x\ Gy}$) then compares it to our generic dose reporting goal. A pass or fail is indicated depending on whether the dose goals and constraints were achieved or not. This sheet is a generic document and does not take into account the tumour location with respect to OAR. It is a useful tool in providing a quick source of information as to what areas of the plan required more investigation when assessing the quality of the treatment plan and its clinical acceptability. In this project it was used during the planning process in combination with the DVH plots to indicate where the plan was failing to meet the constraint and where compromises could be made to ensure the optimal plan was produced.

2.3.2 Plan Quality Score

Our clinical protocol requires each plan to be checked by a clinician prior to treatment to sign off that it is clinically acceptable. This is not practical for this study due to time requirements of the clinicians, this method would also have been prone to both inter-observer and intra-observer variation when assessing and ranking plan quality. To allow for a more objective and quantifiable quality comparison, a plan quality score sheet was developed as a surrogate to approximate the clinicians' judgement using the DVH information.

A quality score sheet was made for each patient individually with the assistance of experienced clinicians. Each clinician was shown the contoured CT data set specific to their area of expertise and asked to rate the importance of each target volume and OAR dose objective on a scale of 1-10 (10 being most important). They were requested to only take into account the specific geometry of that individual patient anatomy as it was not going to be used for any other patient. In addition to the importance of each dose objective the clinicians were also requested to provide a tolerance (if any) that they would accept if that objective could not be achieved.

A scoring system for the plan quality was developed using the score given to the importance (from here on called the objectives "weighting") and the tolerance for each dose objective. If a dose objective was met, points were given equal to the weighting of that objective. If the plan failed to meet the objective then points were assigned based on the objectives weighting and the ratio of the tolerance to the amount that the plan failed to meet the objective. The extent to which the weighting was reduced was broken into two gradient segments as shown in Figure 2.4. If the ratio was less than 0.5 then the points assigned would be reduced by up to a third; if the ratio was between 0.5 and 1.0 then the points would be reduced proportional to the remaining 2/3; if the ratio was more than 1.0, zero points were assigned to the dose objective. The final plan quality is the sum of all the points for a plan normalised to the score of the plan created using the clinical machine parameters. For a detailed list of the weightings applied to the ROI for each site see Appendix A.

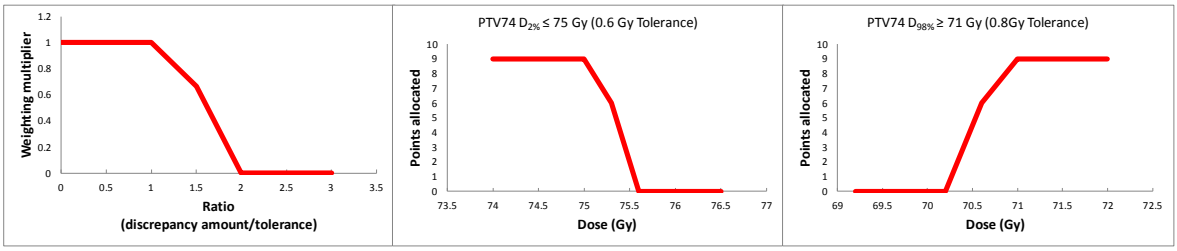

Figure 2.4 Template and example of how points were allocated in the Plan Quality score sheet. The left image is a general example with normalised volume, the middle plot displays the points allocation scheme for $D_{2\%} \leq 75$ Gy and the right image shows the points allocation scheme for $D_{98\%} \geq 71$ Gy.

2.3.3 Conformity and Homogeneity

The Conformity index (CI) and Homogeneity Index (HI) were determined individually for each of the prescribed PTVs using the DVH data exported from pinnacle. The CIs were calculated from the formula proposed by van't Riet et al.[27].

$$CI = \frac{TV_{RI}}{TV} \times \frac{TV_{RI}}{V_{RI}} \quad (1)$$

Where CI is the conformity index, TV_{RI} is the target volume covered by reference isodose (RI), TV is the target volume, V_{RI} is the volume of the reference isodose and RI was defined as 95% of the prescribed dose to that PTV. The first term in the equation defines the quality of the coverage of the target, while the second term defines the volume of healthy tissue exposed to the reference isodose or greater.

The definition of HI was taken from Yoon et al.[28] and is given by

2

$$HI = D_{SD} = \sqrt{\sum (D_i - D_{mean})^2 \times \frac{v_i}{V}}$$

This equates to the standard-deviation of the *d*DVH of the ROI. Where HI is the homogeneity index, D_{SD} is the standard deviation of the dose to the ROI, D_i is the dose D_{mean} is the mean dose to the ROI, V is the volume of the ROI and v_i is the bin size for the *d*DVH data.

In the analysis of CI and HI the PTV that was prescribed the largest dose, $TV_{95\%}$, TV and $V_{95\%}$ were defined based on its actually contoured volume. For the plans with two PTVs a new volume was created for analysis of the PTV with a lower prescription (Figure 2.5). The new volume was created by combining the lower prescription PTV and a 3 mm expansion of the PTV with the larger prescribed dose. This was used to define the TV and $TV_{95\%}$ while the $V_{95\%}$ remained as the volume of the 95% isodose of the second PTV. This was done as the lower PTV conformity would not have been correctly represented in the presence of a volume with a higher prescription. The 3 mm margin was selected based on the observed dose fall off gradient in the initial patients' plans.

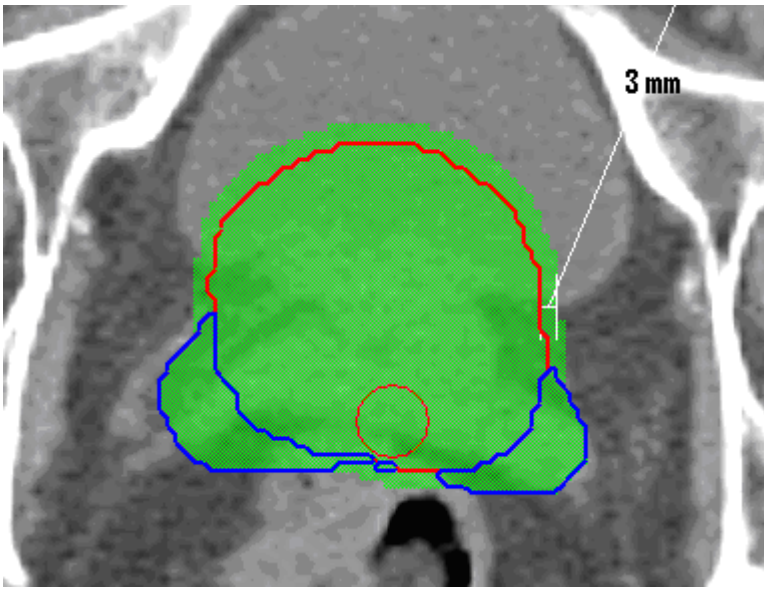

Figure 2.5 An example of the new volume used in the analysis of the conformity and homogeneity of PTV65 in a prostate case where two target volumes were present. The green shading is the new volume, the blue line defines the edge of PTV65 and the red line defines PTV74.

2.4 Plan Quality Assurance

QA is an important part of any radiation therapy and it takes on a more important role when a complex treatment modality such as IMRT or VMAT is used. It is considered best practice to conduct patient specific QA on all patients prior to their initial treatment to ensure that the dose distribution of the treatment we are intending to deliver to the patient is correct. This adds an extra layer of safety to treatments reducing the risk of an error which could compromise the patient's treatment. This section will cover the equipment and procedures that were used in the QA measurements and analysis.

2.4.1 QA Equipment

The equipment that was used to perform QA is a Varian iX model linac with a 120-leaf millennium MLC, an ArcCHECK™ device (Sun Nuclear, Melbourne, FL) in combination with SNC Patient V6.1.3 (Sun Nuclear, Melbourne, FL) and an Iba CC04 ionisation chamber attached to a NE 2570/1 electrometer.

The ArcCHECK device (Figure 2.6) is a diode array designed to measure the 3D dose or the dose fluence patterns in radiation therapy. It consists of 1386 SunPoint™ 0.8 x 0.8 mm diodes arranged in a helical array with 1 cm spacing in both the radial and longitudinal planes. It has 3.2 cm of water equivalent build-up and was used with the CavityPlug™ (Sun Nuclear, Melbourne, FL), which is constructed of PMMA as an additional core designed to house a 0.4 CC cylindrical chamber. ArcCHECK has been shown to be suitable for the assessment of patient specific plan QA [15,16]. It should be noted that all ArcCHECK analysis papers point out that there is a directional dependence of the diodes but this is only significant when the beams cross the diodes at large angles which occur when laterally large fields are used. This is not a problem in the typical clinical setting nor is it a problem for the geometries or field sizes required in this thesis; it is also compensated for in the analysis software to further reduce the error.

ArcCHECK was used in combination with SNC Patient software. SNC Patient is designed to work with the Sun Nuclear products, its principal function is to compare measured dose distributions to ones that have been exported from the user's TPS. It has a variety of corrections and interpolation methods that are applied to the measurement points that can be used in the interpretation of results. It is capable of not only comparing the overall dose distribution but also to make comparisons of the dose delivered at each control point.

An Iba CC04 ionisation chamber in combination with a NE 2570/1 electrometer was used to measure the dose at isocentre. This chamber has an application range of 100 kV-50 MV, an

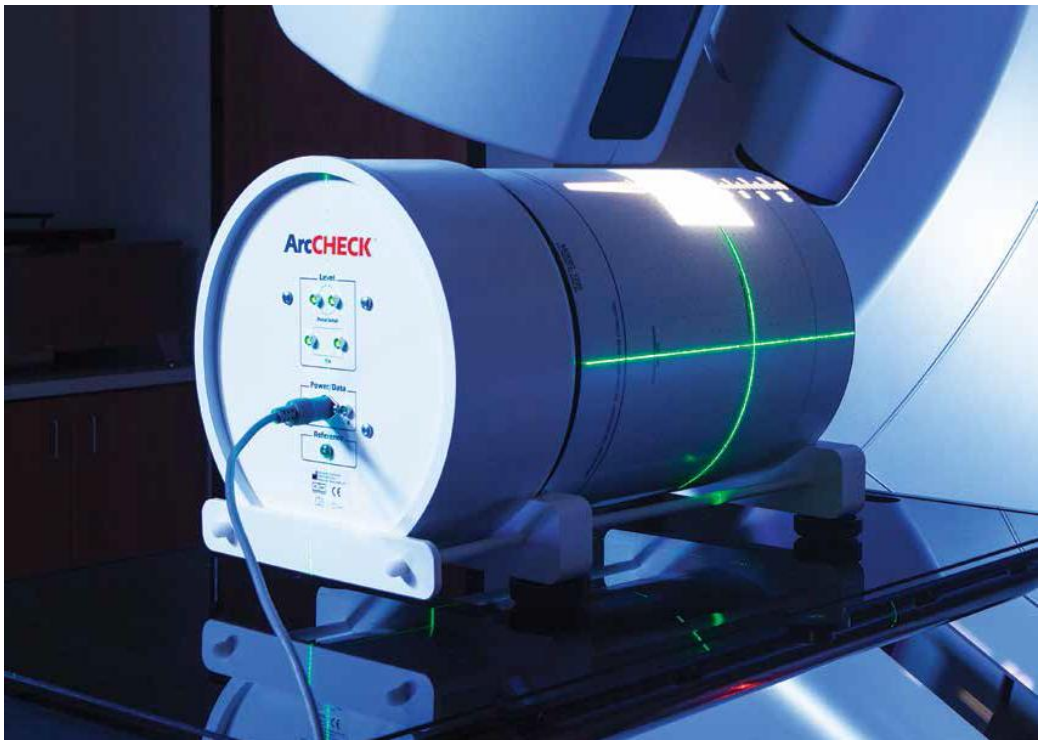

Figure 2.6 ArcCHECK, reproduced from Sun Nuclear Corporation promotional material

active volume of 0.04 cm^3 with a recommended polarising voltage applied of 250 V and sensitivity of approximately 1.10 $x10^{-9}$ C/Gy.

2.4.2 QA Preparation and Delivery

The QA measurements used in this thesis were adapted from out clinical protocol. Dose comparisons between planned and delivered treatments were performed by copying the optimised plans onto a CT image dataset of the ArcCHECK device with a solid Perspex core positioned correctly on the couch with a new set of couch contours. All patient-related density overrides were removed. The density of the volume of the ArcCHECK device was overridden to 1.18 gm/cm^3 [29]. The beams were attached to the ArcCHECK centre and a dose calculation was performed using a 3 mm grid that covered the entire ArcCHECK volume.

The point dose at the ArcCHECK centre was recorded for the total number of fractions prescribed before the prescription was changed to a single fraction then the final overall dose distribution, the dose per CP distributions and RT plan DICOM was exported.

As some of the machine characteristics had been modified in the TPS, they no longer matched what the Aria record and verify system expected based on its initial setup, this meant the plans had to be delivered using the DICOM RT mode of the Aria system. An in-house MATLAB code was used to modify the metadata of the exported plan files to allow the plans to be delivered in the DICOM RT mode without requiring processing through the normal clinical pathway of using Aria RT chart. It had been verified during the commissioning of our

VMAT treatments that this code does not alter the plan in any other way. By using the DICOM RT delivery pathway it avoids the need to perform any machine overrides which would have invalidated some of the restrictions applied in the TPS.

2.4.3 QA Delivery Procedure

An accurate setup of the QA equipment is essential to ensure the accuracy of the measurements. Our VMAT QA regimen also guarantees that the measurements are reproducible. In our centre VMAT QA is conducted at predefined longitudinal and lateral couch position. This is done so that the couch, which thickness varies along its length, can be accurately modelled in the TPS. Lateral lasers and the optical field from the linac are aligned with the reference marks on the ArcCHECK, to make sure that the centre of ArcCHECK is at the machine isocentre. A CC04 ionisation chamber is inserted into the ArcCHECK such that it is located at isocentre.

Once the ArcCHECK and ionisation chambers are in position, a calibration needs to be performed on the ion chamber before any measurements are taken to compensate for machine output fluctuations.

The ArcCHECK array dose also needs to be calibrated prior to measurements commencing. This is done using a 200 MU of a 6 MV beam at a field size of 10 cm ×10 cm. This is expected to deliver a dose of 237.6 cGy to the central diode on the anterior section of the array. This was checked regularly throughout the course of measurements to ensure that it was consistent over the entire day whilst measurements were being conducted. The same field was also used to determine the ratio between the ionisation chamber output and the theoretical dose to isocentre for that beam, which was used to determine the dose that has been measured by the ionisation chamber.

Each treatment plan was delivered without interruption while recording the delivery statistics, fluence patterns from the ArcCHECK, point doses and MLC positioning using the Dynalog data.

2.4.4 QA Analysis

The analysis of the QA measurements were done in a variety of ways. The dose fluence maps acquired with ArcCHECK were analysed through the SNC Patient software. The results of the point dose measurements and beam delivery parameters (i.e., beam on time, Standard Deviation Values (STDV) of both MU and gantry angle) were analysed using polynomial regression, while MLC positional errors were evaluated using a simple statistical analysis of the Dynalog data.

2.4.4.1 Point Dose

The point dose to the isocentre was converted to absolute dose in Gy by taking the ratio of the raw chamber reading for the treatment delivery to the reference beam (200 MU, 10 × 10 fields) and multiplying this by an appropriate conversion factor. Using this value a dose comparison was able to be made between the expected and delivered point doses and the percentage difference was determined.

2.4.4.2 Delivery Parameters

The actual delivery times were compared to the TPS predicted delivery times to confirm the accuracy of the latter. The STDV of the discrepancy between true gantry position and expected position and the STDV of the delivered MU at the check points and the planned MU were also recorded for each treatment delivery.

2.4.4.3 ArcCHECK Dose Fluence

The measurements were analysed using the SNC Patient software where a comparison was made between the expected dose distribution which were calculated by the TPS and the recorded measurements from the actual beam delivery on the linac (Figure 2.7). A comparison was made of the overall treatment's dose fluence map. They were analysed using 3%/3 mm, 2%/2 mm and 1%/1 mm gamma analysis criteria to observe the changes shown for a complete treatment. A 10% dose threshold and Van Dyk correction was applied to the data. Furthermore, a 3D model was selected for the DTA analysis. The 3%/3 mm and 2%/2 mm gamma analysis criteria represent what is used to analyse the quality and delivery accuracy of our clinical treatment plans. The same criteria was chosen for this study to determine how clinically relevant or detectable the effects of the MLC speed and dose rate constraints on the plans are.

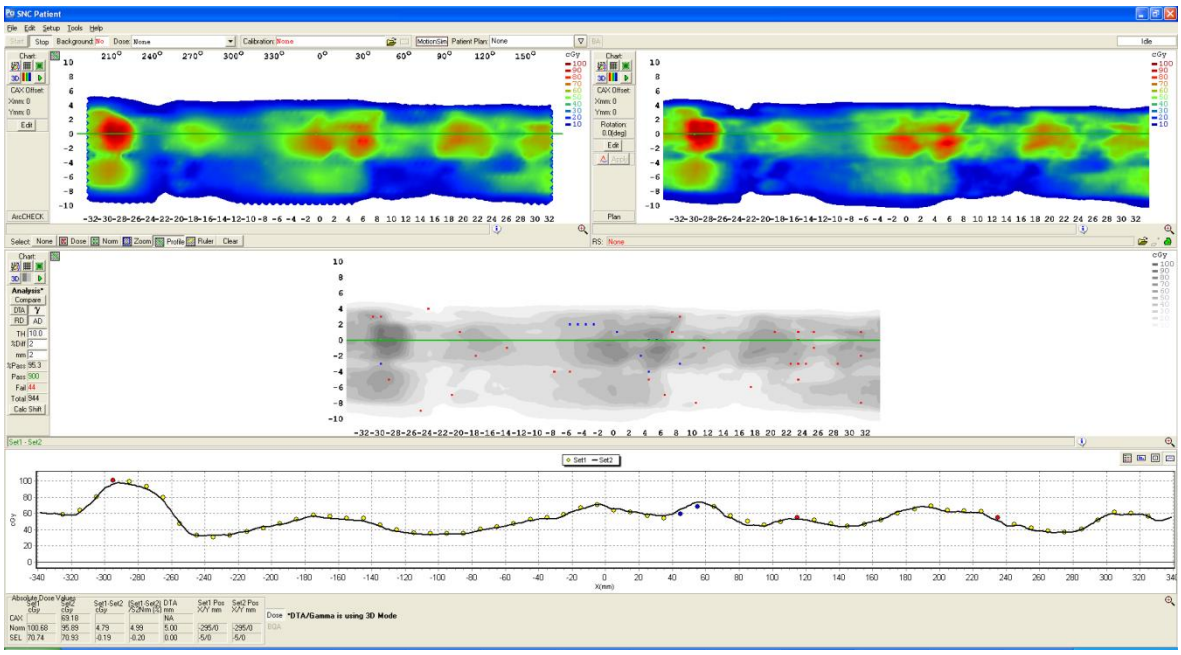

Figure 2.7 Example of the SNC Patient software analysis of a H&N plan delivery using a 2%/2 mm gamma. The top row shows the measured data on the left and expected on the right, the middle plot shows the comparison highlighting the failed points and the bottom plot is the dose profile of the line shown in the other images.

2.4.4.4 ArcCHECK CP Fluence

The SNC software allows a comparison of predicted and measured dose at each control point through its CP analysis function. This requires the expected dose distribution exported from the TPS to be separated into CPs and the ArcCHECK measurements to be recorded in a movie format. All individual CP data analysis was performed using the absolute dose mode and the same gamma criteria that were used in the analysis of the overall dose fluence in the previous section.

SNC produces a plot (Figure 2.8) that graphically shows the number of measurement points that passes and fails the gamma criteria for each CP as a percentage. Each segment represents a CP and its location within the circle shows its position within the arc. The red and blue stacks in each segment represent the percentage of points within the field that did not meet the gamma criteria. The percentage of points that are colder than the predicted dose are given in blue and the percentage that are hotter than the expected dose are given in red. The green section shows the percentage of points that pass. The data in the "Current Dose Difference Result" box midway down on the left side of Figure 2.8 can also be exported along with the rest of the CPs numeric dose difference results. These numeric values were tallied per plan based on the percent of points which failed to meet the gamma criteria, using the following ranges: 10-19.99%, 20-29.99% and above 30%.

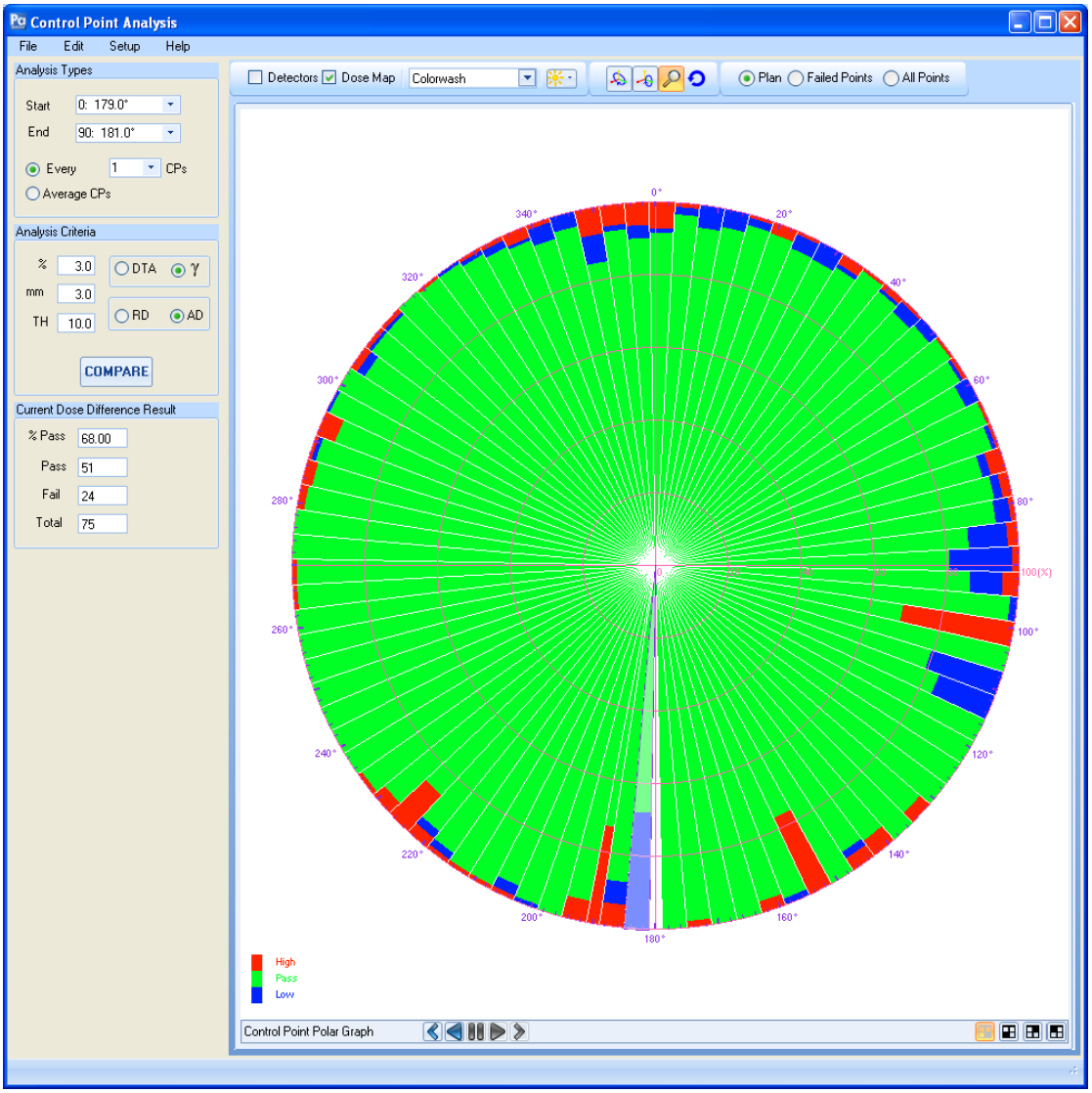

Figure 2.8 Plot from the CP analysis of a VMAT delivery analysed using a 3%/3 mm gamma criteria. Each section represents a CP, the magnitude of the colours show the percentage of the detection points in the field exposed that either pass or fail. Green represent passing the gamma criteria, red and blue represent points failing the gamma criteria above and below respectively.

2.4.4.5 Dynalogs

Dynalog files are a record data produced by the Aria record and verify system that contain the position of the collimator jaw, the gantry angle, and the position of each MLC leaf as well as their planned initial, final and predicted position for a particular time interval (note this interpolation is done at delivery and not in the TPS). All this information is recorded every 50 ms and is stored at the end of the treatments.

The raw Dynalog files were processed using an in-house MATLAB code. This code produced error histograms to allow the observations of any variation in the distribution of the MLC leaf position errors between the plans.

3. Results and Discussion

This chapter is divided into two major sections detailing the results when either the maximum MLC speed or the maximum dose rate is constrained. Each section covers the analysis of the treatment plans produced in terms of the plan characteristics, the conformity, homogeneity and the overall plan quality. The delivery of each treatment was analysed to investigate how the delivery statistics, point dose comparison, dose fluence, CP dose fluence and Dynalog results were affected by the restricted parameter. Wherever appropriate the data was analysed using a statistical polynomial regression, from linear relationship up to a fourth order polynomial to identify correlation and establish trends. The suitable trend for each set of data was determined based on the correlation coefficient (r^2), the statistical significance of r^2 in terms of its p-value and the statistical significance of the improvement in r^2 at higher order polynomial fit. Figure 3.1 provides an example of the analysis of MU per fraction for patient B. The correlation coefficient increases as the polynomial order increases, but improvements in the r^2 are shown to have poor statistical significance meaning that this improvement is likely due to chance. Therefore, in Figure 3.1, the best fit to the change in MU relative to the maximum MLC speed would be a linear fit.

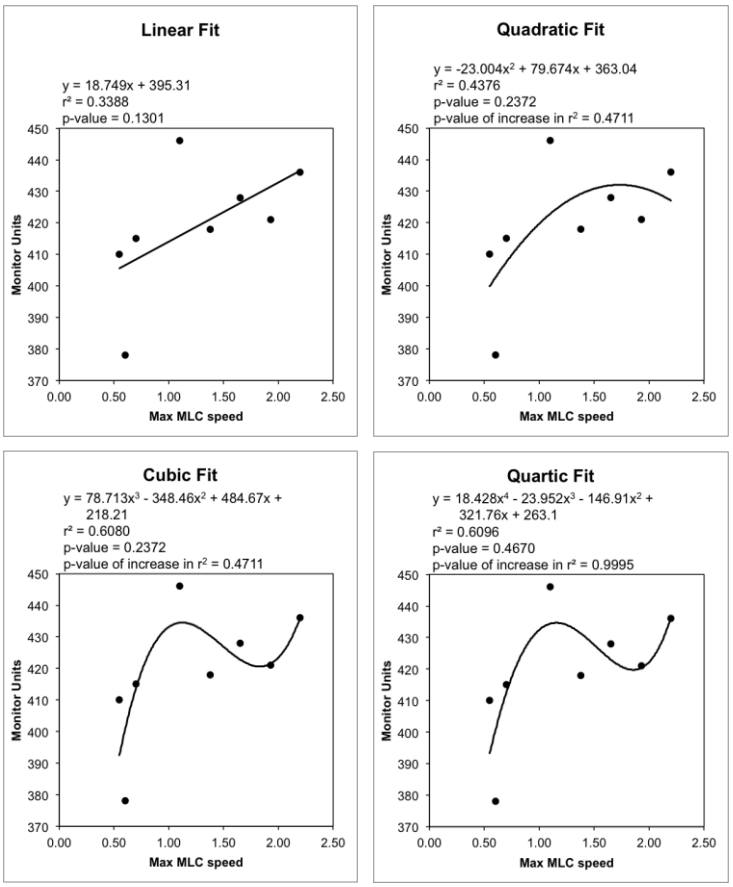

Figure 3.1 An example of the test for correlation between the maximum MLC speed and the treatment plan monitor units. Linear and polynomial regression was applied to the data obtained in order to determine the best function that described the relation between these parameters.

3.1 Effect of MLC Leaf Speed Constrains on VMAT Plans

3.1.1 Plan Characteristics

In this section the characteristics of the plans will be analysed and discussed. Complete tables of all the characteristics mentioned in this section as well as the conformity and homogeneity data can be found in Appendix B.

3.1.1.1 Monitor Units

Shown in Figure 3.2 are the variations in MU with respect to the maximum MLC speed allowed for plans generated for the prostate and H&N cases evaluated in this study. The MU for the plans created using the same objectives as the clinically approved plan and the re-optimised plans are both shown in Figure 3.2.

Plans for both prostate cases, given in Figure 3.2a and 3.2b, exhibited higher MU as the maximum allowed MLC speed was increased. A difference of about 80 MU and 90 MU between the plans with the smallest and largest maximum MLC speed allowed was obtained from prostate patients A and B, respectively. A smaller variation and a less consistent pattern in the change in MU, with respect to the maximum MLC speed allowed, can be seen in the H&N plans, as shown in Figure 3.2c and 3.2d. In the nasopharynx case (Figure 3.2c), a monotonically increasing MU was obtained for the plans which were calculated with the original optimisation objectives at increasing maximum MLC speeds. The re-optimised plans, however, resulted in a smaller range of MU variation and a less obvious dependence of MU on the maximum MLC speed allowed. Similar trends can be seen for the oropharynx case in Figure 3.2d.

Polynomial regression analysis of the data in Figure 3.2 showed that the MU and the maximum MLC speed allowed can best be described by a linear relationship between these two parameters. For patient A, a correlation coefficient of 0.829 (p-value = 0.001) was obtained for the plans generated from the original planning objectives and 0.642 (p-value = 0.018) for the re-optimised objective plans, indicating a dependence of the plan MU on the maximum MLC speed allowed. Patient B had a correlation coefficient of 0.314 (p-value = 0.116) for the original objective plans and 0.567 (p-value = 0.031) for the re-optimised objective plans. For this patient, only the re-optimised plans indicated a dependence of the MU and the maximum MLC speed allowed. For patient C the plans that indicated dependence were the opposite of patient B. The plans using the original objectives had a correlation coefficient of 0.798 (p-value = 0.001) while the correlation coefficient of the re-optimised plan was 0.014 (p-value = 0.780). The final patient, patient D, appeared to have

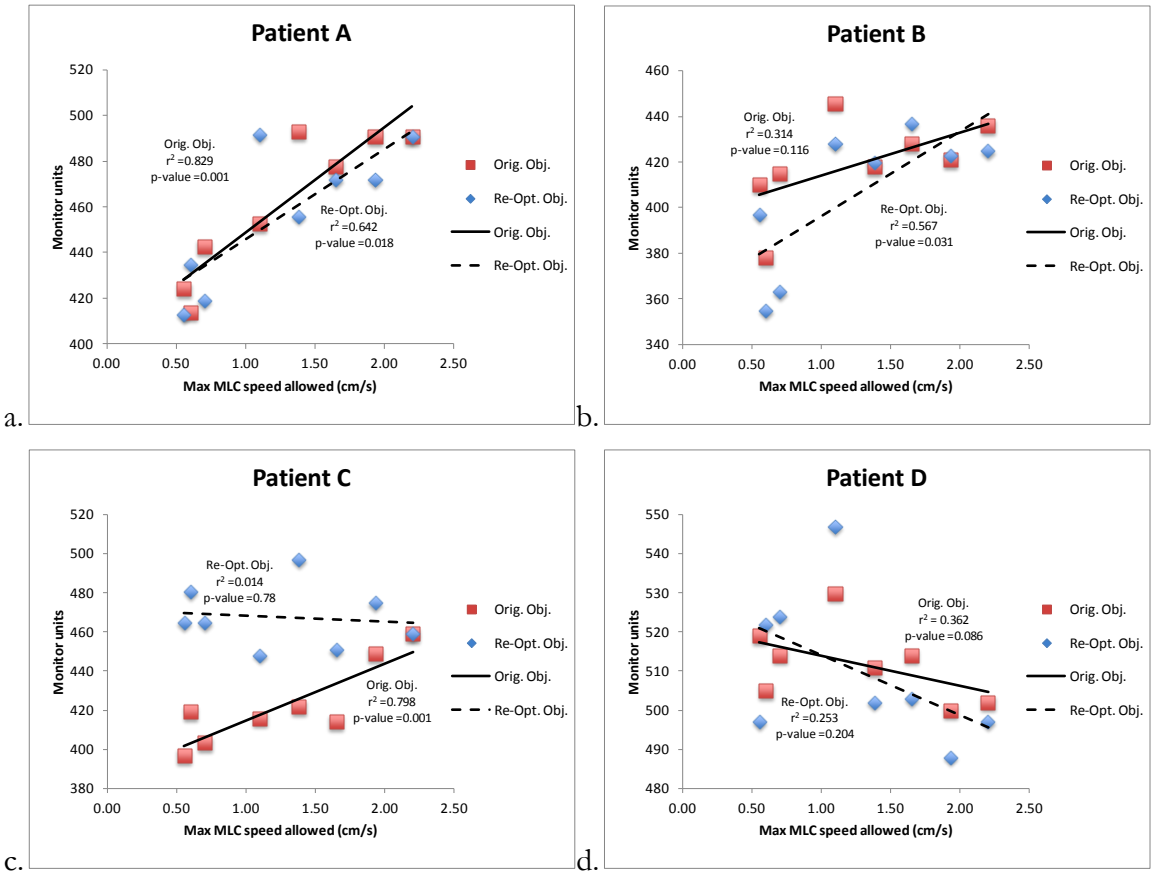

Figure 3.2 Variation in the MU per fraction with respect to the maximum MLC leaf speed allowed in planning. The MU required for each plan for prostate (Patient A, Patient B) and H&N (Patient C, Patient D) cases are given.

no correlation in either the plans from the original or the re-optimised objectives, producing correlation coefficients of 0.362 (p-value = 0.0864) and 0.253 (p-value = 0.204) respectively.

In the treatment of the prostate site using a single arc it can be seen that the lower the maximum MLC leaf speed the less MU required. This could be caused by a reduction in modulation that can be achieved in the plan. By restricting the leaf speed the ability of the leaves to move quickly and produce small fields to smooth out doses is reduced. However the trend of a lower number of MU per fraction with lower maximum MLC leaf speed is not clearly observed in the H&N sites. These sites require dual arcs to ensure that the dose to the OARs is minimised. This provided twice the number of CPs to the TPS when it is optimising the plan. The higher number of modulation points could be why the effect is so minimal. The amount of modulation that can be done is proportional to the number of control points and machine parameters. If the number of available CPs exceeds what is required to achieve the optimisation objectives, then the additional (non-essential) CPs only serve to improve the accuracy of the calculated dose distribution (by reducing the beam spacing)[18] and not the quality of the plan. If the machine characteristics are changed (i.e., maximum MLC leaf speed restricted) the non-essential CPsmay provide enough additional modulation points to allow

the TPS to produce a plan that can still meet the optimisation objectives therefore showing minimal effect.

3.1.1.2 Estimated Delivery Times

The variation in calculated delivery times with respect to the maximum leaf speed are shown in Figure 3.3 for plans generated for the prostate and H&N sites that were evaluated in this study. Each plot in Figure 3.3 displays the set of plans generated using the original objectives and plans created with re-optimised objectives.

The delivery times for the single arc treatment decreased as the maximum leaf speed was increased. The maximum difference between the shortest and longest delivery time was 0.08 minutes and 0.07 minutes for patients A and B respectively as shown in Figure 3.3a and b. The H&N sites also had lower estimated delivery times for the faster leaf speeds, although the difference was significantly less. The times required to deliver both arcs were 2.49-2.51 min and 2.49-2.52 min for patients C and D respectively, meaning the total variation in these plans is around 1%. The data distribution and small range in Figure 3.3c and d make any dependence less likely.

The polynomial regression analysis of the data shown in Figure 3.3 indicated that the best function to describe any correlation was a linear relationship. Both the original objectives and re-optimised objectives of patient A indicated some level of correlation between estimated delivery time and maximum MLC speed, giving correlation coefficients of 0.605 (p-value = 0.014) and 0.732 (p-value = 0.007), respectively. The analysis of patient B indicated correlation ($r^2 = 0.645$, p-value = 0.017) for the plans with re-optimised objectives, this was in contrast to the plans which were generated using the original objectives which appear to have no correlation ($r^2 = 0.390$, p-value = 0.0721). Neither of the H&N patients appeared to show correlation with correlation coefficients of 0.182 (p-value = 0.292) and 0.257 (p-value = 0.200) for patient C plans with original and re-optimised objectives respectively, and patient D gave 0.390 (p-value = 0.0720) and 0.437 (p-value = 0.0789) respectively.

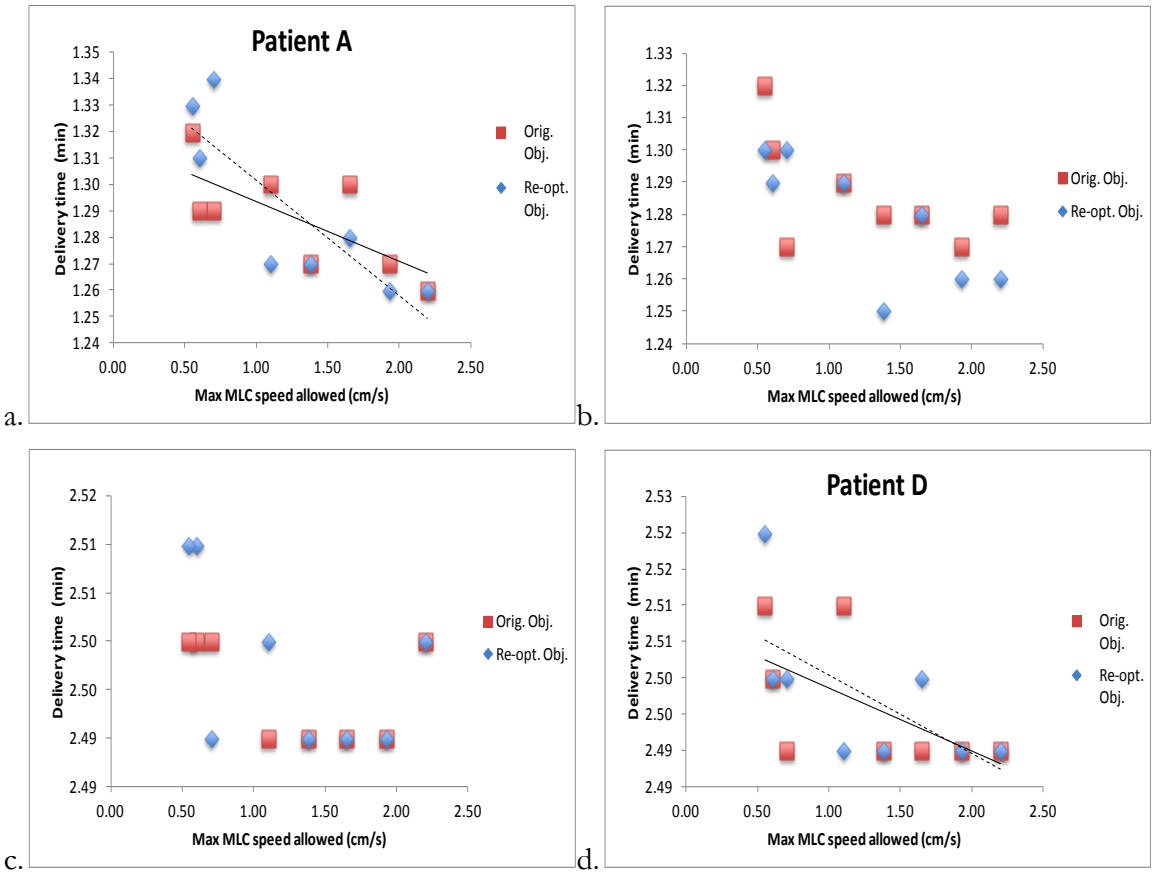

Figure 3.3 Variation in the estimated delivery time with respect to the maximum MLC leaf speed allowed in planning. The delivery time required for each plan for prostate (Patient A, Patient B) and H&N (Patient C, Patinet D) cases are given.

The trend for the prostate treatments, where a single arc is used, indicated correlation between the estimated delivery time and the maximum MLC leaf speed in three of the four cases. This implies that in order to allow the leaves to travel to the required position, the gantry rotation needs to be slowed. This would also mean that the changes in leaf position that require the gantry to slow are essential to achieving planning objectives and cannot be replaced with an alternative leaf sequence elsewhere in the plan. It should be noted that for a single arc the maximum change in estimated delivery time is 0.08 minutes, which is very minimal when compared to a 10 min. treatment slot usually allocated for VMAT treatments. The varied delivery time with a small range for dual arc treatments in H&N cases produced no significant correlation. This indicates that the TPS is more capable of coping with the leaf speed restrictions when more than one arc is used, partly because of the number of control points in the plan.

3.1.1.3 Overall Mean Leaf Speed

The overall mean leaf speed for each plan is shown in Figure 3.4, with prostate cases in the top row and the H&N in the bottom. This is the mean speed of all the leaves that were in motion during beam delivery. Each plot in Figure 3.4 shows the plans which were generated using the original objectives and plans calculated using re-optimised objectives. The error bars represent one standard deviation.

As expected, there is an increase in the mean leaf speed as the maximum MLC leaf speed allowed is increased. Additionally, the spread of leaf speeds increased, meaning that there is more variation in the speed used when higher leaf speeds are available. Although the range covered in each site was similar, none of the mean leaf speeds exceeded 0.68 cm/s which is less than 40% of the manufactures specified maximum MLC leaf speed.

The analysis of mean overall leaf speed using the polynomial regression tool showed that a linear relationship could describe all sites, although there were a couple of cases where the plans showed a stronger correlation for a quadratic relationship over the evaluated range. Patient A produced a correlation coefficient for the linear model of 0.939 (p-value < 0.0001) and 0.948 (p-value < 0.0001) for the original objectives and re-optimised respectively. For Patient B the plans with the original objectives had a correlation coefficient of 0.962 (p-value < 0.0001) for the linear fit. Although the linear fit produced an adequate correlation coefficient of 0.849 (p-value = 0.001) for the re-optimised plans of patient B, a quadratic relationship yielded a superior correlation coefficient of 0.952 (p-value = 0.0005). The H&N sites had a similar trend to the prostate plans with the some cases indicating a linear relationship while others have a closer relationship with a quadratic fit. Patient C expressed a linear relationship for plans that use the original objectives having a correlation of 0.988 (p-value < 0.0001), the re-optimised objective had a marginally closer relationship to a quadratic model with correlation coefficients of 0.982 (p-value = 4×10^{-5}) for quadratic and 0.946 (p-value = 5×10^{-5}) for the linear model. The original objective plans for patient D demonstrated a higher degree of correlation with a quadratic relationship than a linear one with correlation coefficients of 0.994 (p-value = 2×10^{-6}) and 0.956 (p-value = 2×10^{-5}) respectively. Plans generated using re-optimised objectives resulted in a linear correlation between mean overall leaf speed and maximum MLC leaf speed with a correlation coefficient of 0.942 (p-value = 6×10^{-5}).

A close relationship between the mean overall leaf speed and the max MLC speed was expected. There was also a linear relationship between the overall leaf speed and the total distance covered by the MLC leaves. This can be seen in the full tables in Appendix B. The relationship is likely to be due to the minimal variation in the delivery times. If the mean

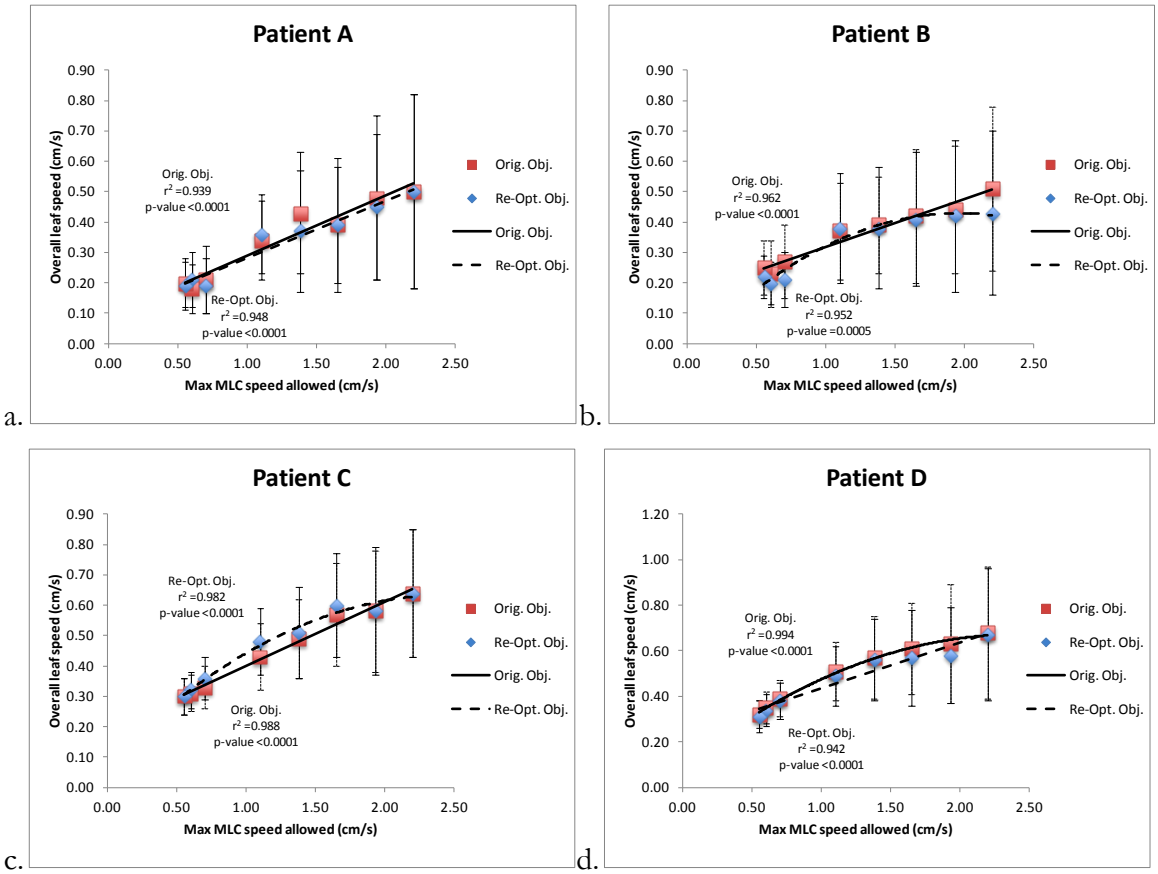

Figure 3.4 Variation in the mean leaf speed with respect to the maximum MLC leaf speed allowed in planning. The mean leaf speed required for each plan for prostate (Patient A, Patient B) and H&N (Patient C, Patient D) cases are given, with error bars representing one standard deveation

speed of the leaves change while the delivery time remains the same then the total distance travelled would be proportional to the change in speed.

Some of the mean leaf speed results showed a linear relationship while the others were better characterised by a quadratic relationship between maximum MLC speed allowed and mean overall leaf speed. In the prostate cases three out of four cases had better correlation with the linear relationship while for the H&N cases two had a linear relationship between mean leaf speed and maximum MLC speed and two had a quadratic relationship. This indicates that in some plans, continually increasing the allowed maximum MLC speed does not necessarily result in all the MLCs travelling faster. This could be the case once all the leaves are able to travel at a speed that allows them to cover the distance required per CP so that the optimal plan is achieved. As we approach this speed more leaves will be able to travel at the required maximum speed and variation in the mean leaf speed will reduce until all leaves are travelling at the maximum speed that they require. This study showed that the more arcs a plan has, the less leaf motion is needed between CPs and hence the maximum MLC speed that is required to meet the planning objectives is likely to be lower. This could be why the dual arcs showed a stronger quadratic relationship compared to the single arc treatment.

3.1.1.4 Overall Mean Dose Rate

Shown in Figure 3.5 are the variations in mean dose rate compared to the maximum MLC speed allowed by the TPS. The overall mean dose rate is the mean of the dose rates that the TPS predicts would be required to deliver the prescribed MU over the arc length of the CPs in the shortest possible time. The time is typically restricted by the maximum gantry speed. However, when a high MU is prescribed for a CP the maximum dose rate becomes the limiting factor.

The prostate cases (Figure 3.5a and b) show an increase in the mean dose rate as the maximum MLC speed is increased. The means increased by around 80 MU/min and 50 MU/min for patients A and B, respectively. A large portion of the increases occur after the initial few increments on MLC speed. The results for the H&N cases are again a lot more varied with less identifiable trends. The range of mean dose rates involved in the plans is around 20 MU/min for both patients. Despite what appears to be very little correlation for the re-optimised plans of patient C (Figure 3.5c), the plans generated from the original objectives exhibited a continually rising mean dose rate for increasing maximum MLC leaf speed.

The data in Figure 3.5a for patient A is best characterised by a linear relationship between the mean dose rate for a plan and the maximum MLC speed, with correlation coefficients of 0.847 (p-value = 0.0004) and 0.722 (p-value = 0.007) for plans with original objectives and re-optimised objectives respectively. Results for patient B, on the other hand, only showed correlation for plans generated with the re-optimised objectives (r^2 = 0.667 p-value 0.01). For the H&N cases, linear correlation was found only for plans generated using the original optimisation objectives of patient C (r^2 = 0.866, p-value = 0.0003). No apparent correlation between the overall mean dose rate and the maximum MLC speed was observed in the plans with the re-optimised objectives and in all the plans for patient D.

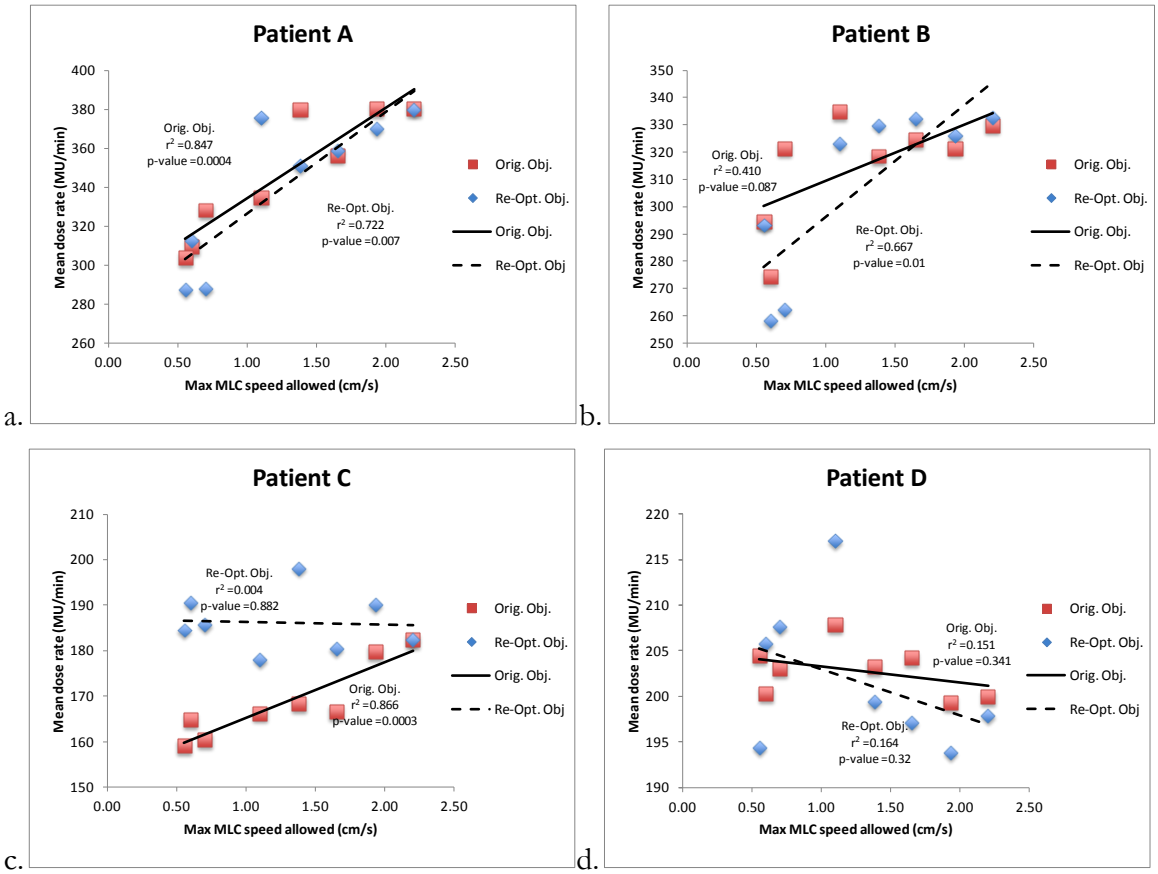

Figure 3.5 Variation in the mean dose rate with respect to the maximum MLC leaf speed allowed in planning. The mean dose rate required for each plan for prostate (Patient A, Patient B) and H&N (Patient C, Patient D) cases are given.

The mean dose rate is implicitly linked to the delivery time and the MU per fraction. For the prostate plans, when the MU and delivery time had a good correlation with the maximum MLC speed the mean dose rate was also found to have a high dependence on the maximum MLC speed settings. In the H&N plans, where the delivery time is largely unchanged even with varying maximum MLC speed setting, the variation in MU had the largest influence on mean dose rate, as reflected in the similarities in the data distributions of Figure 3.2c-d and Figure 3.5c-d.

3.1.2 Plan Conformity and Homogeneity

3.1.2.1 Conformity Index

Figure 3.6 displays how the conformity index (CI) of each PTV varied as the maximum MLC speed was modified. The conformity indices in all plans were computed based on Equation 1. It can be seen that for the single arc prostate plans (Figure 3.6a-d) that the maximum MLC speed influenced the CI of the plans. This was observed across all the plans although there were a few outliers with lower than expected CIs. In Figure 3.6e-g, the small CI range for H&N plans (0.04) and its relatively large variations with respect to the allowed maximum MLC speed indicated that there was no obvious relation between these parameters.

The results of the polynomial regression analysis of the relationship between the CI and maximum MLC speed for the PTVs in the plans evaluated in this study are listed in Table 3.1, where the correlation coefficient and its corresponding p-value are listed for each PTV. Comparing the two prostate cases, patient A had one of its PTVs demonstrating a linear dependence of the CI on MLC speed and the other did not. On the other hand, patient Bs PTVs both had very good correlation between these parameters. It should be noted that the regression analysis for patient B was performed without the outlier data. For the H&N cases, the PTVs in patient C and D did not exhibit a conclusive dependence between the CI and maximum MLC speed as evident in the correlation coefficients listed in Table 3.1.

As with the other parameters discussed in the preceding sections, the dependence of the CI on the maximum allowed MLC speed was more evident in the prostate than the H&N cases. In the prostate plans, the PTVs have a higher weighting applied to the planning dose objectives so the reduction in conformity comes at the cost of an increase in the dose to the healthy tissue. The reduction in the maximum MLC speed would have reduced the ability of the TPS to move MLC leaves at large distances between CPs reducing the ability to conform to target volume concavities. The H&N sites overall showed a lack of dependency of the CI on the MLC leaf speed. As noted earlier, the doubled number of control points in the dual arc H&N plans could have allowed the TPS to generate plans that satisfied the required CI regardless of the maximum MLC speed. The outliers in some of the data in Figure 3.6 could be attributed to the fact that the plans generated in this study were optimised to achieve specific dose objectives rather than to produce a plan that satisfied a specific CI.

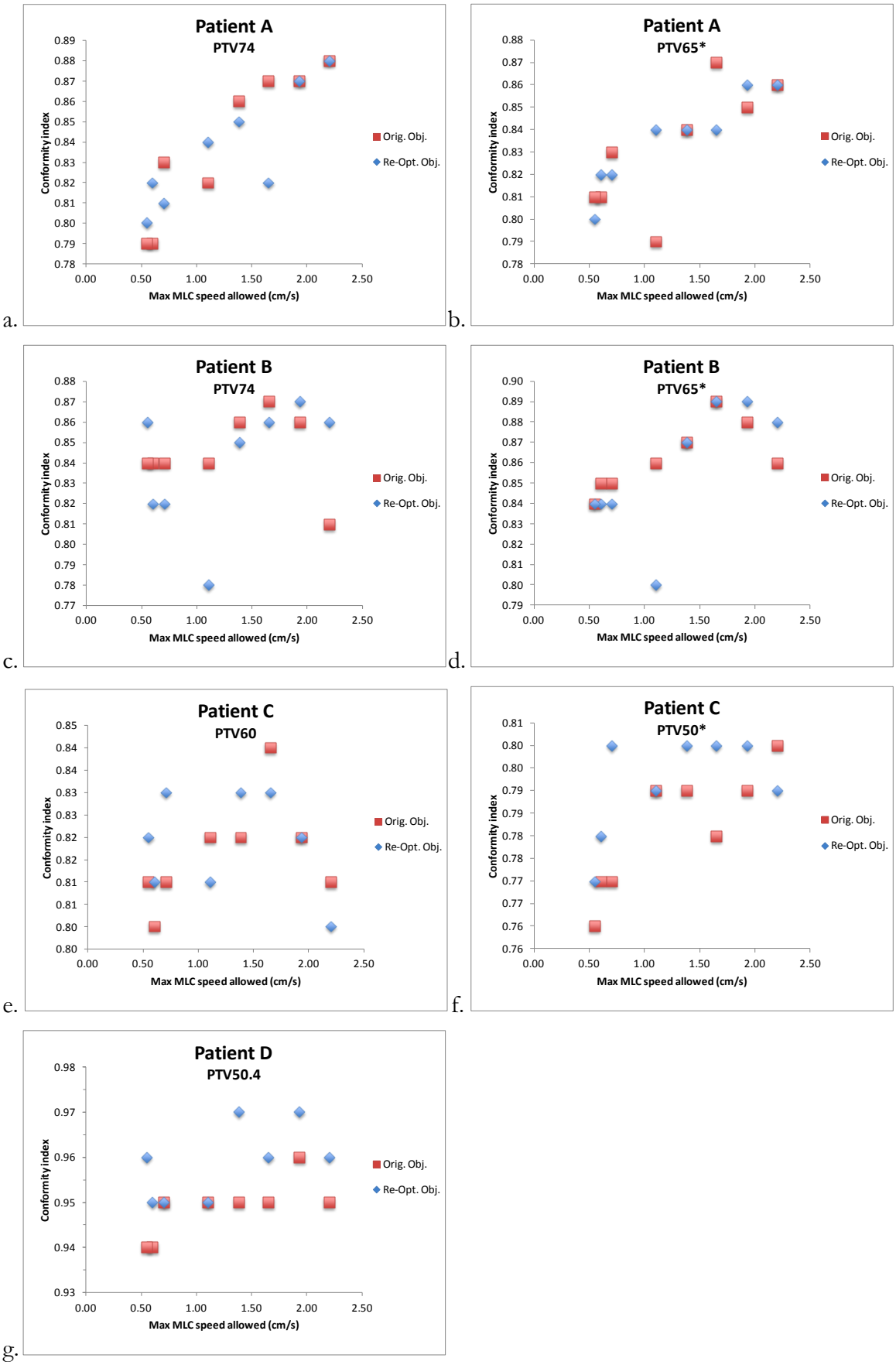

Figure 3.6 Variation in the conformity index with respect to the maximum dose rate allowed. Shown here are the results for each PTV in the plans generated for the prostate (PTV74, PTV65*) and H&N (PTV60, PTV50.4, PTV50*) evaluated in this study.

Table 3.1 Correlation coefficients of the conformity indices shown in Figure 3.6. Enclosed in parenthesis is the corresponding p-value.

Patient	Optimisation Objectives	PTV74	PTV60	PTV50.4	PTV65*	PTV50*
A	Orig.	0.015 (0.757)			0.5711 (0.019)	
	Re-Opt.	0.250 (0.207)			0.5164 (0.045)	
B	Orig.	0.876 (0.000)			0.6175 (0.012)	
	Re-Opt.	0.747 (0.006)			0.8701 (0.001)	
C	Orig.		0.027 (0.671)			0.7157 (0.004)
	Re-Opt.		0.050 (0.596)			0.2949 (0.164)
D	Orig.			0.624 (0.011)		
	Re-Opt.			0.349 (0.123)		

3.1.2.2 Homogeneity Index

The variation of homogeneity for each PTV, as the maximum MLC speed allowed is changed, can be seen in Figure 3.7. The homogeneity Index (HI) was calculated using Equation 2 which equates to the standard deviation of the *d*DVH of the PTV.

The HI was found to be higher for slower maximum MLC speed. As the HI is a measure if the spread of doses within the target volume, the lower the HI value the more homogeneous the dose distribution is for the volume. It can be seen that Figure 3.7b and d have a high HI, these volumes are encompassing the seminal vesicles. The seminal vesicles are adjacent to the prostate so the dose fall off from the 74 Gy prescription to the prostate means that there is a high dose gradient across this volume (PTV65). As with the CI there are a few outliers in the data, these occur in the plans generated from the re-optimised objectives in Figure 3.7b, d, and f.

Error! Reference source not found. shows the result of the polynomial regression analysis of relationship between the homogeneity indices and maximum MLC speed available, the correlation coefficient and the corresponding p-value for a linear relationship are listed. Of the prostate cases patient A demonstrated a dependence between HI and maximum MLC speed for all the plans generated from the original planning objectives, as well as the PTV65 volume of the plans using the re-optimised plans. Conversely patient B demonstrated a dependence of both PTVs in the plans generated from the original objectives, despite the outlier data being excluded. When the H&N cases were analysed the PTV60 of patient C and PTV50.4 of patient D both demonstrated dependence between the HI and maximum MLC speed for all sets of planning objectives. The only H&N target volume that did not demonstrate the linear dependence for any planning objectives was the PTV50 of patient C as can be seen from its coefficients seen in **Error! Reference source not found.**.

The trend that was indicated in most test cases was that the higher the maximum MLC speed the more homogeneous the prescribed treatment plan will be. This would imply that the high leaf speeds are used to smooth out variation in the dose distribution either through small fields or leaves blocking higher dose region. For slower leaf speed settings, the ability of the TPS to remove the inhomogeneities is restricted. The fact that it is present in about equal proportions between sites is likely due to the larger target volumes in the H&N cases which makes it more difficult to achieve and maintain homogeneous dose distributions across them. For this parameter it might be that the number of modulation points that are needed to achieve homogeneity is enough.

a.
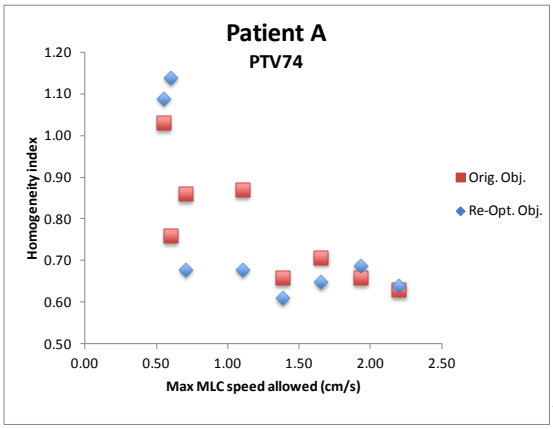

b.
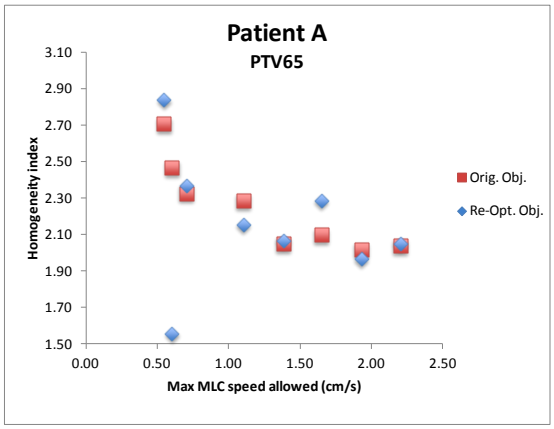

c.
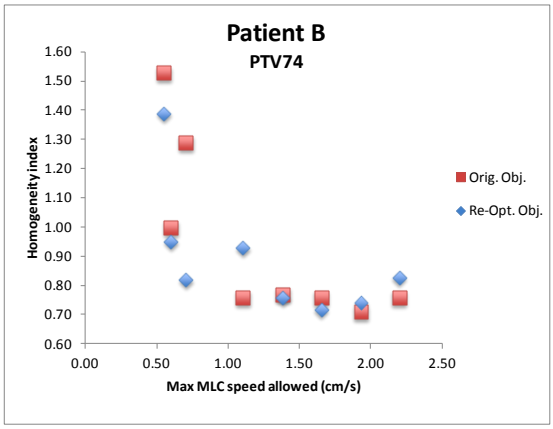

d.
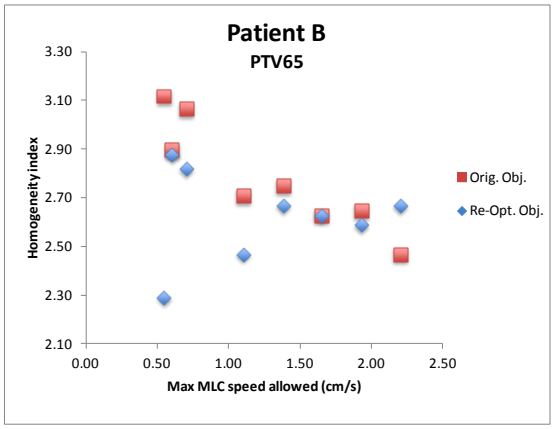

e.
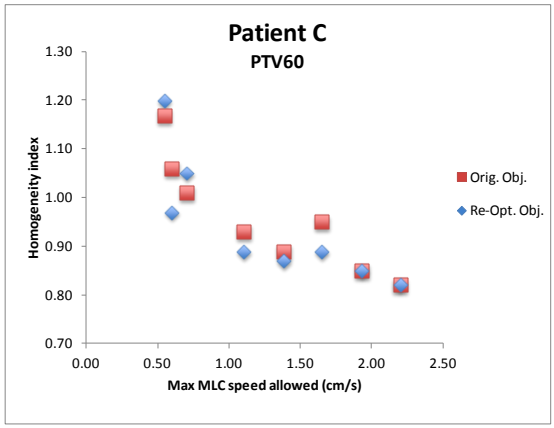

f.
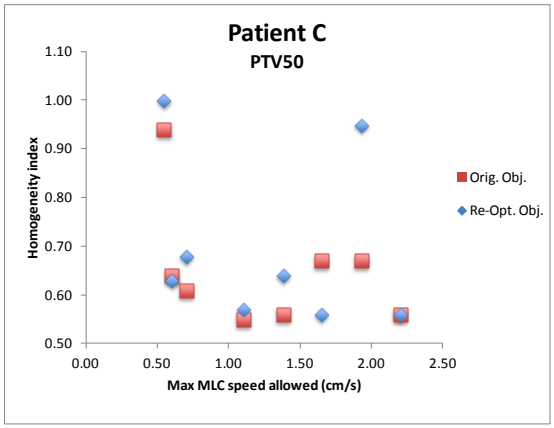

g.
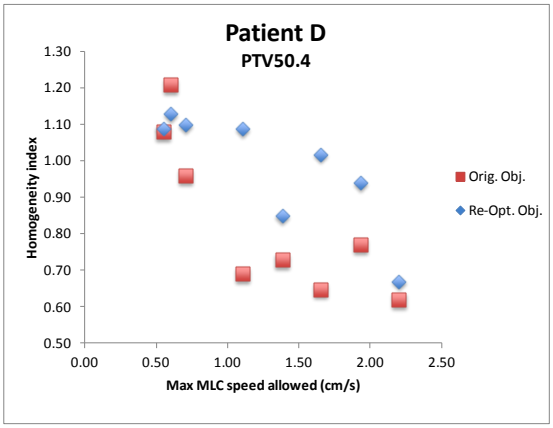

Figure 3.7 Variation in the homogeneity index with respect to the maximum MLC leaf speed allowed. Shown here are the results for each PTV in the plans generated for the prostate (PTV74, PTV65) and H&N (PTV60, PTV50.4, PTV50) cases evaluated in this study.

3.2 Correlation coefficients of the homogeneity indicies shown in Figure 3.7 . Enclosed in parenthesis is the corresponding p-value

Patient	Optimisation Objectives	PTV74	PTV60	PTV50.4	PTV65	PTV50
A	Orig.	0.673 (0.007)			0.767 (0.002)	
	Re-Opt.	0.475 (0.06)			0.612 (0.04)	
B	Orig.	0.547 (0.02)			0.782 (0.002)	
	Re-Opt.	0.391 (0.1)			0.0002 (1.0)	
C	Orig.		0.826 (0.0007)			0.225 (0.2)
	Re-Opt.		0.672 (0.01)			0.042 (0.6)
D	Orig.			0.692 (0.005)		
	Re-Opt.			0.685 (0.01)		

3.1.3 Plan Quality Scores

The plan quality score (Table 3.3) decreased at lower MLC leaf speed. This was more prominent in the single arc plans for the prostate cases. For small reductions in leaf speed, the TPS was able to compensate effectively and an optimum plan with no significant degradation in plan quality was produced. When the maximum MLC leaf speed was reduced to less than 50% of the manufacturer's recommendation, the plan quality in single arc treatments declined with decreasing maximum MLC leaf speed in the plans generated from both the original and re-optimised planning objectives. Plans that were generated with the re-optimised objectives had a lower rate of decline when compared to the plans from the original objectives. Despite this, the limited numbers of modulation points that were available in a single arc proved to limit the TPS ability to maintain high plan quality scores at low MLC leaf speeds.

Although the plan quality score for the H&N sites also suffered from some degradation in the plans using the original objectives, this was to be expected as these objectives were optimised for a plan with different initial parameters. When the planning objectives were re-optimised it was possible to maintain a plan quality score that was consistent with the plans generated with high maximum leaf speeds, even down to the lowest speeds tested. This is potentially due to the increase in the number of modulation points that are provided through the use of dual arcs. The results suggest that if a dual arc was used to treat the prostates then they would also be able to improve the ability of the TPS to cope in the more restrictive setting, although this would lead to an increased treatment delivery time and potentially excessive modulation.

Table 3.3 Plan Quality Scores

Max. MLC speed	Planning objectives	Patient A	Patient B	Patient C	Patient D
2.20	**Orig. Obj.**	1.00	1.05	1.00	0.99
1.93		1.00	1.31	0.96	1.05
1.65		0.99	1.31	0.95	1.00
1.38		1.00	1.21	0.99	1.01
1.10		0.88	1.10	0.98	0.98
0.70		0.83	0.69	0.95	1.00
0.60		0.89	0.90	0.95	0.98
0.55		0.77	0.45	0.95	0.93
2.20	**Orig. Obj.**	1.00	1.00	1.00	1.00
1.93	**Re-Opt. Obj.**	1.00	1.30	1.07	1.08
1.65		1.00	1.22	1.07	1.06
1.38		1.00	1.29	1.07	1.05
1.10		0.92	0.96	1.07	1.06
0.70		0.99	0.75	1.06	1.07
0.60		0.78	0.87	1.07	1.05
0.55		0.71	0.78	1.07	0.99

3.1.4 Point Dose Measurements

The majority of the point dose measurements (Figure 3.8) were within ±3% of the predicted dose, which is well within the accepted clinical tolerance. As can be seen in the same figure, there appears to be no significant trend in the results. The majority of the point doses that failed were within the -3% to -4% range. However, our patient specific QAs have shown a systematic error of approximately -1%, the source of which is still being investigated. Considering this systematic error, it is likely that the failing point dose results would also be within the clinically acceptable threshold.

The point dose measurements for the prostate plans showed a consistent result with a mean difference between predicted and measured doses being 2.04% ± 0.06% (range: 1.95% to 2.15%) and 1.70% ± 0.03% (range: 1.66% to 1.76%) for patients A and B, respectively. This is in contrast with the dual arc H&N treatments which were more varied, -1.95% ± 0.91% (range: -3.89% to -0.18%) and -2.55% ± 0.77% (range: -4.27% to -0.83%) for patients C and D, respectively. The difference in the agreement between predicted and measured doses for the two sites is likely due to the difference in the complexity of the plans. H&N cases require more modulation due to the number of organs at risk in close proximity to the target volumes. Less modulation is needed in prostate plans since the organs at risk that are of major concern are only the rectum and bladder. The location of the point of measurement could have also influenced the results obtained in this work. In prostate cases, the point of measurement (isocentre) was in the middle of the target volume, where the dose is relatively uniform. In the H&N plan, the point of measurement could have been in a high dose gradient region.

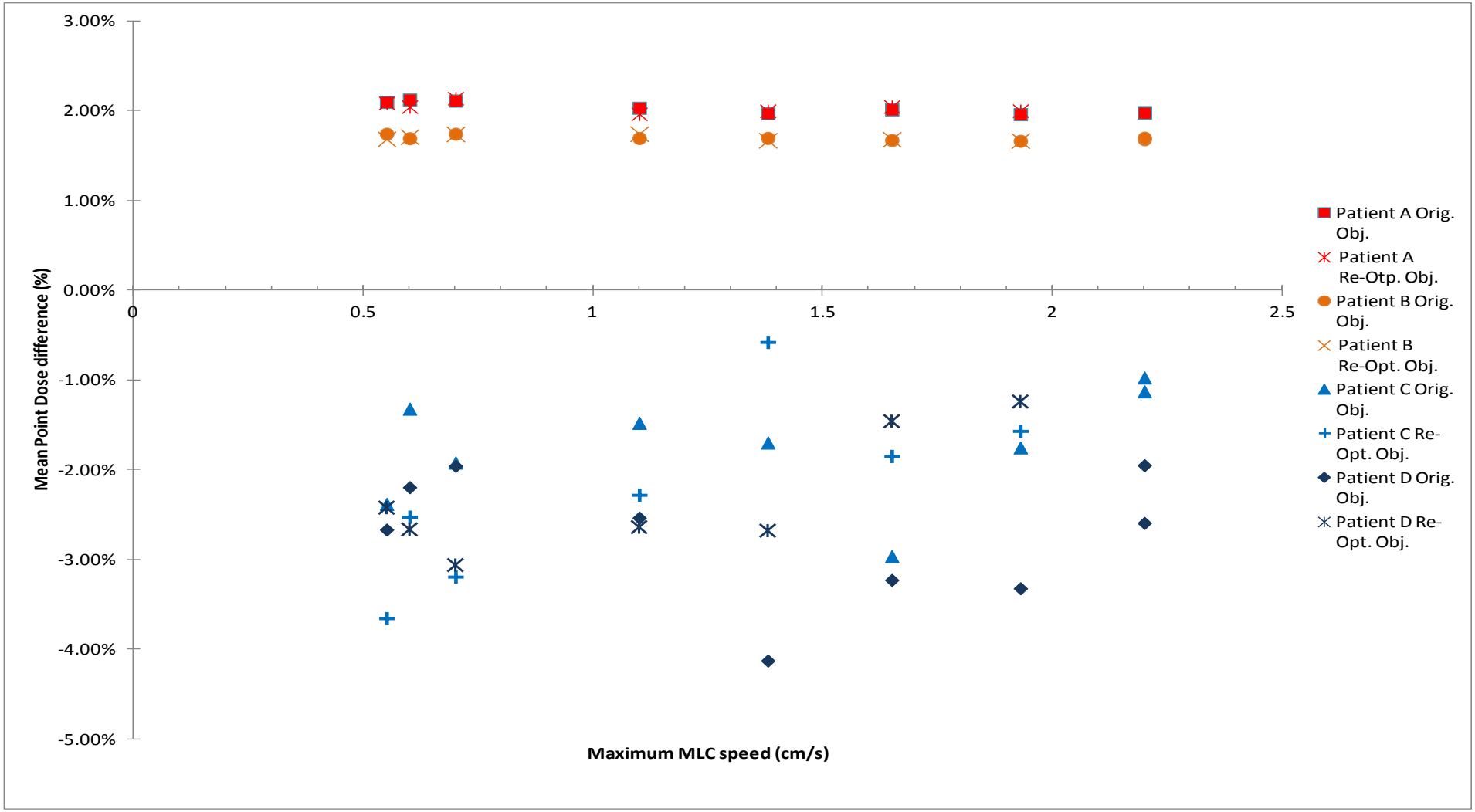

Figure 3.8 Variation in Point dose measurements with respect to the maximum MLC speed allowed. Each patient has been divided into plans using the original objectives represented as a solid shape and plans with re-optimised objectives represented with a cross pattern.

3.1.5 Dose Maps

The gamma analysis of the fluence maps recorded by the ArcCHECK can be seen in Figure 3.9. There is minimal difference between the planned and recorded treatments when using a gamma pass rate of 3%/3 mm or 2%/2 mm. All the prostate plans had a gamma pass rate of above 98.7% and 91.5% for the 3%/3 mm and 2%/2 mm, respectively. The H&N plans showed marginally lower gamma pass rates at 97.4% and 90.0%, respectively. These results are all within the clinically acceptable passing limit at our centre of 95% and 85% for 3%/3 mm and 2%2 mm, respectively. When the gamma values for a 1%/1 mm were calculated the results became less consistent and significantly lower, with gamma pass rate for all plans falling within the 55%-80% range.

There was a linear relationship detected for all gamma criteria in the plans that used the original objectives in patients A and D, with all having correlation coefficients of more than 0.75 (p-value < 0.002). Neither of the other patients showed any correlation for the original objective plans. When the re-optimised plans were analysed the trend that was indicated in patients A and D were no longer observed except in the 3%/3 mm gamma criteria analysis of patient A. Wherever a trend was indicated it expressed a decrease in agreement between planned and delivered dose maps for increasing leaf speed. Given the inconsistencies in what is indicated between the data sets and the range of gamma pass rates, especially for the 3%/3 mm and 2%/2 mm criteria, it was not possible to conclude that there is a definitive trend between gamma pass rate and leaf speed. If further research indicated a trend similar to the ones seen here it is unlikely that it would be clinically significant based on the values seen in this investigation.

a.

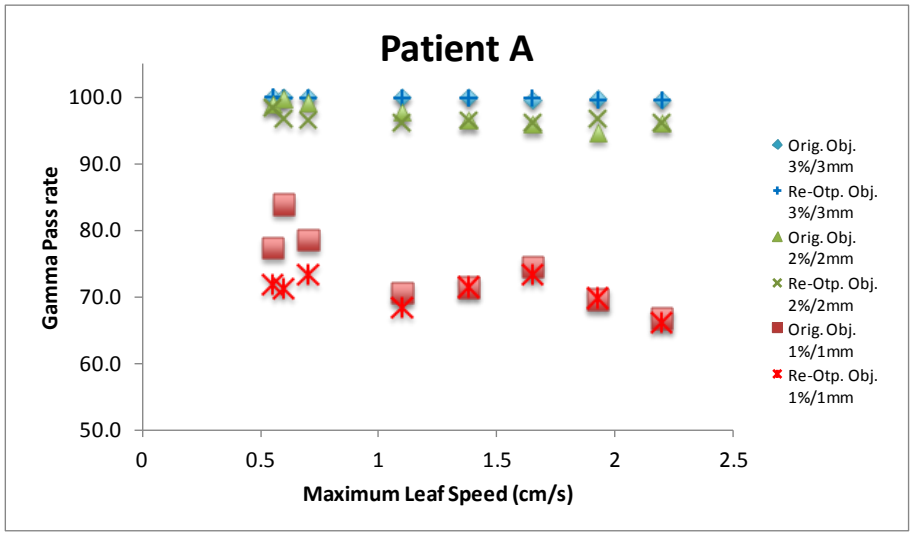

b.

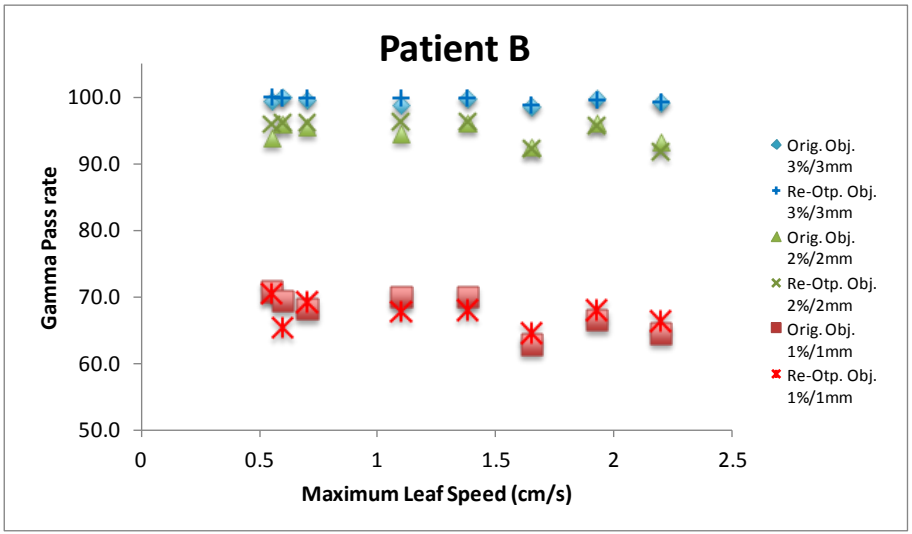

c.

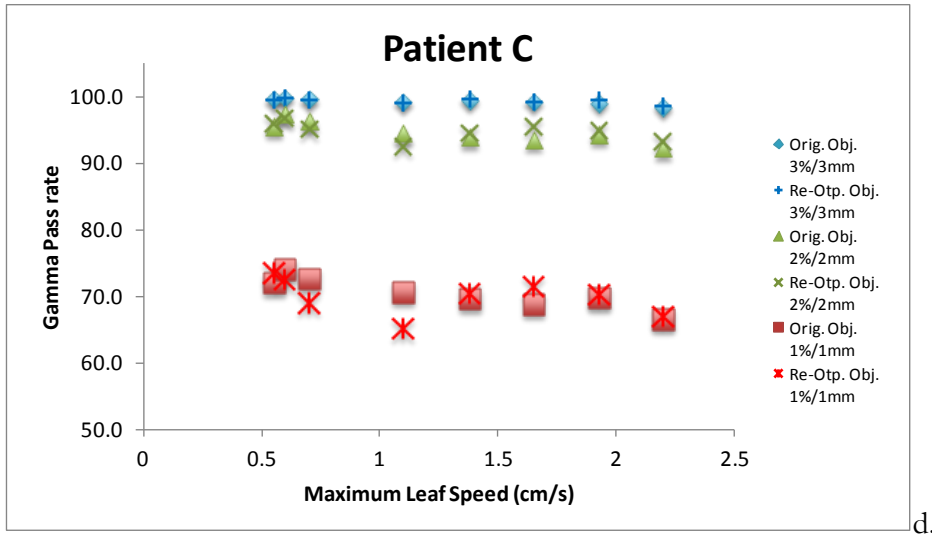

d.

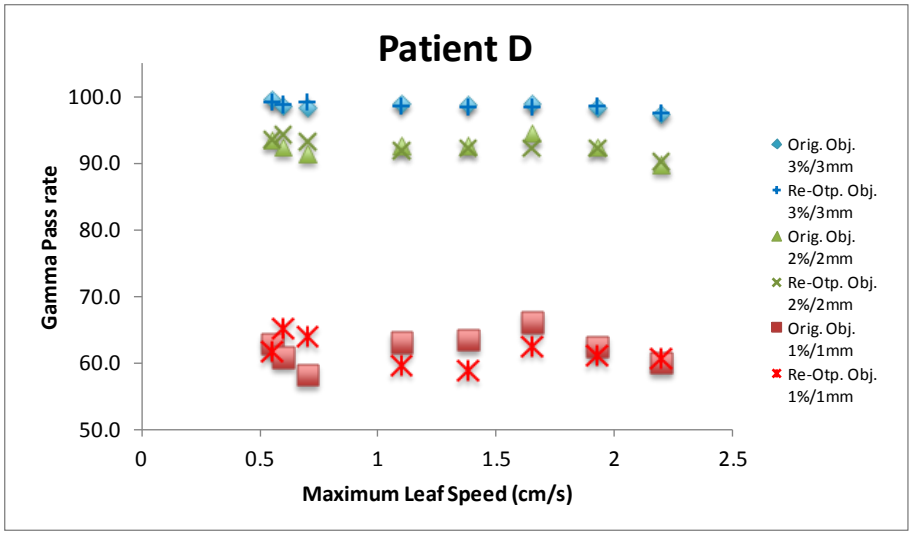

Figure 3.9 Shows the variation in the gamma pass rates for each plan when the maximum MLC leaf speed available is changed. Each plot contains a seires for each of the three gamma criteria (3%/3 mm, 2%/2 mm and 1%/1 mm) and each of the planning objective methods.

3.1.6 Control Point Analysis

Although there was very little difference noticed when the ArcCHECK results were analysed as the overall fluence delivered, this was not the case when the fluence at individual CPs were analysed. Figure 3.10 gives a clear indication of the observed trend with both single and dual arc treatments and is further supported by the numerical analysis in Table 3.4. The figures show an increase in the number of measurements that did not meet the corresponding gamma criteria for higher leaf speed in both the 2%/2 mm and 3%3 mm gamma analysis. Both Figure 3.10b, c and Table 3.4 show that there are twice as many CPs where over 20% of measurement points fail to pass the 2%/2 mm or 3%/3 mm gamma test when the leaf speed allowed in planning is 2.20 cm/s compared to the restriction to 0.55 cm/s. The difference between the 2.20 cm/s and 1.10 cm/s leaf speed plans is lower, this is likely to be a result of the restriction being less significant on the required motion of most leaves. The mean leaf speeds that were required in the plans using the 2.20 cm/s restriction are highest for H&N treatments at 0.68 cm/s which is much less than the maximum allowed leaf speed of the 1.10 cm/s restricted plan. This means that the majority of leaves are still able to move the required distances for both MLC leaf speed settings. The difference between the entire fluence and individual CP evaluation is indicative of possible dose averaging and smearing that occurs. This means that the results may not necessarily be a significant clinical issue.

Table 3.4 Shows the mean number of CPs in a given treatment that have a percentage of detection points failing the gamma criteria within each range. Each single arc had 90 CPs in total and the dual arcs had 180.

Single Arc						
	3%/3 mm			2%/2 mm		
Failure range	2.20 cm/s	1.10 cm/s	0.55 cm/s	2.20 cm/s	1.10 cm/s	0.55 cm/s
10-10.99%	13.25	10.5	2.75	27.25	21.75	15.00
20-20.99%	6.50	6.00	2.25	16.00	16.75	7.00
30%+	1.00	1.75	1.50	6.50	5.50	2.75
Dual Arc						
	3%/3 mm			2%/2 mm		
Failure rate	2.20 cm/s	1.10 cm/s	0.55 cm/s	2.20 cm/s	1.10 cm/s	0.55 cm/s
10-10.99%	28.50	21.75	13.75	64.75	57.50	52.75
20-20.99%	14.00	11.00	5.00	36.00	28.25	17.25
30%+	4.50	3.00	1.75	16.50	16.25	7.50

a.

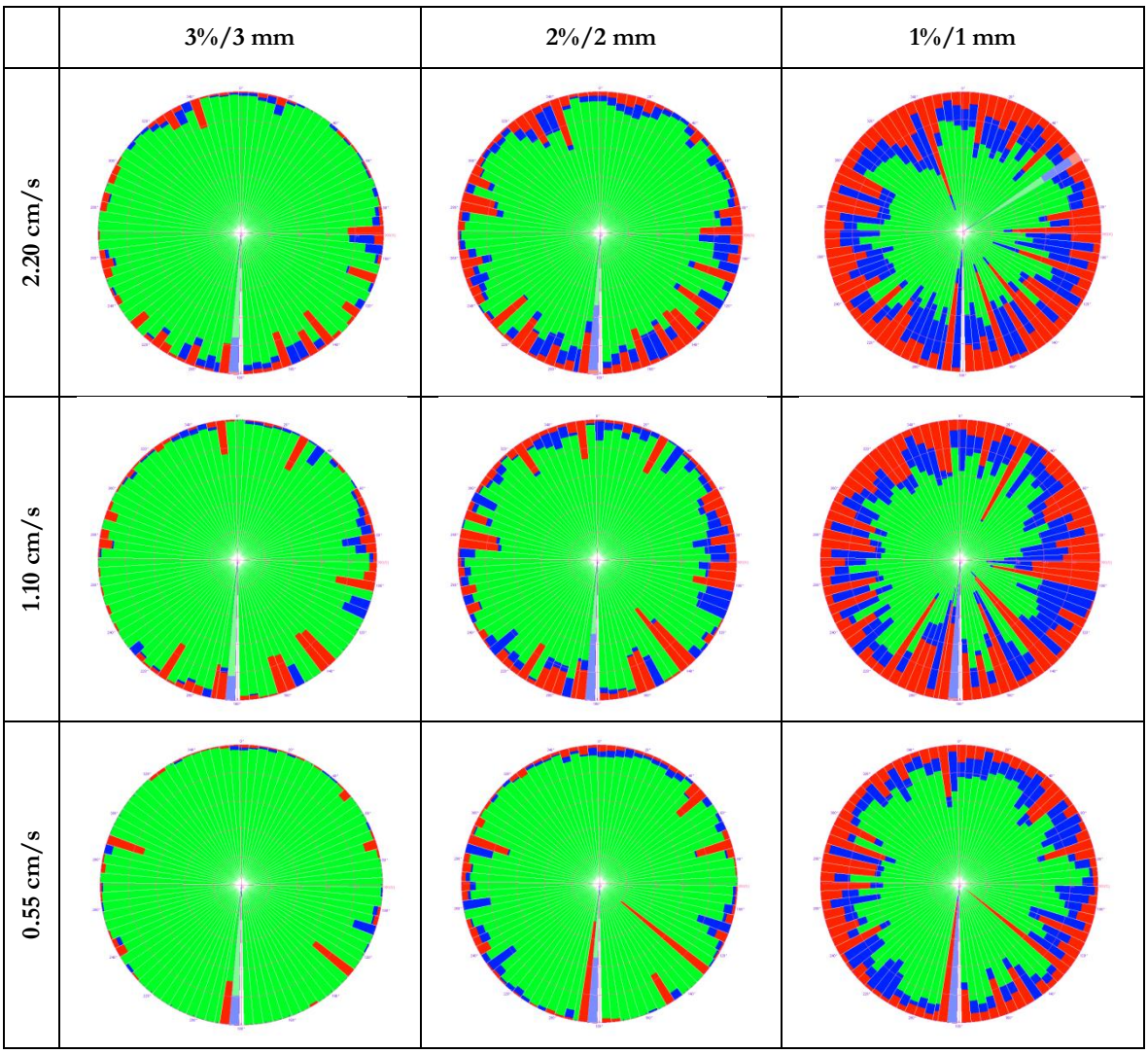

b.

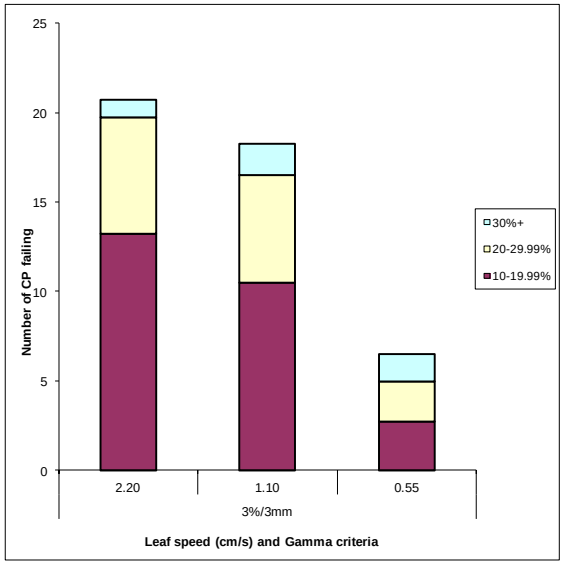

c.

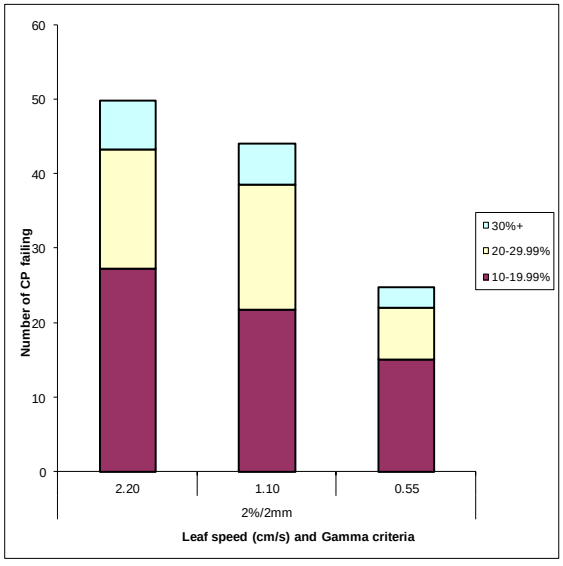

Figure 3.10 a. Shows the CP analysis charts for a slection of leaf speeds for a prostate patient when analysed using three different gamma criteria. b and c show the mean number of CPs per arc that have the given range of points failing to meet either a 3%/3 mm or 2%/2 mm gamma criteria.

3.1.7 Dynalog Analysis

The Dynalog data showed that there was an increase in the larger positional errors for plans that were allowed higher leaf speeds as can be seen in Figure 3.11. The plans where the MLC leaf speed is most restricted have the vast majority of the leaf position errors occurring at less than 0.05cm. It is not until the leaves are allowed to travel up above 1.38 cm/s that we see any positional errors above 0.1 cm. Using the recommended value from the linac manufacturer for the maximum leaf speed, between 5.5% and 11% of all recorded leaf positions deviate from the expected position by 1.0 mm to 1.5 mm. This clearly shows an increase in the failures of the MLC leaves to reach their planned location within the allocated time. These results support the increase in errors that were detected in the CP analysis of ArcCHECK measurements that differed from the overall dose distribution analysis.

To check the clinical relevance of these results, MLC positions at every 2° increment of gantry position were extracted and imported back into pinnacle to determine how these errors affected the dose distribution. A plan quality analysis was done using the same requirements applied in the analysis of the original plan. A plan quality score of 84.8 for the plan with the imported positions was obtained, whereas it was 95 for the original plan. Despite this drop in plan quality, it is not as significant as it may first appear. The imported plan was marginally hotter than the initial one. The slight increase in the near maximum doses ($D_{2\%}$) for both the CTV and the PTV74 is the source of the decrease in plan quality score. These objectives were given high weights and very conservative tolerances (i.e., $D_{2\%} \leq 75.0$ Gy with a 0.3 Gy tolerance) in the plan quality score calculation. This objective and tolerance was decided by our clinicians as the general planning target and is well below the ICRU 83 recommendation of defining the $D_{2\%}$ equal to 107% of the dose prescription of 79 Gy. The CI and HI had a slight reduction as well, but this is also minimal and all organs at risk doses were below the specified dose constraints. When a comparison of the DVH and isodose profiles was performed (Figure 3.12), it was found that that the plans are very similar. The increase in the dose across the entire plan can be seen in the larger 74 Gy and 75 Gy isodose areas. It is difficult to see any difference in the dose deposited in the OAR except for the right femoral head which has slightly increased coverage by the 29.6 Gy isodose. The minimal difference is best illustrated in Figure 3.12c where the similar DVH curves are seen for the original and re-calculated plan, with the latter being only marginally hotter.

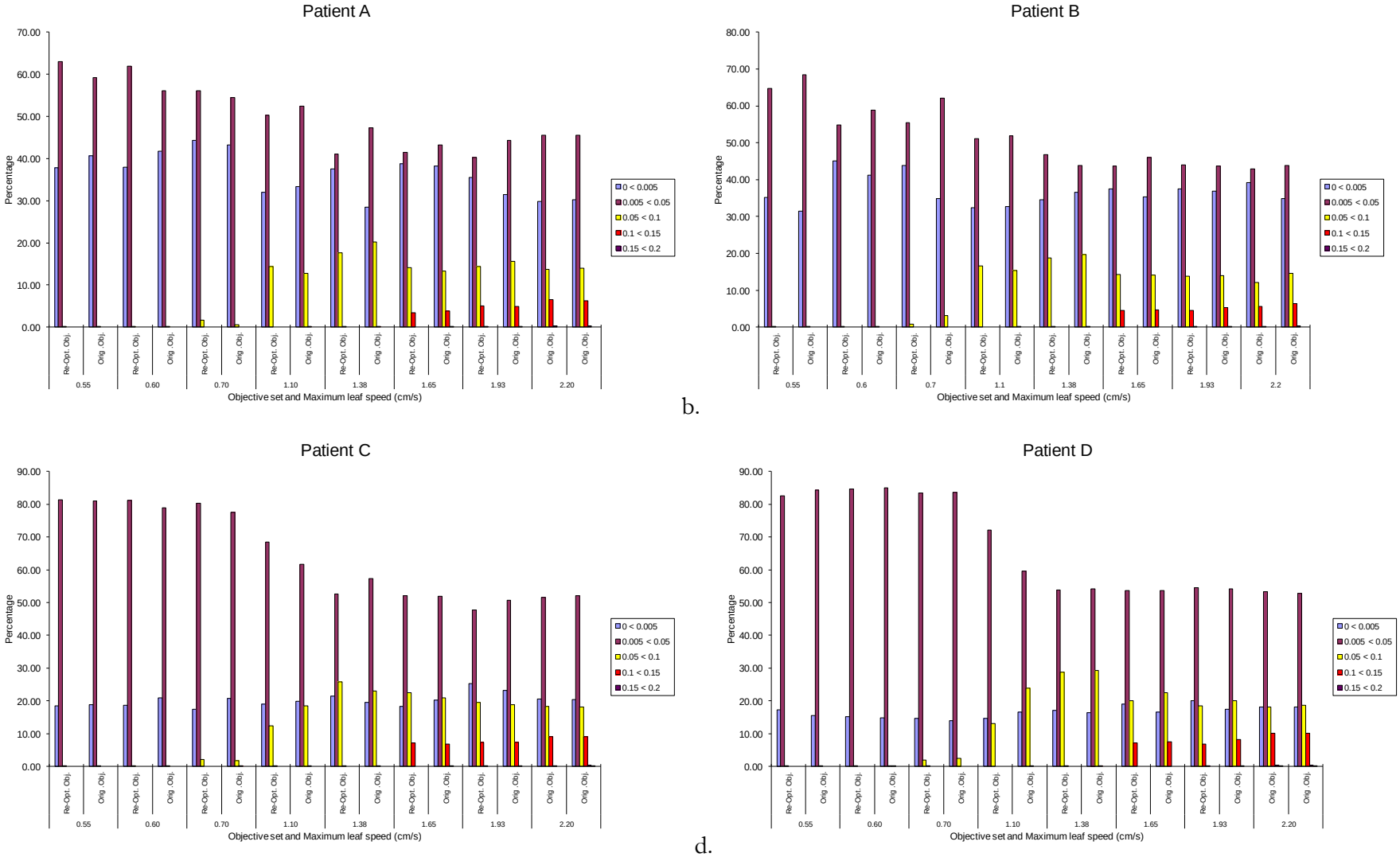

Figure 3.11 Dynalogs produced from each plan delivery. Each plan is given along the x axis and the coresponding histogram of the percentage of point from the dynalog files that have a positional error within the specified range in cm.

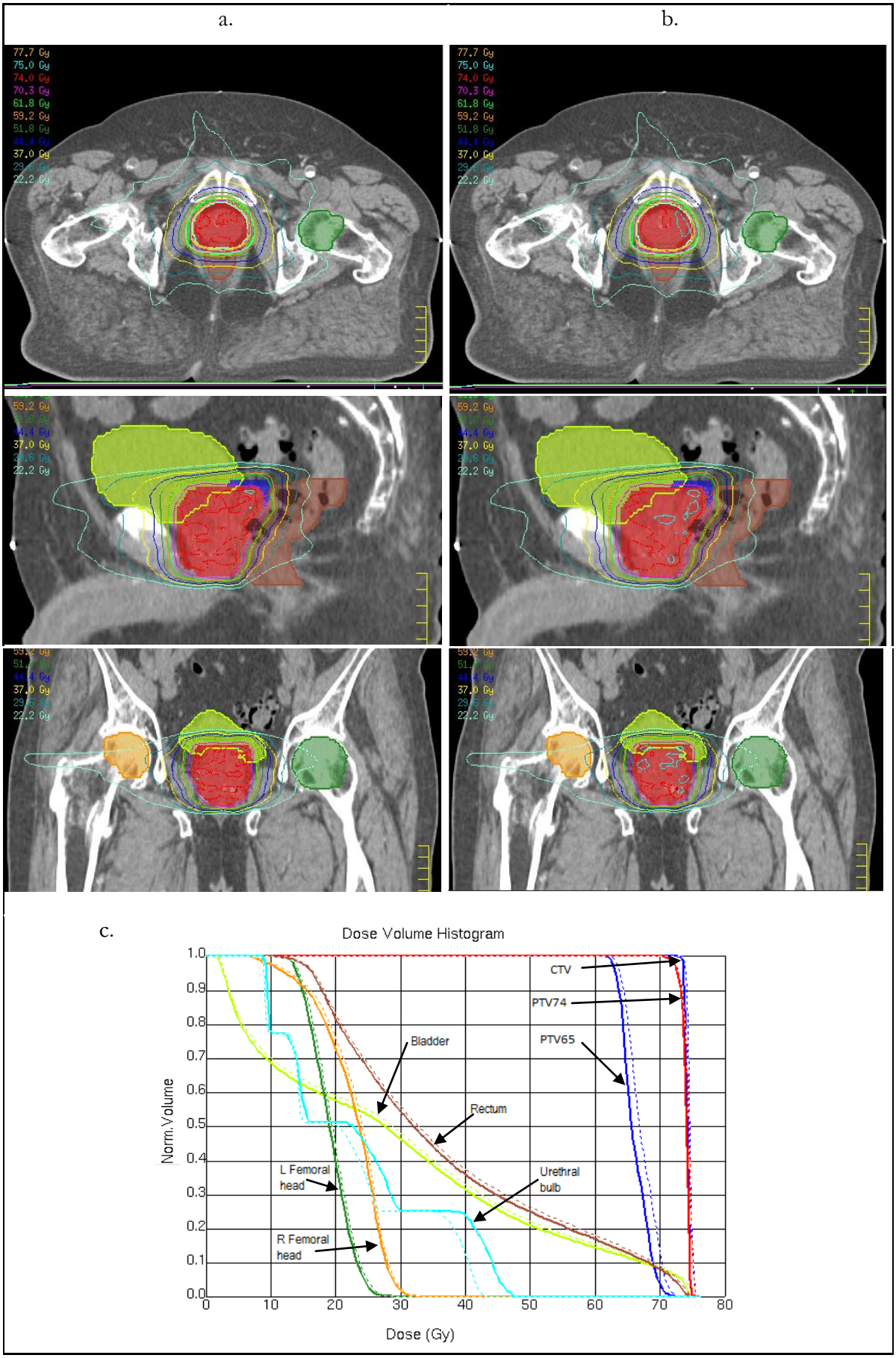

Figure 3.12 Comparison of dose distributions for the orignial plan (a) and the re-calculated plan (b) based on Dynalog MLC positions. c)The DVH shows the original dose distribution as the thick solid line and the thin dotted is the re-calculated plan.

3.2 Restricted Maximum Dose Rate

The range of dose rates that were tested in this study were restricted to 100 MU/min increments and the highest maximum dose rate setting evaluated was 600 MU/min. This was due to the constraints in the usable maximum dose rates in our linear accelerators. The lowest maximum dose rate setting applied in each plan differed for the different sites.

One of the major benefits of VMAT over IMRT is its faster treatment delivery times. To ensure this faster delivery time was maintained, the lowest maximum dose rate implemented was 300 MU/min for prostates and 200 MU/min for H&N. These limited the delivery times to less than 2 min. per arc.

3.2.1 Plan Characteristics

This section covers the analysis of the variation in the plan characteristics of each plan that were produced using different maximum dose rates settings. Full tabulated data for each of the characteristics discussed in this section can be found in Appendix C.

3.2.1.1 Monitor Units

The variations in MU per fraction are shown in Figure 3.13 with respect to the maximum dose rate allowed for all plans of each site. The prostate cases are in the top row (Figure 3.13a, b), while the H&N cases are in the bottom row (Figure 3.13c, d).

The MU variation for the prostates plans was minimal with a range in the order of 15 MU and 20 MU for plans generated from the original and re-optimised objectives of patient A (Figure 3.13a) respectively. There was a MU variation of approximately 20 MU for both plan groups for patient B (Figure 3.13b). No consistent trends were observed for all plots, although some indicate that the TPS generates a plan with a higher MU per fraction when the maximum allowed dose rate was increased.

The polynomial regression analysis of the change in MU as a function of the maximum dose rate didn't show any clear correlation between these two parameters. Patient A had correlation coefficients of 0.017 (p-value = 0.9) and 0.379 (p-value = 0.4) for the original objective plans and plans generated from re-optimised objectives, respectively. Despite patient B having a more regular distribution of results, it did not exhibit a significant correlation for both the original (r^2 = 0.549, p-value = 0.2) and re-optimised (r^2 = 0.307, p-value = 0.4) objectives. The H&N sites did not produce any more predictable results than the prostates. The plans generated for patient C using the original objectives had the best linear correlation (r^2 = 0.671, p-value = 0.09) of all. The plans that were generated for the re-optimised objectives for patient C had correlation coefficients of 0.129 (p-value = 0.6). For the other H&N site, patient D was like all the others with no apparent correlation between the MU per

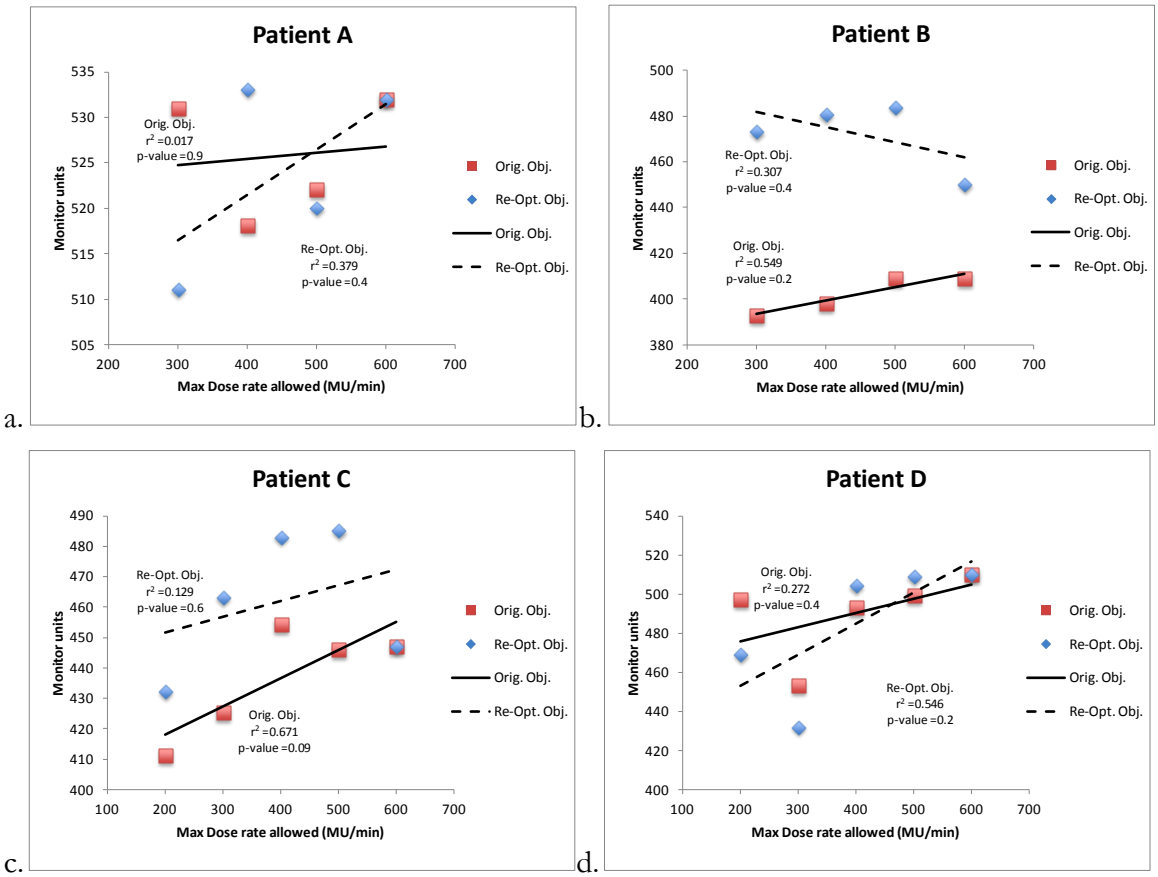

Figure 3.13 Variation in the MU per fraction with respect to the maximum dose rate allowed in planning. The MU required for each plan for prostate (Patient A, Patient B) and H&N (Patient C, Patinet D) cases are given.

fraction and the maximum dose rate available with r^2 of 0.272 (p-value = 0.4) and 0.546 (p-value = 0.2) for plans generated using the original and re-optimised objectives, respectively.

The fluctuations seen in Figure 3.13 indicate that the maximum dose rate settings in the TPS did not affect the number of MU that were used per fraction. This independence of the MU per fraction indicates the effect of changing the dose rate will only affect the time taken to deliver the required number of MU and not how many will be required. This is achieved by slowing down the gantry speed which results in longer delivery time as will be discussed in the next section. This association was also noted in the work of Nicolini et al.[20] where the robust compensation mechanism between gantry speed and maximum dose rate available was shown.

3.2.1.2 Estimated Delivery Time

Figure 3.14 shows the variations that arose in the estimated delivery time when the maximum dose rate available was modified. Figure 3.14a and b correspond to the prostate cases and Figure 3.14c and d to H&N cases. Each plot shows the estimated delivery time with respect to the maximum dose rate for plans generated using the original objectives and re-optimised objectives.

The general trend in all patients was a reduction in the estimated delivery time for increasing maximum dose rate allowed, which reduces the chances of intra-fractional motion. The prostate cases had a significant decrease in delivery time when the dose rate was increased from 300 MU/min to 400 MU/min. This corresponded to a drop in the delivery time by 0.35 min and 0.28 min for plans generated for patient A (Figure 3.14a) using the original and re-optimised planning objectives, respectively. For the total change in dose rate of 300 MU/min, the delivery time was shortened by 0.51 min and 0.49 min. Patient B (Figure 3.14b) had a similar result with 0.18 min and 0.28 min reductions in delivery time when the dose rate was set from 300 MU/min to 400 MU/min for the two sets of plans, respectively. The difference between the delivery time for a dose rate of 300 MU/min and 600 MU/min were 0.25 min and 0.41 min for the same two sets of plans.

The delivery times for the H&N cases also significantly dropped at the first 100 MU/min change in the dose rate. The results shown in Figure 3.14c and d all exhibited a continually shortening delivery times as the dose rate increased. However, the change in delivery times was smaller for the same increment of dose rate at the higher dose rates tested.

Over for the range of dose rates evaluated, the data in Figure 3.14 was best described by a quadratic relationship between the dose rate and delivery time, except for patient B where a linear dependence between these parameters was found to best characterise the data for plans generated using re-optimised objectives. Also given in Figure 3.14 are the correlation coefficients and the corresponding p-values obtained from the polynomial regression analysis of the data for each patient.

Although a quadratic relationship fitted most of the data in Figure 3.14, it is unlikely that this would hold true if higher dose rates were allowed. As the maximum dose rate was increased the difference in the delivery times continually decreased, this would imply that it is likely that the delivery time will be asymptotic to a certain value regardless of the maximum dose rate set. At this point the delivery time will only be dependent on the speed the gantry can rotate. This is limited to the TPS recommendation of 4.8 deg/s. This means that the shortest possible time for an arc the same length as was used in this study can be safely delivered is 74.24 s or 1.24 min. Figure 3.14c and d show the dual arc treatments approaching the minimum delivery time at lower maximum dose rates than a single arc. This is

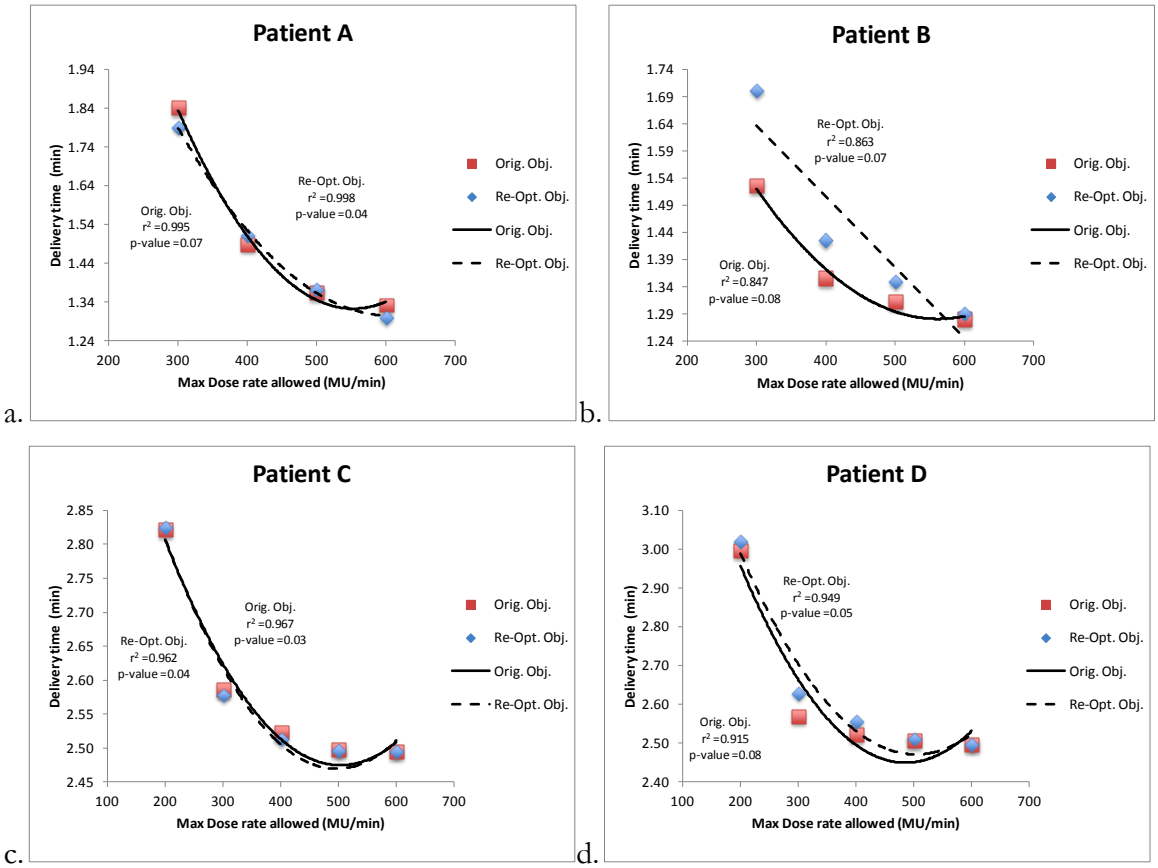

Figure 3.14. Variation in the estimated delivery time with respect to the maximum dose rate allowed in planning. The delivery time required for each plan for prostate (Patient A, Patient B) and H&N (Patient C, Patient D) cases are given.

again a likely consequence of the higher number of modulation points that a dual arc has compared to a single arc.

3.2.1.3 Overall Mean Leaf Speed

The changes in overall mean leaf speed with respect to the maximum dose rate are shown in Figure 3.15. The error bars show one standard deviation. The mean leaf speeds in the prostate plans were generally increasing with increasing dose rate (Figure 3.15a, b). This can be more clearly seen in the numerical data in Appendix C. For the H&N sites the major difference in leaf speeds occurs when the dose rate increased from 200 MU/min to 300 MU/min, after this point the overall mean leaf speed stays fairly constant.

For patient A, there appeared to be no significant correlation between mean leaf speed and the dose rate setting for the plans optimised with the original objectives. The plans with re-optimised objectives, however, exhibited a linear relationship between these parameters with correlation coefficient of 0.894 (p-value = 0.05). For patient B, the original objectives produced plans with a good correlation coefficient 0.916 (p-value = 0.04), whereas the re-optimised objectives showed no apparent correlation with an r^2 of 0.136 (p-value = 0.6). Both H&N cases yielded plans that exhibited a quadratic dependence of the mean leaf speed on the maximum dose rate allowed in the plans.

The variations in overall mean leaf speed were closely linked to the delivery time. The MLC leaf speed is set so that as the gantry rotates from one CP to the next, the MLC leaves travel at a constant speed so they reach their next specified position at the same time as the gantry does. This is optimised in the TPS and recalculated by the record and verify system to check the correct delivery of the plan. The data in Appendix C shows that the overall mean distance travelled by the MLC leaves were consistent with each other for all maximum dose rate tested. If there is no change in the distance travelled by the MLC leaves with respect to increasing maximum dose rate available and there is a decrease in the estimated delivery time, then the overall mean leaf speed will increase as the MLCs are required to cover the same distance in less time.

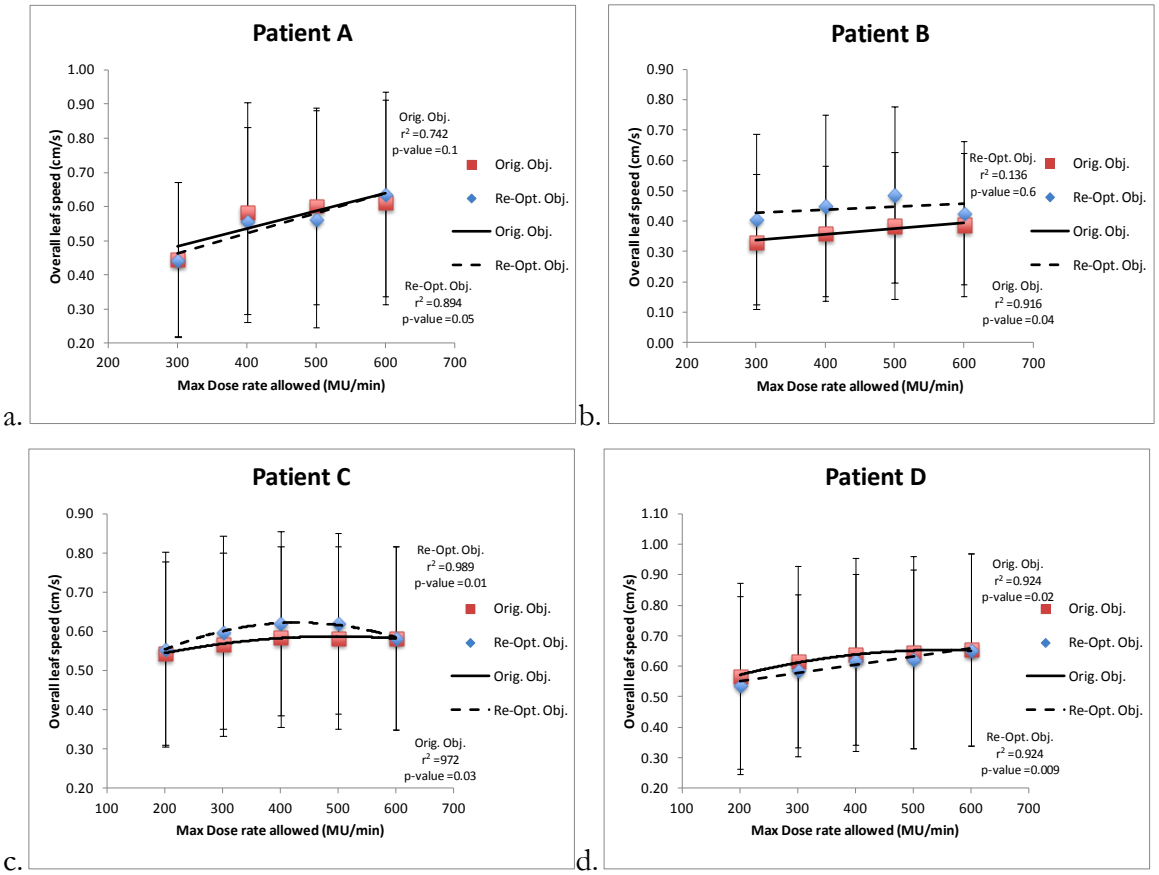

Figure 3.15 Variation in the mean leaf speed with respect to the maximum dose rate allowed in planning. The mean leaf speed required for each plan for prostate (Patient A, Patient B) and H&N (Patient C, Patient D) cases are given.

3.2.1.4 Overall Mean Dose Rate

The change in mean dose rate with respect to the maximum dose rate is shown in Figure 3.16. The graphs correspond to the plans generated using the original planning objectives and the re-optimised objectives.

As expected, a higher maximum dose rate setting resulted in higher mean dose rate. For patient A (Figure 3.16a) the mean delivered dose rate increase by over 110 MU/min over the range tested for both sets of planning objectives. Patient B had a smaller increase of around 70 MU/min. The majority of the change in the mean dose rate in the H&N sites occurs between 200 MU/min and 400 MU/min as seen in Figure 3.16c and Figure 3.16d.

The degree of dependence of the mean dose rate on the maximum dose rate allowed in each plan were not consistent across the cases evaluated in this study. This is evident in the best-fit lines of the graphs in Figure 3.16. However, the mean dose rates were seen to have monotonically increased with the maximum allowed dose rate.

Given that the number of MU required appeared to be independent of maximum dose rate and the delivery time showed a tendency to approach the minimum delivery time as dose rate was increased. When the maximum dose rate allowed exceeds what is required to deliver the maximum MU prescribed for a single CP, within the minimum time required for the gantry to cover the length of that CP, the mean dose rate will become independent of increasing maximum dose rate. We can already see this maximum dose rate being approached in each patient by the mean dose rate levelling off as the maximum dose rate was increased, but all plans still required the gantry to be slowed at some point to deliver the prescribed MU.

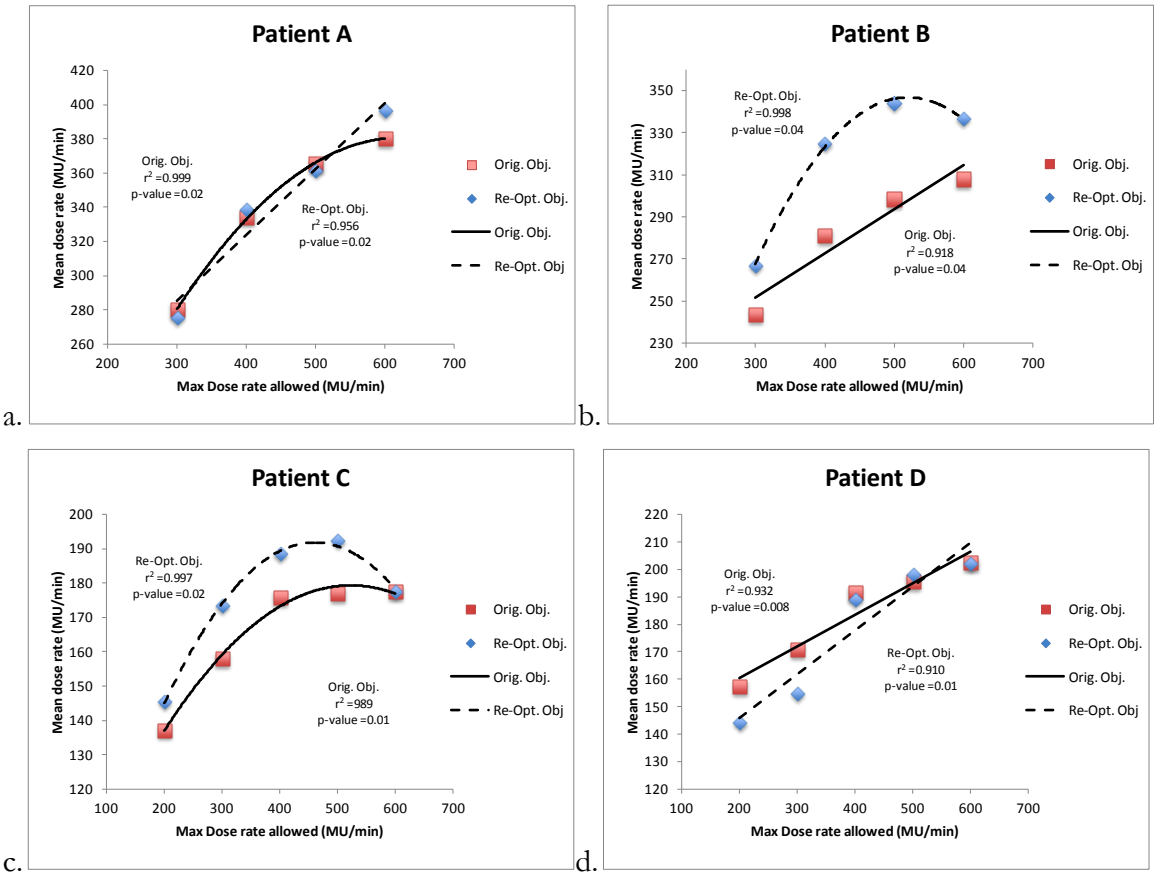

Figure 3.16 Variation in the mean dose rate with respect to the maximum dose rate allowed in planning. The Mean dose rate for each plan for prostate (Patient A, Patient B) and H&N (Patient C, Patient D) cases are given.

3.2.2 Conformity and Homogeneity

3.2.2.1 Conformity Index

The variation of the CI compared to the change in maximum dose rate available for each plan is shown in Figure 3.17. When the maximum dose rate available was varied, the CI of the plans showed minimal variation (Figure 3.17). On two occasions (Figure 3.17c and d), a set of plans had constant CI for all does rates. The largest variation of 0.06 was seen in patient A (Figure 3.17a). For cases where a relationship between these variables was apparent, the CI decreased as the maximum dose rate available increased.

From the results of the polynomial regression analysis (**Error! Reference source not found.**), there was no significant relationship indicated between the CI and the maximum dose rate available. Of the prostate cases, the only target volume that came close to expressing a linear dependency between CI and maximum MLC leaf speed was PTV74 of patient B for the plans generated from the original objectives. However, the corresponding plans produced with the re-optimised planning objectives showed no variation in the CI at all. If the outlier data for Patient C is disregarded the only significant variation occurred when the dose rate was changed from 200 MU/min to 300 MU/min.

In general, the variations in CI were minimal for all plans and many were constant for maximum dose rates above 300 MU/min. This all indicates that the maximum dose rate does not affect the ability of the TPS to produce a highly conformal plan within the range of dose rate that are seen clinically.

a.

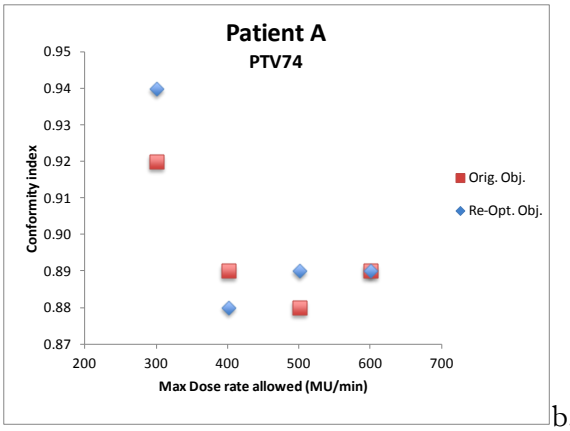

b.

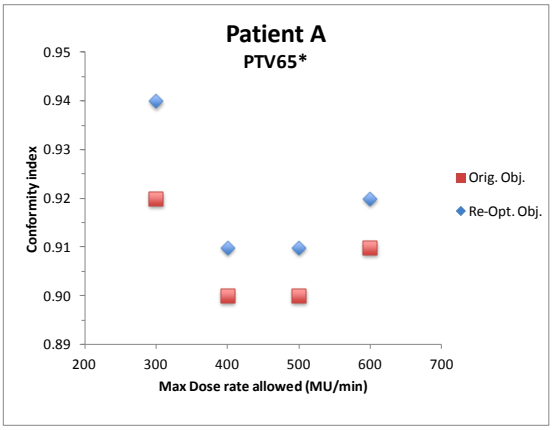

c.

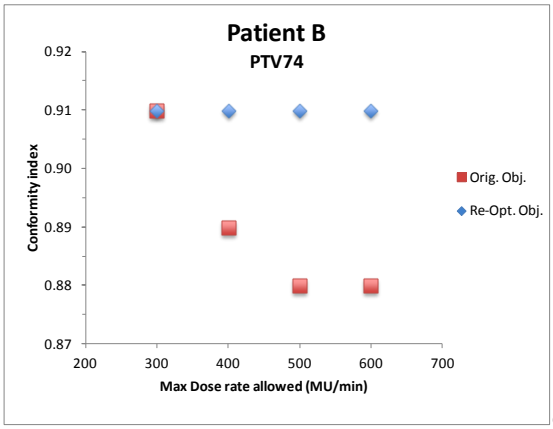

d.

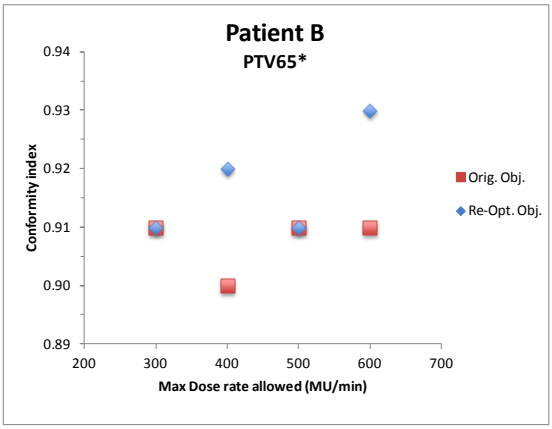

e.

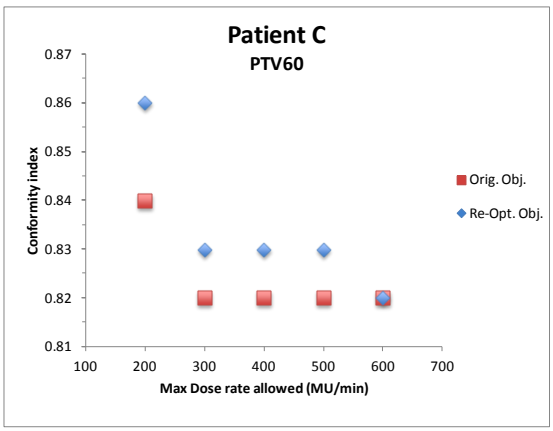

f.

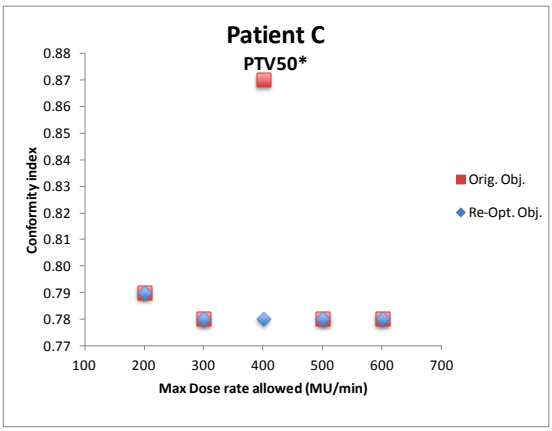

g.

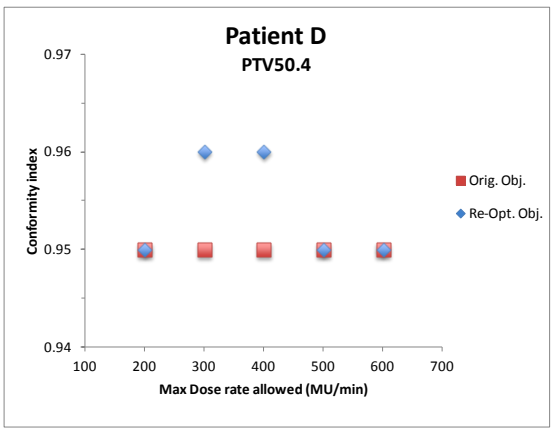

Figure 3.17 Variation in the conformity index with respect to the maximum dose rate allowed. Shown here are the results for each PTV in the plans generated for the prostate (PTV74, PTV65*) and H&N (PTV60, PTV50.4, PTV50*) evaluated in this study.

Table 3.5 Correlation coefficients of the conformity indicies shown in Figure 3.17 Enclosed in parenthesis is the corresponding p-value.

Patient	Optimisation Objectives	PTV74	PTV60	PTV50.4	PTV65*	PTV50*
A	Orig.	0.556 (0.3)			0.164 (0.6)	
	Re-Opt.	0.445 (0.3)			0.3 (0.5)	
B	Orig.	(0.833) 0.09			0.067 (0.7)	
	Re-Opt.	na			0.455 (0.3)	
C	Orig.		0.5 (0.2)			0.533 (0.3)
	Re-Opt.		0.696 (0.08)			0.5 (0.2)
D	Orig.			na		
	Re-Opt.			0.083 (0.6)		

3.2.2.2 Homogeneity Index

The effect of changes in the maximum dose rate available in planning on the homogeneity of the dose distribution of the target volumes for each site is shown in Figure 3.18. The HI is obtained for each PTV by taking the standard deviation of the *d*DVH data that was exported from Pinnacle.

With the exception of the PTV65 of patient A (Figure 3.18b), the HI showed minimal variation as the maximum dose rate was varied. The plans generated from the re-optimised objectives with the exception of the PTV65 volumes (Figure 3.18b, d) showed a decrease in HI as the maximum dose rate increased. Since HI is a measure of the spread of data, the implication was that the higher the maximum dose rate available the more homogenous the dose distribution was across the target volumes. The PTV65 volumes in the two prostate cases that encompass the seminal vesicles showed an increase in the HI as the maximum MLC dose rate was increased. They additionally had a higher HI as they were adjacent with the PTV74 and hence were in the fall off region of the PTV74 giving them poor homogeneity.

For most of the cases investigated the HI did not appear to be dependent on the maximum dose rate allowed in the TPS as evident from the correlation coefficients listed in Table 3.6. Of the prostate cases the plans generated using the original objectives showed a linear dependence between their parameters for the PTV65 volume. None of the other cases for patient A or any of the plan sets for patient B showed any significant dependence. Each H&N site had one set of plans which displayed some dependence. For instance, despite the PTV60 of patient C having no apparent correlation ($r^2 = 0$) for the plans generated by the original optimisation objective, the re-optimised objectives did exhibit a very good correlation ($r^2 = 0.9$, p-value = 0.01). On the other hand, patient D also exhibited some dependence for the plans generated from the re-optimised objectives but not for those produced with the original objectives.

a.

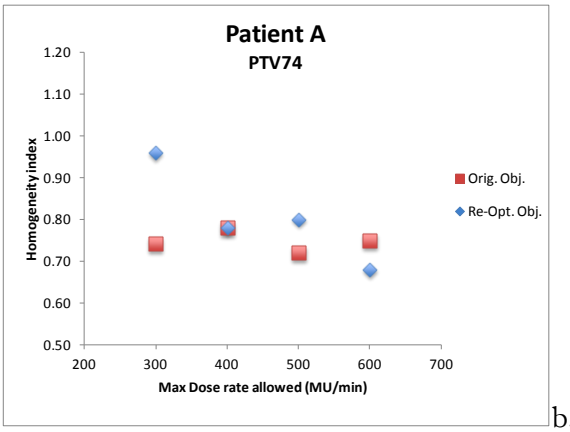

b.

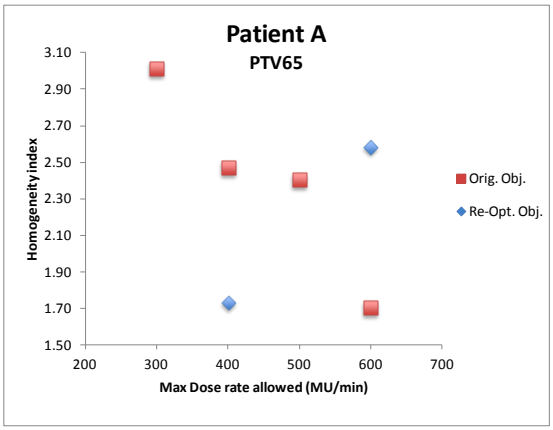

c.

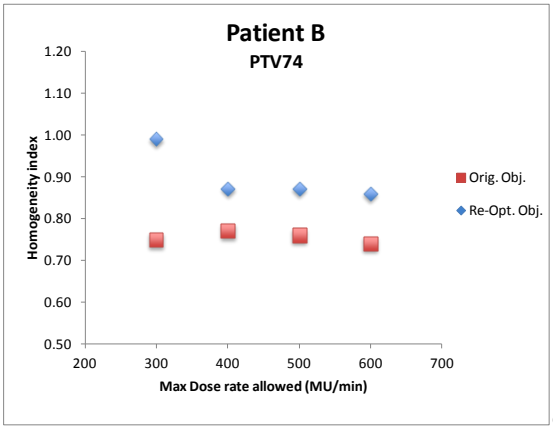

d.

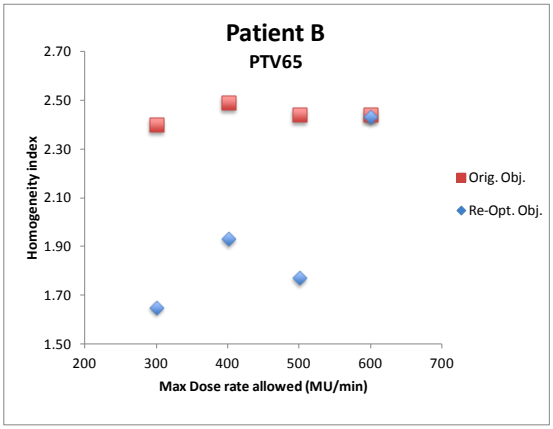

e.

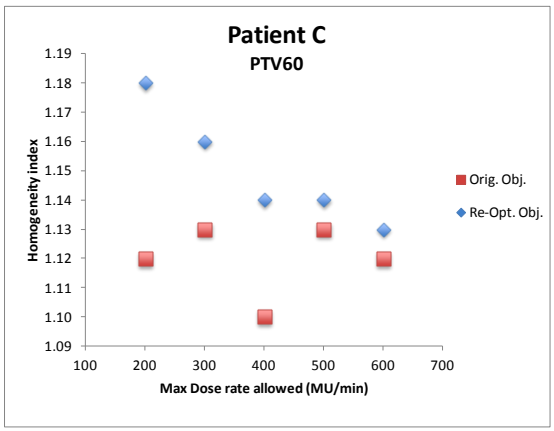

f.

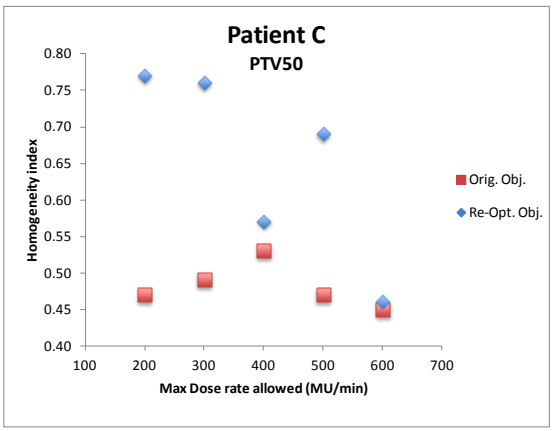

g.

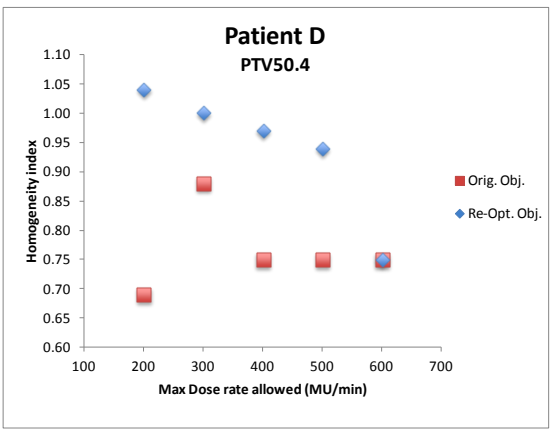

Figure 3.18 Variation in the homogeneity index with respect to the maximum dose rate allowed. Shown here are the results for each PTV in the plans generated for the prostate (PTV74, PTV65) and H&N (PTV60, PTV50.4, PTV50) cases evaluated in this study.

Table 3.6 Correlation coefficients of the homogeneity indicies shown in Figure 3.18. Enclosed in parenthesis is the corresponding p-value.

Patient	Optimisation Objectives	PTV74	PTV60	PTV50.4	PTV65	PTV50
A	Orig.	0.025 (0.8)			0.923 (0.04)	
	Re-Opt.	0.834 (0.09)			0.359 (0.4)	
B	Orig.	0.16 (0.6)			0.060 (0.7)	
	Re-Opt.	0.663 (0.2)			0.673 (0.2)	
C	Orig.		na			0.098 (0.6)
	Re-Opt.		0.9 (0.01)			0.674 (0.09)
D	Orig.			0.001 (1.0)		
	Re-Opt.			0.809 (0.4)		

The general indication for the plans using the original objectives was that there is little difference in the homogeneity of the plans generated with changing maximum dose rate; given only one out of seven indicated any variation. This was in contrast to the results of the plans from re-optimised objectives which had a higher likelihood of correlation occurring. The influence of the higher dose rates producing more conformal plans is likely to have caused the PTV65 volumes to have the opposite trend for HI than the rest of the plans. PTV65's, location relative to PTV74 resulted in steeper dose gradient in its volume giving a less homogeneous dose distribution. From these results it can be inferred that the homogeneity is more influenced by the planning objectives rather than the maximum dose rate available, especially for non-adjacent target volumes.

As with the CI there was no significant correlation indicated between the dose rate restrictions and the HI of the plans produced. This is evident in the lack of significant observable trends seen in Figure 3.18.

3.2.3 DVH analysis of Plan Quality Scores

The plans quality scores with respect to varying restricted maximum dose rate remained consistent with the 600 MU/min maximum setting in all treatment sites with the exception of patient A. For this patient, a decline in the quality of the plans was observed when dose rate was restricted to 300 MU/min with the normalised plan quality score falling over 10% in both plans with the original objectives and the re-optimised objectives. The fact that only one out of all four tests showed any clear trend supports the finding of Nicolini et al.[20] that restrictions applied to the dose rate have a minimal effect on the plan quality. This is likely due to the ability of the TPS to regulate the speed of gantry rotation to ensure that there is no change to the MU that can be delivered per CP.

Table 3.7 Plan quality scores for varing maxumin dose rate available when planning.

Maximum Dose rate	Planning objectives	Patient A	Patient B	Patient C	Patient D
600	**Orig. Obj.**	0.95	1.06	1.00	1.00
500		0.99	1.04	1.00	1.00
400		0.96	1.03	1.00	1.00
300		0.88	0.99	0.99	1.00
200				0.99	0.98
600	**Orig. Obj.**	1.00	1.00	1.00	1.00
500	**Re-Opt. Obj.**	1.00	1.03	1.05	1.09
400		0.98	1.00	1.05	1.08
300		0.86	1.01	1.05	1.09
200				1.05	1.10

3.2.4 Delivery Parameters

Only the results of the single arc plans showed a trend of a decline in the STDV of the MU (Appendix D) as the maximum available dose rate was reduced; correlation coefficients of above 0.9 (p-value < 0.02) were recorded for all single arc treatments. This was not reflected in the dual arc plans where no significant trend was detected. It should be noted that the analysis only had four points for the single arc treatments (300-600 MU/min). In the dual arc plans there was an additional data point at 200 MU/min, which typically produced a STDV equal to the 600 MU/min reading. Without this additional data included, the same trend as the single arc treatment was obtained. This could either mean that the results for the 200 MU/min plans were outliers or that there was no dependence between these parameters to begin with. To clarify this, further investigation would need to be done which should include a

single arc delivery with 200 MU/min maximum dose rate, despite this dose rate not being a practical clinical setting because it would result in a longer delivery time.

The gantry STDV (Appendix D) only showed a significant trend in three of the cases where r^2 for a linear relationship were all above 0.83 (p-values < 0.01). The trend identified was that the lower the maximum dose rate, the lower the STDV for gantry position. Although not all of the plans had a clear correlation between both the maximum dose rate and the STDV of gantry position, they all followed a similar pattern where the more restricted dose rates had fewer errors. A linear relationship between delivery time and gantry STDV was identified in six out of the eight cases. This shows that as the treatment time went up, which corresponded to a decrease in the mean gantry speed, the STDV of the gantry position decreased. Therefore, the gantry is more likely to be in the correct position if it is moving slower. However, this effect is minimal with the maximum change going from 0.29° to 0.21° for a 32 second increase in delivery time.

The beam on time (BOT) showed trends that were consistent with the estimated delivery times. The BOT recorded was less than the estimated time due to the BOT not including when the beam was on hold.

3.2.5 Point Dose Measurements

The changes in the point dose measurements with respect to the change in maximum dose rate available are shown in Figure 3.19. Once again the majority of the point dose differences between the predicted and measured doses were within the acceptable clinical tolerance of ±3%. There are three points that had a difference of between -3% and -4% difference. There was no significant trend detected when the point dose results were compared to their corresponding maximum dose rate. The prostates were once again the more consistent of the two sites selected, with the mean difference being -2.33% ± 0.65% (range: -4.07% to -1.42%) and -1.41% ± 0.41% (range: -2.31% to -0.63%) for patient A and B respectively. The H&N sites had mean difference of -0.36% ± 0.83% (range: -4.38% to -0.59%) and -1.39% ± 0.78% (range: -2.61% to 0.65%) for patient C and D respectively. The lack of trends and the broad distribution of data in Figure 3.19 suggest that there is no relationship between the point dose difference and the maximum dose rate available at planning.

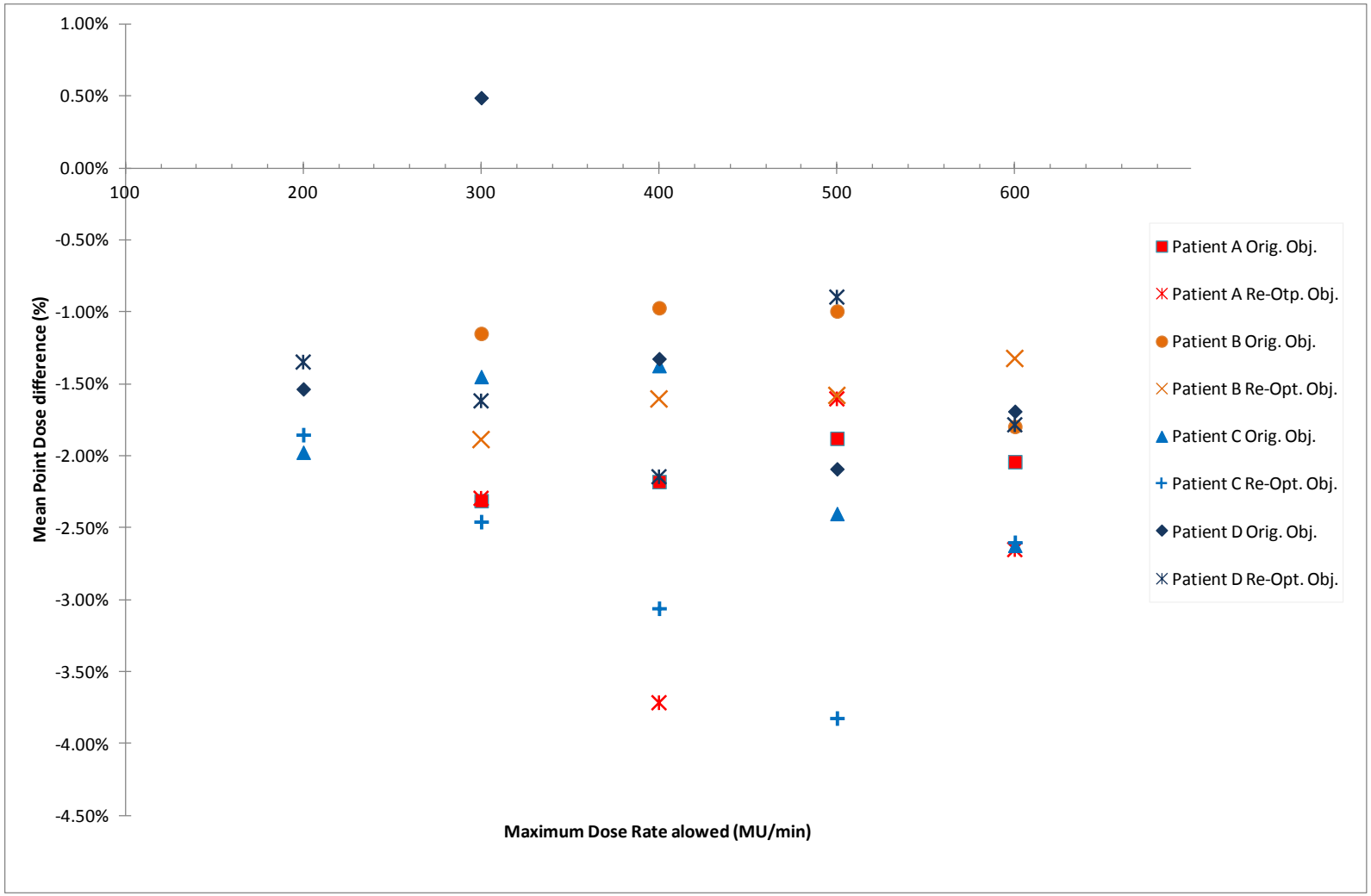

Figure 3.19 Variation in Point dose measurements with respect to the maximum dose rate allowed. Each patient has been divided into plans using the original objectives represented as a solid shape and plans with re-optimised objectives represented with a cross pattern.

3.2.6 Dose Maps

The variation in the gamma pass rates of the dose distributions measured with ArcCHECK are shown in Figure 3.20. The range of pass rates was consistent across plans with respect to the gamma criteria. All plans passed our clinical criteria in terms of the gamma analysis with the 3%/3 mm criteria having a mean of 99.2% ± 0.6% (range: 97.4% to 100.0%) and the 2%/2 mm criteria being 94.8% ± 1.5% (range: 90.3% to 97.9%), with the acceptable criteria being 95% and 85% gamma pass rate respectively. Although there is no clinical criteria for the stricter gamma criteria of 1%/1 mm, the consistency of results (mean: 70.1% ± 3.6%, range: 61.2% to 77.9%) is encouraging.

The majority of the plans appeared to express no relationship between gamma pass rate and the maximum dose rate available regardless of the gamma criteria applied. The minimal variation in the gamma pass rates within and across sites imply that the maximum dose rate that was available in planning had no clear effect on the ability of the linac to deliver an overall accurate treatment, over the range measured. This is consistent with the results of the planning study where the number of MU are largely independent of the maximum dose rate setting. It also shows that the slight improvements that were seen in the MU and gantry position STDV had negligible effect on how well the planned and delivered dose distributions matched.

a.

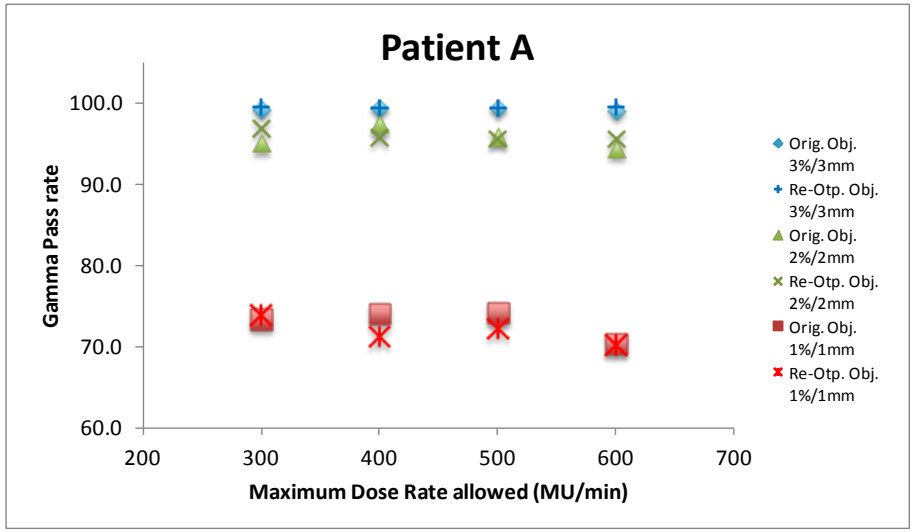

b.

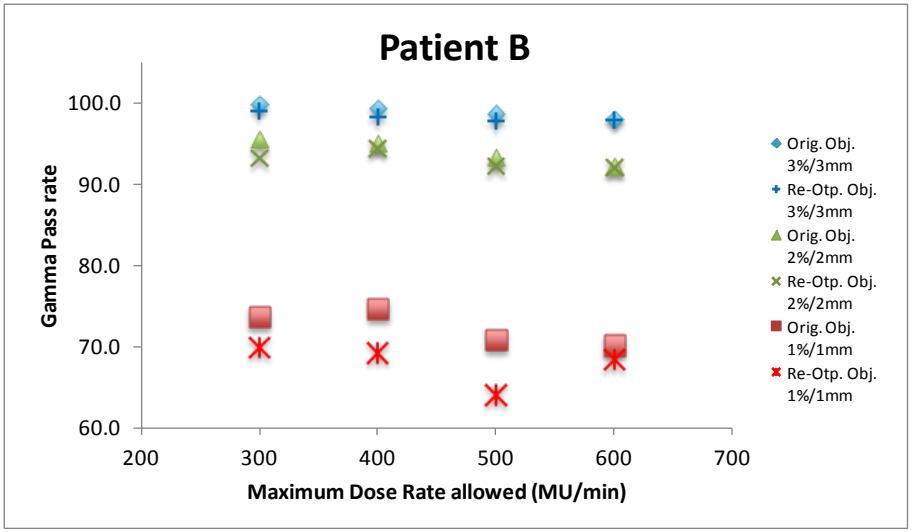

c.

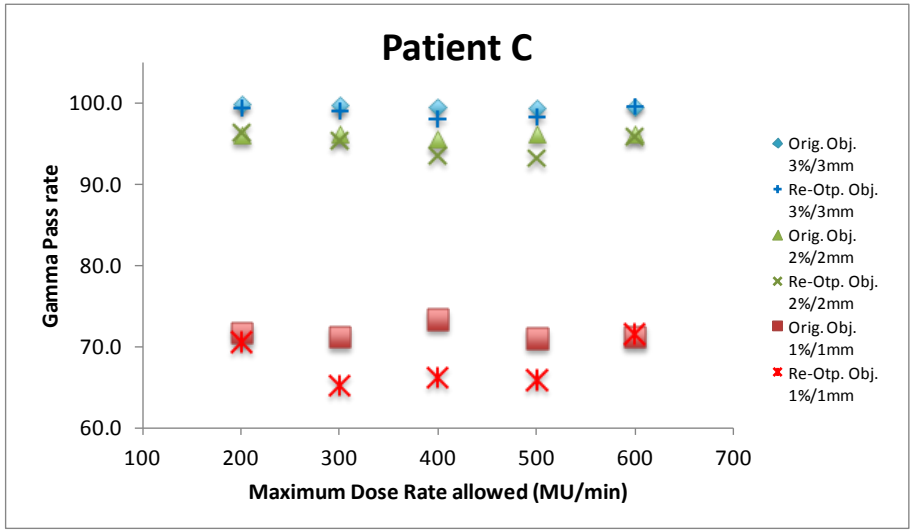

d.

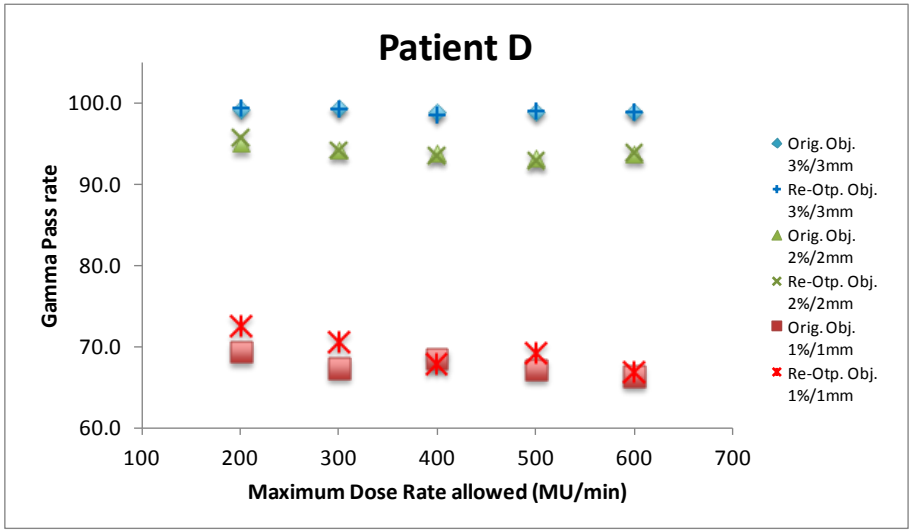

Figure 3.20 Shows the variation in the Gamma pass rates for each plan when the maximum dose rate available is changed. Each plot contains a seires for each of the three gamma criteria (3%/3 mm, 2%/2 mm and 1%/1 mm) and each of the planning objective methods.

3.2.7 Control Point Analysis

Figure 3.21a shows the charts produced in the analysis of the individual CP pass rates for one set of patient B's trials. Figure 3.21b and c show the mean number of CPs that have a given percentage of points failing either the 3%/3 mm or the 2%/2 mm gamma criteria for prostate treatments. A summary of this data is listed in Table 3.8 as well as those of the dual arc plans for the H&N cases.

It is most apparent from the results of the 2%/2 mm gamma analysis in Figure 3.21a that as the maximum dose rate available was reduced the number of segments with a high failure rate (seen as blue or red spikes) was reduced. This was also seen in the 3%/3 mm images, but to a lesser extent. The stricter requirements of the 1%/1 mm gamma analysis criteria resulted in a large number of CPs failing. It can be seen in Figure 3.21b and c and the data in Table 3.8 that for a 3%/3 mm gamma analysis criteria, the number of measurement points that fall within the 10-19.99% range for a single arc treatment is largely independent of the maximum dose rate available. The total number of CPs that was failing by more than 10% was decreasing overall. This is in contrast to what was seen when a 2%/2 mm gamma analysis was applied to the single arcs. The overall number of CPs that have more than 10% of measurement points failing was constant while the number of points in the 10 to 19.99% range increases and the number of points in the 20% and above range decreased. When the same analysis was done on the dual arc plans, both the 3%/3 mm and 2%/2 mm gamma criteria showed minimal variation in the total number of CPs having more than 10% of measurement points failing.

The reductions in the pass rate of the single arc treatments using a 3%/3 mm gamma criteria suggest that for an individual CP, there is a better match between the predicted and the measured data when the maximum dose rate is reduced. This looks to be consistent with the results of the 2%/2 mm gamma analysis of the single arc treatment but was shown to be minimal as only the number of CPs with a high percent of measurement points failing are reduced. The small improvements given the large change in dose rate make it unlikely that it was a direct result of the change in dose rate and may be linked more to one of the other parameters such as mean leaf speed or delivery time.

a.

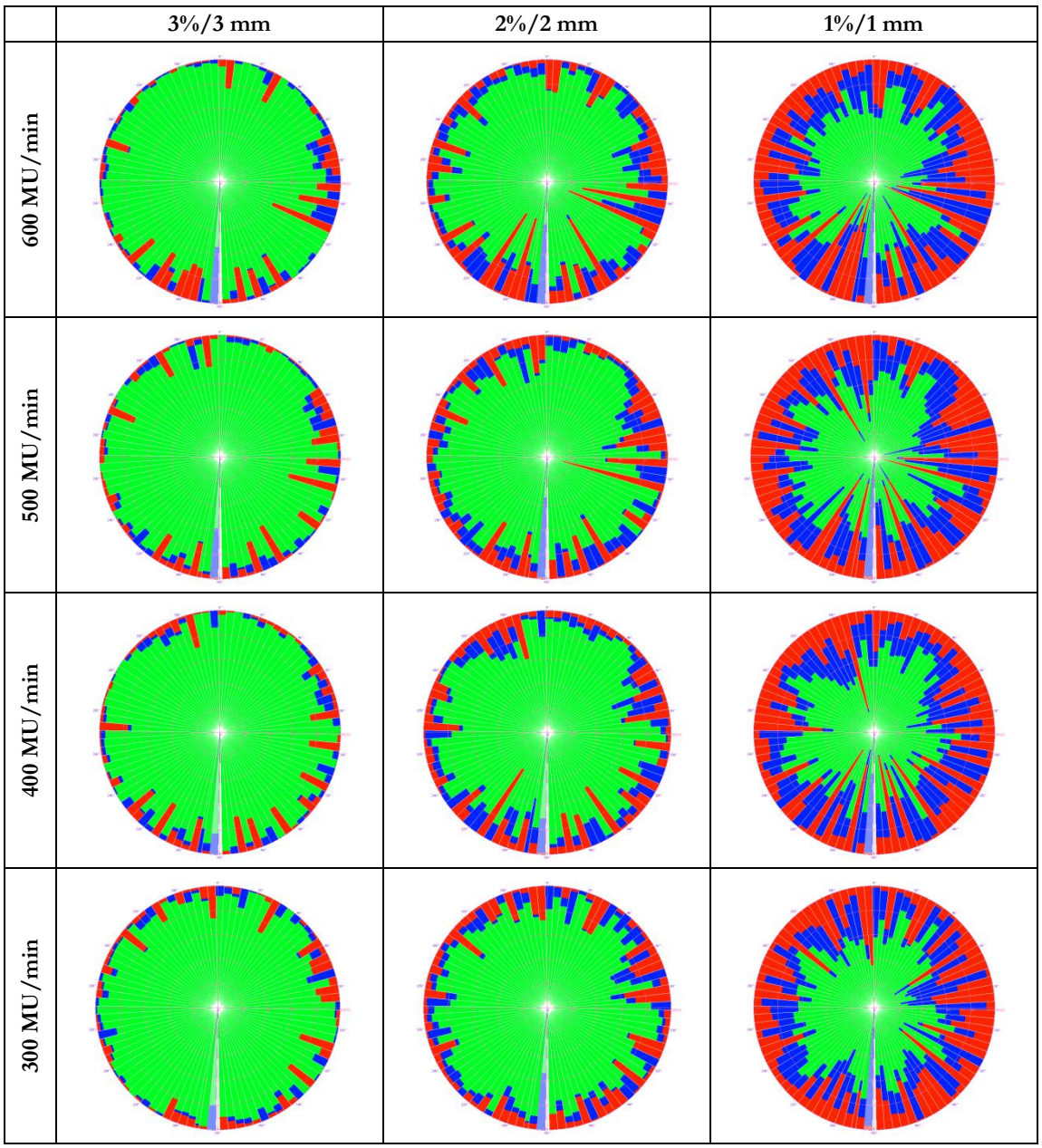

b.

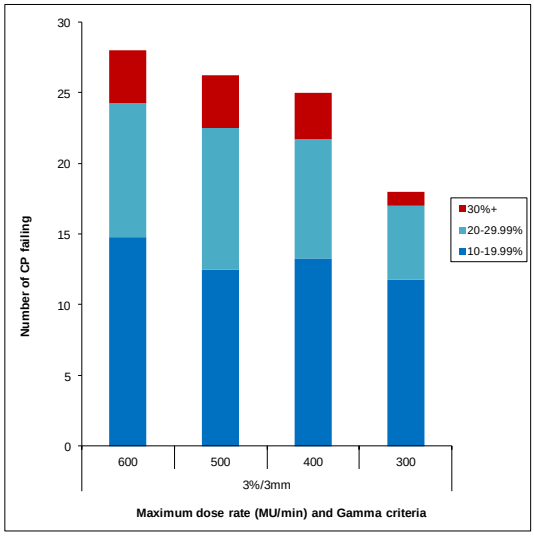

c.

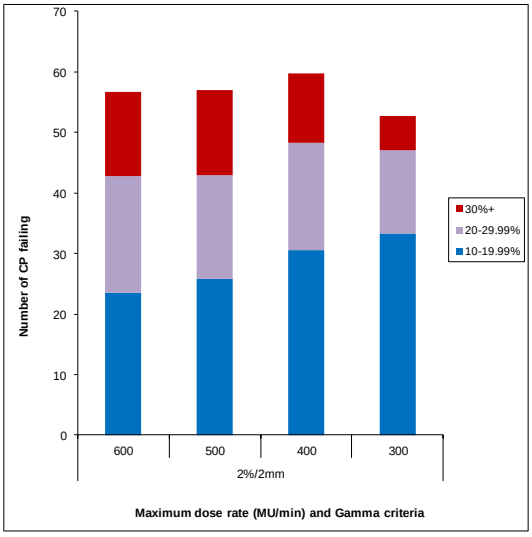

Figure 3.21 a Shows the CP analysis charts for a prostate patient when analysed using three different gamma criteria. b and c show the mean number of CPs per arc that have the given range of points failing to meet either a 3%/3 mm or 2%/2 mm gamma criteria.

Table 3.8 The mean number of points that failed for an individual arc with 90 control points.

3%/3 mm									
	Single Arc				Dual Arc				
Failure range	**600**	**500**	**400**	**300**	**600**	**500**	**400**	**300**	**200**
10-19.99%	14.75	12.5	13.25	11.75	12.88	14.00	14.88	13.63	15.88
20-29.99%	9.5	10	8.5	5.25	5.88	5.38	5.38	7.63	4.25
30%+	3.75	3.75	3.25	1	2.63	1.38	1.13	2.50	1.75
Total Failing CP	28.00	26.25	25.00	18.00	21.38	20.75	21.38	23.75	21.88
2%/2 mm									
	Single Arc				**Dual Arc**				
Failure rate	**600**	**500**	**400**	**300**	**600**	**500**	**400**	**300**	**200**
10-19.99%	23.5	25.75	30.5	33.25	28.75	29.50	32.00	22.50	28.13
20-29.99%	19.25	17.25	17.75	13.75	15.38	18.63	16.00	20.75	17.75
30%+	14	14	11.5	5.75	8.25	7.88	8.25	8.50	5.75
Total Failing CP	56.75	57.00	59.75	52.75	52.38	56.00	56.25	51.75	51.63

3.2.8 Dynalog Analysis

The histograms of the Dynalog data showing the MLC positional errors for each maximum dose rate can be seen in Figure 3.22. The single arc plan (Figure 3.22a and b) yielded a reduction in the large positional errors as the maximum dose rate was reduced, and a corresponding increase in the 0.0 to 0.5 mm range. The H&N plans (Figure 3.22 c and d) also showed a slight decrease in large MLC positional errors as the maximum dose rate was decreased but this primarily occurred when the dose rate went from 300 MU/min to 200 MU/min.

The change in the MLC positional error was minimal in all patients and the results in Figure 3.22 shows that the dose rate settings and MLC positional error are not directly linked. The steady change that was observed in the single arc prostate cases is similar to the trend that was seen in the effect of delivery time which caused a change in the mean leaf speed. The change in MLC positional error seen between 200 MU/min and 300 MU/min for the H&N cases is consistent with what was seen in the estimated delivery time and mean leaf speed. The slight changes that are seen in the MLC positional errors, as the maximum dose rate was changed, is likely to be related to the increased delivery time which causes a reduction in the mean MLC speed.

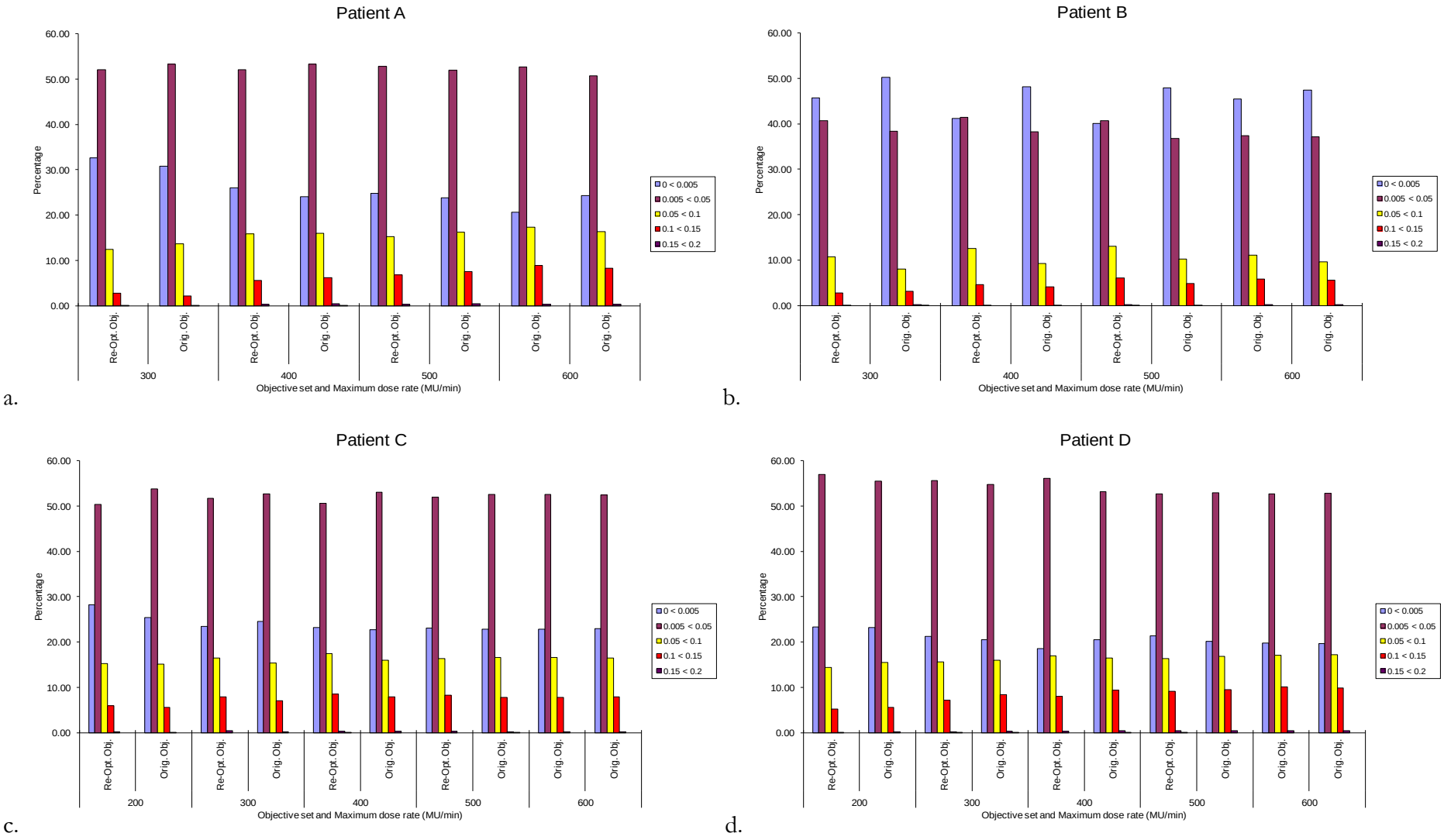

Figure 3.22 Dynalogs produced from each plan delivery. Each plan is given along the x axis and the coresponding histogram of the percentage of point from the dynalog flie that have a positional error within thespecified range in cm.

4. Summary and Conclusions

The dependence on the maximum allowed MLC speed and dose rate settings in the Pinnacle treatment planning system of VMAT plan parameters were investigated in this study. A survey on how these two machine parameters affected the plans monitor units (MU), estimated delivery time, mean dose rate, mean MLC speed, dose conformity and homogeneity in the generated plans was carried out. Additionally, the quality of the plans produced at different maximum MLC speeds and dose rates were evaluated by means of the plan quality score, a metric defined in this work based on the weighted importance of clinical dose objectives. This study also attempted to find out the effect of MLC speed and dose rate settings on the accuracy of plan delivery as demonstrated by the pass-fail rate of the quality assurance measurements and MLC leaf position errors.

The MU per fraction was found to be lower for slower MLC leaf speeds in single arc plans. As faster maximum MLC leaf speeds were allowed, the TPS generally created control points with field apertures that required the leaves to travel faster as evidenced by the increase in mean leaf speeds. Additionally, the delivery times for faster leaf settings were found to be shorter. This meant that in order to deliver the necessary dose to achieve the optimisation objectives, the TPS had to modify the extent of modulation based on the complexity of the treatment site and machine parameter restrictions. With slower leaf speeds, the delivery times were extended slightly longer but at fewer MU which means lower scattered dose and potentially reduced associated secondary cancer risks.

The dual arc plans, however, showed no apparent dependence on the MU and estimated delivery time on the MLC leaf speed setting. Although the same pattern of faster mean leaf motion at higher maximum MLC leaf speed setting was observed, the delivery times were not as variable for dual arc plans. With double the number of control points available to produce an optimum plan, the TPS was able to generate an optimised plan without varying the extent of modulation when the maximum MLC speed was varied. This meant that the MU per control point did not have to vary significantly, thus, a total MU per fraction was independent of the maximum allowed MLC leaf speed. Consequently, the mean dose rate was also found to be independent of the MLC leaf speed setting.

In terms of three measures of the plan quality (i.e., CI, HI and plan quality score), all showed that as the maximum MLC leaf speed increased so did the plan quality in single arc treatments resulting in better conformity, more homogeneous dose distributions and improved plan quality scores. In addition to the MLC leaf speed, the optimisation objectives were found to have a significant influence in the degree at which the quality of the plans varied. A reduction in maximum MLC speed can possibly be made without affecting

the capability of the TPS to achieve high quality plans. For dual arc plans the only quality indicator that was significantly affected was HI; the CI showed minimal variation and the plan quality scores were only slightly reduced for plans that used the original planning objectives.

The deliverability and dosimetric accuracy of the plans as indicated by their QA measurement results exhibited very little dependence on the maximum MLC speed setting allowed during plan optimisation, both for single and dual arc plans. The agreement between the planned and delivered dose fluence maps was influenced by the MLC speed setting for plans generated using the same planning objectives. However, this was not true for plans created with re-optimised objectives. The individual CP analysis of the dose fluence revealed that it was affected by the change in the MLC leaf speed setting. The lower leaf speeds showed better agreement between planned and delivered CP dose fluences, despite this not being observed in the overall dose fluence maps. The recorded MLC positional errors during plan delivery were also found to be affected by the MLC leaf speed, with higher maximum leaf speeds having more errors, however these were all within the clinically acceptable tolerance.

This study also investigated the effect of the maximum dose rate setting on the same evaluation metrics mentioned earlier. The MU in the plans were unaffected by the dose rate setting but the estimated delivery time was inversely affected by changing the maximum allowable dose rate in the plan. While the conformity index remained independent of the dose rate, the dose in the target volumes became less homogenous at lower dose rates. Plan QA results exhibited no clinically significant dependence of the QA evaluation indices on the maximum dose rate setting applied when optimising the treatment plans.

The number of VMAT fields and consequently the number of CPs in the plan was found to have a significant role on how much the MLC leaf speed setting affected the optimised plans in Pinnacle. Plans with multiple VMAT fields, in general, will be independent of the MLC speed setting but would require longer optimisation and delivery times. The degree at which the plans can be improved by using multiple fields should therefore be carefully weighed against the efficiency of generating plans for clinical use.

It was also evident in this study that the optimisation objectives influenced how the MLC speed and dose rate settings used in planning affected the parameters and quality of the plans generated in Pinnacle. By choosing the appropriate optimisation objectives, optimum MLC and dose rate settings may be used without significantly altering the plan parameters and plan quality metrics evaluated in this work.

The results of the MLC leaf speed evaluation showed that the lower the maximum leaf speed the more accurate the delivered treatment, but the quality of the plan is also reduced. This indicates that there could be an optimum maximum MLC leaf speed that produces high quality plans which can be accurately delivered. Based on this work a maximum MLC leaf speed of 1.38 cm/s was shown to have no reduction in plan quality but did show improved

delivery accuracy. There was no justification found for reducing the maximum dose rate below the recommended 600 MU/min.

5. Future Work

Much of this work was based on the clinically relevant planning techniques and conditions and the equipment used was limited to those available in our treatment facility. This study can be extended to include conditions outside the clinically used values of the parameters investigated here in order to validate the conclusions drawn from our results. Additionally the use of equipment from other manufacturers would establish if the results obtained in this study were manufacturer-specific or can be applied more generally.

It was seen on many occasion that the results of the prostate cases and H&N showed different trends. The likely causes could be the number of arcs used in the plans, the complexity of the site or a combination of the two. To determine this, dual arc treatments could be planned for prostates, single arc treatments could be trialled for H&N sites and potentially a triple arc treatment could be planned for both. These situations may not generally be implemented clinically but would provide necessary data on how the number of arcs and plan complexity affect the treatment plan parameters investigated in this work.

Another possible subject of future work related to this thesis would be to investigate the use of dose rates lower and/or higher than those considered here. Exploring the effect of much higher dose rates would be relevant as flattening filter free linacs, which are capable of delivering dose rates above our current limit of 600 MU/min, become widely used.

The effect of MLC leaf speed and dose rate on the various metrics evaluated here may have been dependent on the equipment used. It is therefore recommended that a similar parametric survey be conducted for linac, TPS and QA equipment other than the ones used in this study. Of key interest would be the effect of MLC speed using other linac manufacturers as these are controlled using different systems and have a different range of speeds. These will likely have an influence on the effect on the accuracy of plan delivery. Different TPS also use different implementations of VMAT which generates plan parameters that may be completely different from those produced in Pinnacle. The use of different QA equipment and methods may also influence the agreement of fluence patterns providing further useful information.

References

[1] A. Jemal, F. Bray, M. M. Center, J. Ferlay, E. Ward, & D. Forman. Global cancer statistics.[Erratum appears in CA Cancer J Clin. 2011 Mar-Apr;61(2):134]. *CA: a Cancer Journal for Clinicians, 61*(2), 69-90.

[2] J.; Shin Ferlay, HR; Bray, F; Forman, D; Mathers, C; Parkin, DM. (2010). GLOBOCAN 2008 v2.0, Cancer Incidence and Mortality Worldwide. Retrieved 02/02/2013, 2013, from http://globocan.iarc.fr

[3] Amato J. Giaccia, & Eric J. Hall. (2006). *Radiobiology for the radiologist*. Philadelphia: Lippincott Williams & Wilkins.

[4] Peter Metcalfe, Tomas Kron, & Peter Hoban. (1997). *The physics of radiotherapy X-rays from linear accelerators*. Madison, Wis: Medical Physics Pub.

[5] A. Brahme. Optimization of stationary and moving beam radiation therapy techniques. *Radiotherapy & Oncology, 12*(2), 129-140.

[6] Thomas Bortfeld. (2006). IMRT: a review and preview. *Physics in Medicine and Biology, 51*(13), R363-R379. doi: 10.1088/0031-9155/51/13/R21

[7] E. J. Hall, & C. S. Wuu. (2003). Radiation-induced second cancers: the impact of 3D-CRT and IMRT. *Int J Radiat Oncol Biol Phys, 56*(1), 83-88.

[8] E. J. Hall. (2006). Intensity-modulated radiation therapy, protons, and the risk of second cancers. *Int J Radiat Oncol Biol Phys, 65*(1), 1-7. doi: 10.1016/j.ijrobp.2006.01.027

[9] J. D. Ruben, S. Davis, C. Evans, P. Jones, F. Gagliardi, M. Haynes, & A. Hunter. (2008). The effect of intensity-modulated radiotherapy on radiation-induced second malignancies. *Int J Radiat Oncol Biol Phys, 70*(5), 1530-1536. doi: 10.1016/j.ijrobp.2007.08.046

[10] B. Wang, & X. G. Xu. (2008). Measurements of non-target organ doses using MOSFET dosemeters for selected IMRT and 3D CRT radiation treatment procedures. *Radiat Prot Dosimetry, 128*(3), 336-342. doi: 10.1093/rpd/ncm363

[11] C. X. Yu. (1995). Intensity-modulated arc therapy with dynamic multileaf collimation: an alternative to tomotherapy. *Physics in Medicine and Biology, 40*(9), 1435. doi: 10.1088/0031-9155/40/9/004

[12] Otto Karl. (2008). Volumetric modulated arc therapy: IMRT in a single gantry arc. *Medical Physics, 35*(1), 310. doi: 10.1118/1.2818738

[13] Li Zhang, Mian Xi, Xiao-Wu Deng, Qiao-Qiao Li, Xiao-Yan Huang, & Meng-Zhong Liu. (2012). Four-dimensional CT-based evaluation of volumetric modulated arc therapy for abdominal lymph node metastasis from hepatocellular carcinoma. *Journal of radiation research, 53*(5), 769-776. doi: 10.1093/jrr/rrs022

[14] D. Palma, E. Vollans, K. James, S. Nakano, V. Moiseenko, R. Shaffer, . . . K. Otto. (2008). Volumetric modulated arc therapy for delivery of prostate radiotherapy: comparison with intensity-modulated radiotherapy and three-dimensional conformal radiotherapy. *Int J Radiat Oncol Biol Phys, 72*(4), 996-1001. doi: 10.1016/j.ijrobp.2008.02.047

[15] V. Feygelman, G. Zhang, C. Stevens, & B. E. Nelms. (2011). Evaluation of a new VMAT QA device, or the "X" and "O" array geometries. *Journal of Applied Clinical Medical Physics, 12*(2), 3346.

[16] G. Li, Y. Zhang, X. Jiang, S. Bai, G. Peng, K. Wu, & Q. Jiang. (2013). Evaluation of the ArcCHECK QA system for IMRT and VMAT verification. *Physica Medica, 29*(3), 295-303. doi: http://dx.doi.org/10.1016/j.ejmp.2012.04.005

[17] S. Webb, & D. McQuaid. (2009). Some considerations concerning volume-modulated arc therapy: a stepping stone towards a general theory. *Physics in medicine and biology, 54*(14), 4345. doi: 10.1088/0031-9155/54/14/001

[18] Fan Chen, Min Rao, Jin-song Ye, David M. Shepard, & Daliang Cao. (2011). Impact of leaf motion constraints on IMAT plan quality, deliver accuracy, and efficiency. *Medical physics, 38*(11), 6106.

[19] D. Tatsumi, M. N. Hosono, R. Nakada, K. Ishii, S. Tsutsumi, M. Inoue, . . . Y. Miki. (2011). Direct impact analysis of multi-leaf collimator leaf position errors on dose distributions in volumetric modulated arc therapy: a pass rate calculation between measured planar doses with and without the position errors. *Physics in Medicine and Biology, 56*(20), N237. doi: 10.1088/0031-9155/56/20/N03

[20] Giorgia Nicolini, Alessandro Clivio, Luca Cozzi, Antonella Fogliata, & Eugenio Vanetti. (2011). On the impact of dose rate variation upon RapidArc implementation of volumetric modulated are therapy. *Medical physics, 38*(1), 264.

[21] Judith Alvarez-Moret, Fabian Pohl, Oliver Koelbl, & Barbara Dobler. (2010). Evaluation of volumetric modulated arc therapy (VMAT) with Oncentra MasterPlan® for the treatment of head and neck cancer (Vol. 5, pp. 110-110). England: BioMed Central.

[22] Matthias Guckenberger, Anne Richter, Thomas Krieger, Juergen Wilbert, Kurt Baier, & Michael Flentje. (2009). Is a single arc sufficient in volumetric-modulated arc therapy (VMAT) for complex-shaped target volumes? *Radiotherapy and Oncology, 93*(2), 259-265. doi: 10.1016/j.radonc.2009.08.015

[23] G. Tang, M. A. Earl, S. Luan, C. Wang, M. M. Mohiuddin, & C. X. Yu. Comparing radiation treatments using intensity-modulated beams, multiple arcs, and single arcs. *International Journal of Radiation Oncology, Biology, Physics, 76*(5), 1554-1562.

[24] V. Grégoire, & T. R. Mackie. (2011). State of the art on dose prescription, reporting and recording in Intensity-Modulated Radiation Therapy (ICRU report No. 83). *Cancer radiothérapie : journal de la Société française de radiothérapie oncologique, 15*(6-7), 555-559. doi: 10.1016/j.canrad.2011.04.003

[25] The Institute of Cancer Research: Royal Cancer Hospital. *Conventional or Hypofractionated High Dose Intensity Modulated Radiotherapy for Prostate Cancer (CHHiP)*. Clinical Trial. Retrieved from http://clinicaltrials.gov/ct2/show/NCT00392535?term=CHHiP&rank=1

[26] Quantitative Analyses of Normal Tissue Effects in the Clinic. (2010). *International journal of radiation oncology, biology, physics, 76*(3).

[27] L. Feuvret, G. Noel, J. J. Mazeron, & P. Bey. (2006). Conformity index: a review. *International Journal of Radiation Oncology, Biology, Physics, 64*(2), 333-342.

[28] Myonggeun Yoon, Sung Yong Park, Dongho Shin, Se Byeong Lee, Hong Ryull Pyo, Dae Yong Kim, & Kwan Ho Cho. (2007). A new homogeneity index based on statistical analysis of the dose-volume histogram. *Journal of applied clinical medical physics, 8*(2), 9.

[29] Technical bulletin 08-11: ArcCHECK-CT images. (2011): Sun Nuclear Corporation.

Appendix A

Appendix A 1 The weighting for each ROI in the prostate cases used to calculate the plan quality scores

Region of interest	Prostate	
	Dose Objective	Weight
CTV	$D_{98\%} \geq 73.0$Gy	10
	$D_{2\%} \leq 75.0$Gy	10
PTV74	$D_{98\%} \geq 71.0$Gy	9
	$D_{2\%} \leq 75.0$Gy	9
PTV65	$D_{98\%} \geq 62.4.0$Gy	9
	$D_{2\%} \leq 65.9.0$Gy	9
Rectum	$V_{40Gy} \leq 60\%$	8
	$V_{60Gy} \leq 30\%$	6
	$V_{70Gy} \leq 15\%$	6
	$V_{74Gy} \leq 3\%$	8
Bladder	$V_{50Gy} \leq 50\%$	5
Left/ Right Femoral head	$V_{50Gy} \leq 50\%$	5
Urethral bulb	$V_{70Gy} \leq 20\%$	5

Appendix A 2 The weightings assigned by clinicians to the rellevent ROIs for H&N cases, used to calculate the plans quality score.

Region of interest	Oropharynx		Nasopharynx	
	Dose Objective	Weight	Dose Objective	Weight
GTV			$V_{50.4\ Gy}=100\%$	10
PTV60	$V_{57\ Gy}=95\%$	8		
PTV50.4			$V_{47.9\ Gy}=95\%$	7
PTV50	$V_{47.5\ Gy}=95\%$	8		
Spinal cord	$D_{max} < 39$ Gy	10	$D_{max} < 32$ Gy	10
Brainstem	$D_{max} < 46$ Gy	10	$D_{max} < 39$ Gy	10
Left/Right Eyes	$D_{max} < 43$ Gy	10	$D_{max} < 36$ Gy	10
Left/Right Lens	$D_{max} < 7$ Gy	3	$D_{max} < 6$ Gy	3
Left/Right Optic nerve	$D_{max} < 43$ Gy	10	$D_{max} < 36$ Gy	10
Chiasm	$D_{max} < 43$ Gy	10	$D_{max} < 36$ Gy	10
Temporal lobe	$V_{56\ Gy} \leq 1\%$	5		
Left/Right Parotid	$D_{mean} < 22$ Gy	8/6	$D_{mean} < 19$ Gy	8/6
Oesophagus	$D_{mean} < 26$ Gy	5	$D_{mean} < 21$ Gy	
Left/Right Brachial plexus	$D_{max} < 57$ Gy	8	$D_{max} < 47$ Gy	
Left/Right Mandible	$V_{57\ Gy} \leq 1\%$	8/5	$V_{47\ Gy} \leq 1\%$	8/5

Appendix B

Plan characteristics for restricted MLC studies

Appendix B 1 provides the characteristics of plans produced from the patient A data set. * indicates where the analysis is done on the adjusted target volume . ** indicates the plan used for normalisation of the plan quality scores.

Max MLC speed (cm/s)	Optimisation objectives used	MU	Estimated delivery time	Overall Leaf speed (cm/s)		Area change (cm^2)			Overall leaf travel (cm)		Mean Dose rate	Dose rate change			CN		HI		Plan Quality Normalised to Default leaf speed
				Mean	Std Dev.	Mean	Std Dev.	Max.	Mean	Std Dev.		Mean	Std Dev.	Max.	PTV74	PTV65*	PTV74	PTV65	
2.20	Orig. Obj.	491	1.26	0.50	0.32	3.19	2.80	11.21	13.28	8.44	380.15	91.75	94.73	491.49	0.88	0.86	0.63	2.04	1.00
1.93	Orig. Obj.	491	1.27	0.48	0.27	2.86	2.21	9.92	12.76	7.18	380.32	95.45	102.53	399.35	0.87	0.85	0.66	2.02	1.00
1.65	Orig. Obj.	478	1.30	0.39	0.22	2.48	2.23	10.27	10.49	5.96	356.33	100.54	123.27	499.50	0.87	0.87	0.71	2.10	0.99
1.38	Orig. Obj.	493	1.27	0.43	0.20	2.56	1.91	8.03	11.58	5.15	380.08	101.15	103.25	405.82	0.86	0.84	0.66	2.05	1.00
1.10	Orig. Obj.	453	1.30	0.34	0.13	1.91	1.36	5.52	9.21	3.40	334.70	107.69	134.57	499.80	0.82	0.79	0.87	2.29	0.88
0.70	Orig. Obj.	443	1.29	0.21	0.11	1.14	0.95	4.09	5.70	2.83	328.18	52.05	60.76	273.39	0.83	0.83	0.86	2.33	0.83
0.60	Orig. Obj.	414	1.29	0.18	0.08	0.85	0.63	3.25	4.78	1.94	309.49	49.40	67.46	371.98	0.79	0.81	0.76	2.47	0.89
0.55	Orig. Obj.	424	1.32	0.20	0.08	1.26	0.74	2.65	5.52	2.06	303.46	54.52	87.67	442.18	0.79	0.81	1.03	2.71	0.77
2.20	Orig. Obj**.	491	1.26	0.50	0.32	3.19	2.80	11.21	13.28	8.44	379.97	90.19	92.37	482.65	0.88	0.86	0.64	2.05	1.00
1.93	Re-opt. Obj.	472	1.26	0.45	0.24	2.75	2.09	9.69	11.95	6.46	370.14	74.28	78.30	338.66	0.87	0.86	0.69	1.97	1.00
1.65	Re-opt. Obj.	472	1.28	0.39	0.19	2.13	1.55	7.12	10.56	4.94	358.39	104.40	136.65	499.51	0.82	0.84	0.65	2.29	1.00
1.38	Re-opt. Obj.	456	1.27	0.37	0.20	2.06	1.78	6.56	9.99	5.15	350.71	70.74	98.39	489.50	0.85	0.84	0.61	2.07	1.00
1.10	Re-opt. Obj.	492	1.27	0.36	0.13	2.20	1.64	7.97	9.61	3.51	375.98	95.57	107.05	499.22	0.84	0.84	0.68	2.16	0.92
0.70	Re-opt. Obj.	419	1.34	0.19	0.09	1.05	0.76	3.76	5.33	2.09	287.85	112.81	158.42	490.17	0.81	0.82	0.68	2.37	0.99
0.60	Re-opt. Obj.	435	1.31	0.21	0.09	0.99	0.71	3.36	5.71	2.28	312.65	165.20	175.85	499.96	0.82	0.82	1.14	1.56	0.78
0.55	Re-opt. Obj.	413	1.33	0.19	0.08	1.14	0.76	2.77	5.31	1.94	287.47	59.03	105.09	498.69	0.80	0.80	1.09	2.84	0.71

Appendix B 2 provides the characteristics of plans produced from the patient B data set. * indicates where the analysis is done on the adjusted target volume. ** indicates the plan used for normalisation of the plan quality scores.

Max MLC speed (cm/s)	Optimisation objectives used	MU	Estimated delivery time	Overall Leaf speed (cm/s)		Area change (cm^2)			Overall leaf travel (cm)		Mean Dose rate	Dose rate change			CN		HI		Plan Quality Normalised Default leaf speed
				Mean	Std Dev.	Mean	Std Dev.	Max.	Mean	Std Dev.		Mean	Std Dev.	Max.	PTV74	PTV65*	PTV74	PTV65	
2.20	Orig. Obj.	436	1.28	0.51	0.27	2.58	1.96	7.91	11.93	6.16	329.79	132.61	128.29	498.35	0.81	0.86	0.76	2.47	1.05
1.93	Orig. Obj.	421	1.27	0.44	0.21	2.58	1.99	8.41	10.41	4.90	321.45	113.35	126.70	499.42	0.86	0.88	0.71	2.65	1.31
1.65	Orig. Obj.	428	1.28	0.42	0.22	2.15	1.58	6.53	9.84	5.05	324.70	157.25	150.43	497.71	0.87	0.89	0.76	2.63	1.31
1.38	Orig. Obj.	418	1.28	0.39	0.16	2.23	1.54	6.49	9.29	3.71	318.45	129.09	128.26	499.57	0.86	0.87	0.77	2.75	1.21
1.10	Orig. Obj.	446	1.29	0.37	0.16	1.38	1.14	4.22	8.61	3.62	334.65	92.15	102.27	357.21	0.84	0.86	0.76	2.71	1.10
0.70	Orig. Obj.	415	1.27	0.27	0.12	1.41	1.10	4.61	6.36	2.66	321.23	73.46	94.12	430.44	0.84	0.85	1.29	3.07	0.69
0.60	Orig. Obj.	378	1.30	0.23	0.11	1.20	1.01	3.85	5.46	2.41	274.31	91.28	135.20	499.96	0.84	0.85	1.00	2.90	0.90
0.55	Orig. Obj.	410	1.32	0.25	0.09	1.32	0.95	3.28	6.09	2.13	294.61	78.56	92.76	385.11	0.84	0.84	1.53	3.12	0.45
2.20	Orig. Obj.**	425	1.26	0.43	0.26	2.20	1.95	7.81	9.98	6.14	332.57	81.97	88.09	491.82	0.86	0.88	0.83	2.67	1.00
1.93	Re-opt. Obj.	423	1.26	0.42	0.25	2.41	1.99	8.06	9.84	5.80	326.03	111.68	131.14	498.48	0.87	0.89	0.74	2.59	1.30
1.65	Re-opt. Obj.	437	1.28	0.41	0.22	2.08	1.55	6.17	9.70	5.12	332.22	133.59	159.47	499.94	0.86	0.89	0.72	2.63	1.22
1.38	Re-opt. Obj.	420	1.25	0.38	0.20	1.93	1.51	5.79	8.74	4.57	329.92	97.09	100.38	401.69	0.85	0.87	0.76	2.67	1.29
1.10	Re-opt. Obj.	428	1.29	0.38	0.18	1.60	1.20	4.88	8.90	4.15	322.85	104.43	125.63	499.94	0.78	0.80	0.93	2.47	0.96
0.70	Re-opt. Obj.	363	1.30	0.21	0.09	1.09	0.89	4.00	4.99	1.93	262.45	121.30	171.56	499.87	0.82	0.84	0.82	2.82	0.75
0.60	Re-opt. Obj.	355	1.29	0.20	0.07	0.96	0.75	3.37	4.62	1.54	258.14	71.24	137.51	499.98	0.82	0.84	0.95	2.88	0.87
0.55	Re-opt. Obj.	397	1.30	0.22	0.07	0.83	0.74	3.06	5.20	1.66	293.20	69.94	100.85	499.00	0.86	0.84	1.39	2.29	0.78

Appendix B 3 provides the characteristics of plans produced from the patient C data set. * indicates where the analysis is done on the adjusted target volume. ** indicates the plan used for normalisation of the plan quality scores

Max MLC speed (cm/s)	Optimisation objectives used	MU	Estimated delivery time	Overall Leaf speed (cm/s)		Area change (cm²)			Overall leaf travel (cm)		Mean Dose rate	Dose rate change			CN		HI		Plan Quality Normalised Default leaf speed
				Mean	Std Dev.	Mean	Std Dev.	Max.	Mean	Std Dev.		Mean	Std Dev.	Max.	PTV60	PTV50*	PTV60	PTV50	
IMRT	Orig. Obj.	?													0.84	0.73	1.14	0.89	0.95
2.20	Orig. Obj.	459	2.50	0.64	0.21	4.93	4.31	22.05	30.75	10.39	182.40	53.04	86.58	383.41	0.81	0.80	0.82	0.56	1.00
1.93	Orig. Obj.	449	2.49	0.58	0.20	4.95	4.38	21.17	28.04	9.69	179.79	56.56	85.74	449.59	0.82	0.79	0.85	0.67	0.96
1.65	Orig. Obj.	414	2.49	0.57	0.17	4.59	4.21	19.15	27.66	8.15	166.52	40.63	68.16	365.10	0.84	0.78	0.95	0.67	0.95
1.38	Orig. Obj.	422	2.49	0.49	0.13	3.65	3.04	15.16	23.54	6.31	168.24	40.63	79.71	453.80	0.82	0.79	0.89	0.56	0.99
1.10	Orig. Obj.	416	2.49	0.43	0.11	3.16	2.66	12.96	20.87	5.39	166.14	37.01	65.41	420.34	0.82	0.79	0.93	0.55	0.98
0.70	Orig. Obj.	403	2.50	0.33	0.07	2.13	1.47	6.61	15.86	3.29	160.30	34.40	71.29	462.57	0.81	0.77	1.01	0.61	0.95
0.60	Orig. Obj.	419	2.50	0.31	0.06	1.87	1.35	6.38	14.80	3.07	164.85	39.45	80.48	377.79	0.80	0.77	1.06	0.64	0.95
0.55	Orig. Obj.	397	2.50	0.30	0.06	1.98	1.34	5.71	14.32	2.99	158.88	28.43	51.98	214.97	0.81	0.76	1.17	0.94	0.95
2.20	Orig. Obj.**	459	2.50	0.64	0.21	5.02	4.34	21.88	30.82	10.47	182.38	52.60	87.37	407.49	0.80	0.79	0.82	0.56	1.00
1.93	Re-opt. Obj.	475	2.49	0.58	0.21	4.46	3.62	17.23	28.04	9.94	190.08	51.21	81.39	499.24	0.82	0.80	0.85	0.95	1.07
1.65	Re-opt. Obj.	451	2.49	0.60	0.17	4.32	3.43	15.50	28.87	8.50	180.40	52.10	73.47	358.73	0.83	0.80	0.89	0.56	1.07
1.38	Re-opt. Obj.	497	2.49	0.51	0.15	4.11	3.28	15.12	24.68	7.29	198.16	48.04	62.46	310.48	0.83	0.80	0.87	0.64	1.07
1.10	Re-opt. Obj.	448	2.50	0.48	0.11	3.19	2.49	13.07	23.09	5.48	177.95	46.05	63.79	300.19	0.81	0.79	0.89	0.57	1.07
0.70	Re-opt. Obj.	465	2.49	0.36	0.07	2.33	1.62	7.52	17.45	3.46	185.66	42.26	61.93	337.54	0.83	0.80	1.05	0.68	1.06
0.60	Re-opt. Obj.	481	2.51	0.32	0.06	2.02	1.44	6.21	15.63	2.92	190.56	36.90	71.85	412.96	0.81	0.78	0.97	0.63	1.07
0.55	Re-opt. Obj.	465	2.51	0.30	0.06	1.95	1.48	6.39	14.72	2.90	184.42	32.60	53.40	225.31	0.82	0.77	1.20	1.00	1.07

Appendix B 4 provides the characteristics of plans produced from the patient D data set. * indicates where the analysis is done on the adjusted target volume. ** indicates the plan used for normalisation of the plan quality scores

Max MLC speed (cm/s)	Optimisation objectives used	MU	Estimated delivery time	Overall Leaf speed (cm/s)		Area change (cm^2)			Overall leaf travel (cm)		Mean Dose rate	Dose rate change			CN	HI	Plan Quality Normalised to VMAT score
				Mean	Std Dev.	Mean	Std Dev.	Max.	Mean	Std Dev.		Mean	Std Dev.	Max.	50.4	50.4	
IMRT	Orig. Obj.	?													0.86	0.96	0.70
2.20	Orig. Obj.	502	2.49	0.68	0.29	4.89	4.43	25.35	28.18	12.11	199.98	82.35	95.60	355.75	0.95	0.62	0.99
1.93	Orig. Obj.	500	2.49	0.63	0.26	4.55	4.03	22.07	26.07	11.07	199.35	79.86	88.35	345.02	0.96	0.77	1.05
1.65	Orig. Obj.	514	2.49	0.61	0.20	4.04	3.25	18.25	25.37	8.46	204.21	88.04	114.67	473.80	0.95	0.65	1.00
1.38	Orig. Obj.	511	2.49	0.57	0.18	3.62	3.01	16.56	23.53	7.33	203.24	90.60	117.73	456.22	0.95	0.73	1.01
1.10	Orig. Obj.	530	2.51	0.51	0.13	3.04	2.35	13.31	21.03	5.25	207.93	92.71	114.28	497.26	0.95	0.69	0.98
0.70	Orig. Obj.	514	2.49	0.39	0.08	2.03	1.74	7.98	16.23	3.29	203.08	70.62	103.01	493.67	0.95	0.96	1.00
0.60	Orig. Obj.	505	2.50	0.35	0.07	1.87	1.55	6.73	14.34	2.78	200.34	61.22	88.13	457.31	0.94	1.21	0.98
0.55	Orig. Obj.	519	2.51	0.32	0.06	1.64	1.37	5.93	13.41	2.62	204.48	61.86	92.67	404.26	0.94	1.08	0.93
2.20	Orig. Obj.**	497	2.49	0.67	0.30	4.93	4.51	25.59	27.84	12.42	197.87	81.26	91.69	318.59	0.96	0.67	1.00
1.93	Re-opt. Obj.	488	2.49	0.58	0.21	3.70	3.77	25.05	24.42	8.95	193.77	62.66	85.02	426.12	0.97	0.94	1.08
1.65	Re-opt. Obj.	503	2.50	0.57	0.21	3.91	3.62	20.82	23.90	8.65	197.11	81.27	117.41	499.48	0.96	1.02	1.06
1.38	Re-opt. Obj.	502	2.49	0.56	0.18	3.31	2.92	14.45	23.20	7.37	199.43	88.95	115.58	498.46	0.97	0.85	1.05
1.10	Re-opt. Obj.	547	2.49	0.49	0.13	3.18	2.43	12.89	20.96	5.69	217.03	77.26	101.55	387.39	0.95	1.09	1.06
0.70	Re-opt. Obj.	524	2.50	0.38	0.08	2.08	1.93	8.86	15.47	3.07	207.60	67.96	96.88	480.50	0.95	1.10	1.07
0.60	Re-opt. Obj.	522	2.50	0.34	0.07	1.73	1.56	7.32	14.23	2.85	205.73	70.12	100.12	455.95	0.95	1.13	1.05
0.55	Re-opt. Obj.	497	2.52	0.31	0.07	1.46	1.29	5.35	13.07	2.67	194.38	55.25	93.43	499.42	0.96	1.09	0.99

Appendix C

Plan Characteristics for sites with varied maximum dose rate

Appendix C 1 The plan characteristics for patient A when the maximum dose rate available at planning is modified. PTV65* is the analysis volume as described in the methods. Orig. Obj. ** is the plan used for normalisation.

Max Dose Rate (MU/min)	Optimisation objectives used	MU	Estimated delivery time	Overall Leaf speed (cm/s)		Area change (cm²)			Overall leaf travel (cm)		Mean Dose rate (MU/min)	Dose rate change (MU/min)			CN		HI		Plan Quality Normalised to Orig. Obj.**
				Mean	Std Dev.	Mean	Std Dev.	Max.	Mean	Std Dev.		Mean	Std Dev.	Max.	PTV74	PTV65*	PTV74	PTV65	
600	Orig. Obj.	532	1.33	0.61	0.30	4.64	3.42	11.89	22.47	10.35	380.60	159.65	178.25	499.65	0.89	0.91	0.75	1.70	0.95
500	Orig. Obj.	522	1.36	0.60	0.29	4.78	3.01	10.70	22.38	10.02	365.32	125.68	147.36	398.95	0.88	0.90	0.72	2.40	0.99
400	Orig. Obj.	518	1.49	0.58	0.32	4.90	3.47	13.05	23.21	10.99	334.07	69.69	106.44	299.45	0.89	0.90	0.78	2.47	0.96
300	Orig. Obj.	531	1.84	0.45	0.23	4.42	2.96	16.13	21.60	8.47	280.21	25.68	68.67	269.46	0.92	0.92	0.74	3.01	0.88
600	Orig. Obj.**	532	1.30	0.64	0.27	4.31	3.16	13.30	23.00	9.52	396.31	154.24	154.65	499.82	0.89	0.92	0.68	2.58	1.00
500	Re-Opt. Obj.	520	1.37	0.56	0.32	3.92	3.39	14.98	21.26	11.26	361.98	121.45	138.09	399.74	0.89	0.91	0.80	1.17	1.00
400	Re-Opt. Obj.	533	1.51	0.56	0.27	4.36	3.45	16.30	22.64	9.44	338.80	70.08	109.17	299.71	0.88	0.91	0.78	1.73	0.98
300	Re-Opt. Obj.	511	1.79	0.44	0.23	4.10	2.98	10.85	20.82	8.26	275.39	31.98	67.43	260.97	0.94	0.94	0.96	1.45	0.86

Appendix C 2 The plan characteristics for patient B when the maximum dose rate available at planning is modified. PTV65* is the analysis volume as described in the methods. Orig. Obj. is the plan used for normalisation.**

Max Dose Rate (MU/min)	Optimisation objectives used	MU	Estimated delivery time	Overall Leaf speed (cm/s)		Area change (cm^2)			Overall leaf travel (cm)		Mean Dose rate (MU/min)	Dose rate change (MU/min)			CN		HI		Plan Quality Normalised to Orig. Obj.**
				Mean	Std Dev.	Mean	Std Dev.	Max.	Mean	Std Dev.		Mean	Std Dev.	Max.	PTV74	PTV65*	PTV74	PTV65	
600	Orig. Obj.	409	1.28	0.39	0.24	2.73	2.57	10.09	10.58	6.38	308.29	132.32	142.35	499.85	0.88	0.91	0.74	2.44	1.06
500	Orig. Obj.	409	1.31	0.39	0.24	2.68	2.63	10.97	10.68	6.53	298.75	106.84	122.11	399.76	0.88	0.91	0.76	2.44	1.04
400	Orig. Obj.	398	1.35	0.36	0.22	2.72	2.51	10.37	10.26	6.19	281.22	77.52	91.53	299.61	0.89	0.90	0.77	2.49	1.03
300	Orig. Obj.	393	1.53	0.33	0.22	2.44	2.28	9.90	10.05	5.90	243.94	46.99	72.69	269.90	0.91	0.91	0.75	2.40	0.99
600	Orig. Obj.**	450	1.29	0.43	0.26	2.74	2.95	19.82	12.40	7.47	337.00	96.31	113.33	499.60	0.91	0.93	0.86	2.43	1.00
500	Re-Opt. Obj.	484	1.35	0.49	0.29	3.14	2.59	12.92	13.53	7.59	344.39	89.78	113.05	398.94	0.91	0.91	0.87	1.77	1.03
400	Re-Opt. Obj.	481	1.42	0.45	0.30	2.89	2.74	13.00	13.12	8.06	325.13	58.06	82.50	299.64	0.91	0.92	0.87	1.93	1.00
300	Re-Opt. Obj.	473	1.70	0.41	0.28	3.23	2.77	9.94	13.10	7.56	267.19	31.90	65.02	269.48	0.91	0.91	0.99	1.65	1.01

Appendix C 3 The plan characteristics for patient C when the maximum dose rate available at planning is modified. PTV50* is the analysis volume as described in the methods. Orig. Obj. ** is the plan used for normalisation.

Max Dose Rate (MU/min)	Optimisation objectives used	MU	Estimated delivery time	Overall Leaf speed (cm/s)		Area change (cm^2)			Overall leaf travel (cm)		Mean Dose rate (MU/min)	Dose rate change (MU/min)			CN		HI		Plan Quality Normalised to Orig. Obj.**
				Mean	Std Dev.	Mean	Std Dev.	Max.	Mean	Std Dev.		Mean	Std Dev.	Max.	PTV60	PTV50*	PTV60	PTV50	
IMRT	Orig. Obj.														0.84	0.73	1.14	0.89	0.93
600	Orig. Obj.	447	2.50	0.58	0.23	4.91	4.23	20.41	28.15	11.38	177.64	47.21	78.40	484.83	0.82	0.78	1.12	0.45	1.00
500	Orig. Obj.	446	2.50	0.58	0.23	4.76	4.31	21.70	28.18	11.33	176.84	47.09	73.41	377.27	0.82	0.78	1.13	0.47	1.00
400	Orig. Obj.	454	2.52	0.59	0.23	4.71	4.21	20.88	28.55	11.13	175.84	43.49	67.57	296.95	0.82	0.87	1.10	0.53	1.00
300	Orig. Obj.	425	2.59	0.57	0.23	4.91	4.24	18.16	28.06	11.26	157.97	40.50	59.16	266.94	0.82	0.78	1.13	0.49	0.99
200	Orig. Obj.	411	2.82	0.54	0.23	4.62	3.84	19.79	28.55	10.92	137.16	24.04	40.23	169.85	0.84	0.79	1.12	0.47	0.99
600	Orig. Obj.**	447	2.50	0.58	0.23	4.91	4.22	20.42	28.14	11.36	177.64	47.18	78.56	482.65	0.82	0.78	1.13	0.46	1.00
500	Re-Opt. Obj.	485	2.50	0.62	0.23	5.36	4.50	23.44	29.95	11.26	192.30	49.42	76.25	379.87	0.83	0.78	1.14	0.69	1.05
400	Re-Opt. Obj.	483	2.51	0.62	0.23	5.26	4.56	24.44	30.10	11.38	188.61	44.06	68.78	299.06	0.83	0.78	1.14	0.57	1.05
300	Re-Opt. Obj.	463	2.58	0.60	0.25	5.74	4.75	23.00	29.54	11.87	173.54	41.39	55.79	242.55	0.83	0.78	1.16	0.76	1.05
200	Re-Opt. Obj.	432	2.83	0.56	0.25	5.32	4.78	22.59	29.08	11.65	145.39	26.54	40.56	169.67	0.86	0.79	1.18	0.77	1.05

Appendix C 4 The plan characteristics for patient D when the maximum dose rate available at planning is modified. Orig. Obj. ** is the plan that the Plan quality score is normalised to.

Max Dose Rate (MU/min)	Optimisation objectives used	MU	Estimated delivery time	Overall Leaf speed (cm/s)		Area change (cm^2)			Overall leaf travel (cm)		Mean Dose rate (MU/min)	Dose rate change (MU/min)			CN	HI	Plan Quality Normalised to Orig. Obj.**
				Mean	Std Dev.	Mean	Std Dev.	Max.	Mean	Std Dev.		Mean	Std Dev.	Max.	PTV50.4	PTV50.4	
IMRT	Orig. Obj.														0.86	0.96	0.68
600	Orig. Obj.	510	2.50	0.65	0.32	5.16	6.23	27.63	27.22	13.12	202.28	105.59	136.19	497.69	0.95	0.75	1.00
500	Orig. Obj.	499	2.51	0.65	0.31	5.21	6.24	30.67	26.96	13.10	195.55	94.46	113.60	398.86	0.95	0.75	1.00
400	Orig. Obj.	493	2.52	0.64	0.32	5.16	6.22	29.58	26.71	13.08	191.62	80.54	96.04	299.52	0.95	0.75	1.00
300	Orig. Obj.	453	2.57	0.62	0.31	5.21	6.30	29.37	26.15	12.78	170.86	76.07	77.96	269.88	0.95	0.88	1.00
200	Orig. Obj.	497	3.00	0.57	0.30	5.00	5.57	25.34	27.11	12.31	157.20	40.38	56.98	169.61	0.95	0.69	0.98
600	Orig. Obj.**	510	2.50	0.65	0.32	5.16	6.24	27.67	27.21	13.12	202.23	105.43	135.99	497.80	0.95	0.75	1.00
500	Re-Opt. Obj.	509	2.51	0.62	0.29	4.47	4.82	23.36	25.97	12.21	198.16	89.80	112.45	399.95	0.95	0.94	1.09
400	Re-Opt. Obj.	504	2.56	0.62	0.28	4.73	5.03	22.18	26.92	12.12	188.97	64.80	90.51	299.83	0.96	0.97	1.08
300	Re-Opt. Obj.	432	2.63	0.59	0.25	4.53	4.62	22.19	25.12	9.93	154.87	77.87	81.93	269.84	0.96	1.00	1.09
200	Re-Opt. Obj.	469	3.02	0.54	0.29	4.51	4.94	26.77	25.53	12.03	144.06	42.28	57.57	169.93	0.95	1.04	1.10

Appendix D

STDV and BOT data for all plans where dose rate was modulated

Maximum Dose rate	Patient A			Patient B			Patient C			Patient D		
	MU STDV	Gantry STDV (°)	Beam on time (min)	MU STDV	Gantry STDV (°)	Beam on time (min)	MU STDV	Gantry STDV (°)	Beam on time (min)	MU STDV	Gantry STDV (°)	Beam on time (min)
200							0.03	0.28	2.79	0.03	0.30	3.02
300	0.02	0.21	1.89	0.02	0.28	1.54	0.01	0.30	2.53	0.03	0.34	2.51
400	0.03	0.24	1.51	0.03	0.30	1.35	0.02	0.31	2.44	0.02	0.35	2.47
500	0.03	0.28	1.37	0.03	0.32	1.29	0.03	0.31	2.41	0.03	0.35	2.42
600	0.04	0.27	1.33	0.04	0.32	1.25	0.03	0.31	2.41	0.04	0.33	2.43
200							0.03	0.28	2.81	0.03	0.30	3.01
300	0.01	0.23	1.81	0.02	0.26	1.72	0.02	0.29	2.53	0.02	0.33	2.59
400	0.02	0.25	1.53	0.03	0.29	1.43	0.02	0.30	2.44	0.02	0.34	2.49
500	0.03	0.28	1.37	0.03	0.31	1.33	0.03	0.31	2.42	0.03	0.36	2.43
600	0.04	0.29	1.28	0.04	0.31	1.26	0.03	0.31	2.41	0.04	0.34	2.42